Trafficking and Quality Control of Inward-Rectifying Potassium Channels in the Model Eukaryote *Saccharomyces cerevisiae*

by

Timothy Daniel Mackie

Bachelor of Science, Messiah College, 2010

Bachelor of Arts, Messiah College, 2010

Submitted to the Graduate Faculty of the

Dietrich School of Arts and Sciences in partial fulfillment

of the requirements for the degree of

Doctor of Philosophy

University of Pittsburgh

2018

UNIVERSITY OF PITTSBURGH

Dietrich School of Arts and Science

This dissertation was presented

by

Timothy Daniel Mackie

It was defended on

April 18, 2018

and approved by

Karen M. Arndt, Ph.D., Professor, Department of Biological Sciences

Jeffrey D. Hildebrand, Ph.D., Associate Professor, Department of Biological Sciences

Arohan R. Subramanya, M.D., Assistant Professor, Department of Medicine

Andrew P. VanDemark, Ph.D., Associate Professor, Department of Biological Sciences

Dissertation Advisor: Jeffrey L. Brodsky, Ph.D., Professor, Department of Biological Sciences

Trafficking and Quality Control of Inward-Rectifying Potassium Channels in the Model Eukaryote *Saccharomyces cerevisiae*

Timothy Daniel Mackie, PhD

University of Pittsburgh, 2018

Humans express 15 different inward-rectifying potassium (K_{ir}) channels that play a variety of roles in epithelial transport, nerve conduction, and muscle contraction. Polymorphisms in K_{ir} channels underlie numerous genetic diseases. In order to investigate the function and regulation of K_{ir} channels, researchers have long recognized the potential of expressing them in strains of *Saccharomyces cerevisiae* (Bakers' yeast) engineered for sensitivity to growth in a low potassium medium. These studies capitalize on the wide variety of genetic and biochemical tools available in yeast, namely the ease of transforming large quantities of cells with recombinant DNA and the availability of comprehensive mutant libraries for high-throughput screening. Due to the longstanding popularity of yeast as model eukaryotes, the mechanisms underlying cellular phenomena are relatively well-documented and are also conserved in multicellular organisms. In this document, I will first review the history and diversity of techniques for studying potassium channels in potassium-sensitized yeast. Next, I will describe the results of a genetic screen to identify the key regulatory factors for a particular K_{ir} channel: the renal outer medullary potassium (ROMK) channel. ROMK, also known as $K_{ir}1.1$, is the major route for potassium secretion into the pro-urine and plays an indispensable role in regulating serum potassium. However, the cellular machinery that regulates ROMK trafficking has not been fully defined. I used a synthetic genetic array to identify nonessential genes that reduce the plasma membrane pool of ROMK in potassium uptake-deficient yeast. Through this screen, I identified several members of the endosomal complexes required for transport (ESCRT) and the class-C core vacuole/endosome tethering (CORVET) complexes. Moreover, silencing of ESCRT and CORVET components increased ROMK levels at the plasma membrane in a mammalian cell line, therefore establishing that post-endocytic sorting influences the cell-surface density of ROMK and modulates its activity. Finally, I will briefly delineate potential future studies in yeast with ROMK and other K_{ir} channels and will describe several investigations into various aspects of K_{ir} channel biology to which I have contributed through collaboration.

TABLE OF CONTENTS

LIST OF TABLES

LIST OF FIGURES

PREFACE

Acknowledgements and Dedication

Upon reflection, I can't pinpoint with any certainty when my scientific journey began and I certainly see no imminent end to it. It certainly stretches well beyond the investigations circumscribed by my graduate career described in this document. Therefore, an adequate acknowledgement of my influences as a scientist must necessarily start with my parents, David and Maria Mackie. Through their extraordinary investment in my education, my parents gave me the foundational skills to excel academically and instilled in me an implacable desire to seek the truth in all things. My physicist father deserves special gratitude for convincing me to take up biology as a major course of study as an undergraduate, in addition to my preferred major of journalism. I took quickly to my "secondary" discipline, largely through the enthusiastic and adroit instruction of the faculty of the Department of Biology at Messiah College, in particular Drs. David Foster, Erik Lindquist, Gerald Hess, and John Harms, as well as Dr. Roseann Sachs of the Department of Chemistry, a wizard in the classroom who improbably made Organic Chemistry my favorite class of my sophomore year. For three summers during my college years, I had the privilege to conduct research at the US Army Research Laboratory (ARL) through the Department of Defense's Student Temporary Employment Program (STEP), where I received invaluable mentorship from Drs. David Heaps, Paul Pellegrino, Christian Sund, Amethist Finch, and James Sumner. My experiences at ARL, in which I produced my first scientific publication, were instrumental in convincing me to pursue a career in research.

After signing on to the graduate program at the University of Pittsburgh, I was honored to join the research group of Dr. Jeffrey Brodsky. Jeff never fails to impress me with his breadth of scientific knowledge both within his specialty of protein quality control and of other related fields. He is a role model both as a scientist and as a human being, as he has always prioritized graduate student mentorship despite his busy schedule and has a wonderful talent for building

and maintaining collaborations within and across disciplines. Through example, Jeff has taught me that a good scientist must have a sharp mind, but a great scientist must also have a generous heart. The other members of the research group deserve equal recognition for shaping me into the scientist I am today. Dr. Christopher Guerriero chaperoned me into the field of protein quality control by serving as my research rotation mentor. Chris and fellow research assistant professors Drs. Teresa Buck and Patrick Needham have served as intellectual leaders who have shared expertise, helped troubleshoot difficult problems, and kept the rest of us accountable for staying up-to-date on the scientific literature. My contemporaries in the group who have been a wellspring of aid and camaraderie both professionally and socially include postdoctoral fellows Dr. Alexandra Manos-Turvey and Dr. Sara Sannino, previous graduate students Dr. Karen Hecht, Dr. Alexander Kolb, Dr. Joseph Tran, Dr. G. Michael Preston, and Dr. Lynley Doonan, and current graduate students Zhihao Sun, Samuel Estabrooks, and Deepa Kumari. Lab manager Jennifer Goeckeler-Fried keeps the physical aspect of research humming along with nary a snag, to say nothing of her incredible skills and decades of experience as a researcher. She has been aided during my time in the lab by research technician Megan Yates and by numerous undergraduate lab aides who have gone on to spearhead their own research projects.

My thesis committee of Drs. Andrew VanDemark, Karen Arndt, Jeffrey Hildebrand, and Arohan Subramanya has provided a critical yet encouraging voice throughout my graduate career. Each individual member has also provided technical expertise throughout the years, by serving as a research rotation mentor, by writing letters of recommendation that enabled me to get fellowships, and by enlisting members of their lab to train me in several of the skills required to complete this project. I have also been mentored through the Biological Sciences' Teaching Minor program by Drs. Kathryn Gardner and Craig Peebles, who have taken a keen interest in helping me hone my skills in the classroom.

A number of individuals have dedicated time and resources to this project over the years. Dr. Alexander Kolb laid much of the groundwork for this dissertation through careful assay optimization and for training me during my first few months in the lab. Dr. Brighid O'Donnell joined the project as a research fellow and through heroic effort was able to spin off her own project which synthesized my interest in quality control of potassium channels with her medical expertise as a neonatologist. Jackson Parr was an undergraduate researcher who performed much of the groundwork for the ROMK gain-of-function screen (see Appendix A). I also had the

privilege to mentor two excellent rotation students: Matthew Googins, who toiled relentlessly in the tissue culture room to find potential correctors for misfolded ROMK, and Nga (Katie) Nguyen, whose hard work and enthusiasm allowed the gain-of-function screen to really get off the ground (see Appendix A). Dr. Paul Welling at the University of Maryland Baltimore, in addition to laying much of the intellectual foundation of my project, graciously allowed me to work in his lab for several weeks, during which time I received invaluable training on cell surface biotinylation by his lab manager, Bo-Young Kim. Dr. Arohan Subramanya, of Pitt's School of Medicine, in addition to serving on my thesis committee, has provided local expertise on mammalian cell culture and perspective on the role of ROMK in the human body. Dr. Allyson O'Donnell at Duquesne University has taught me innumerable tools of the trade as a yeast researcher and has been a fount of knowledge for all things protein trafficking. In my last year of graduate school, I was honored to receive financial support from the Andrew W. Mellon Foundation through its fellowship program in the Dietrich School of Arts and Sciences.

Science is as much an exercise in perseverance as in creativity, and I've been extremely lucky to have a supportive network of friends in the city of Pittsburgh who cheered me up when experiments failed and celebrated with me when they succeeded. Special recognition is owed to my roommate Kathleen Zawrotniak for tolerating my erratic schedule and jargon-heavy rants over morning coffee, and to my board gaming group of Jacob Czech, Kayleigh Stevenson, Dr. Zara Weinberg, and Dr. Meredyth Wegener for helping me mentally unwind and for being so unflaggingly dependable for 3+ years. I owe a great debt to Drs. Gregory Wier, Adam Wier, and Swarna Mohan for introducing me to great music and taking me under their wings when I was a first-year graduate student. Dr. S. Branden Van Oss has been both a fast friend and an intellectual whetstone who has stuck by me even during the most difficult times. Finally, my girlfriend Anuva Kulkarni has brought light and adventure into my life during this past year.

List of Abbreviations

Note: Abbreviations common to the parlance of molecular biology (*i.e.* DNA, GFP) and closely related disciplines are not included. Standard yeast and human gene names are indicated by italic text; however, genes are often named according to the study in which they were first identified, which may or may not reflect their biological function.

17-AAG: 17-Allylamino-17-DemethoxyGeldanamycin

AAA+: ATPases Associated with diverse cellular Activities

AGA: A-AGlutinin

ApoB: Apolipoprotein B

ARH: Autosomal Recessive Hypocholesteremia protein

BAR: Bin/Amphiphysin/Rvs

BK: Big Potassium channel

BLINK: Blue Light INduced Potassium channel

BSD: Bypass SOD1 Defects

CCD: Cortical Collecting Duct

CCP: Clathrin-Coated Pit

CDC: Cell Division Cycle

CFTR: Cystic Fibrosis Transmembrane conductance Regulator

CIE: Clathrin-Independent Endocytosis

CME: Clathrin-Mediated Endocytosis

COP: Coat Protein

CORVET: class-C cORe Vacuole/Endosome Transport

CUL: CULlin

CYC: CYtochrome C

DALY: Disability-Adjusted Life Year

DDM: n-DoDecyl-β-Maltoside

DOA: Degradation of Alpha factor

DUb: DeUbiquitinating protease

ENA: *Exitus NAtru*

ENaC: Epithelial Sodium Channel

END: ENDocytosis

ER: Endoplasmic Reticulum

ERAD: Endoplasmic Reticulum Associated Degradation

ERQC: Endoplasmic Reticulum Quality Control

ESCRT: Endosomal Sorting Complexes Required for Transport

FAP: Fluorogen-Activated Peptide

FHS: Framingham (MA) Heart Study

GIRK: G-protein activated Inward-Rectifying Potassium channel

GO: Gene Ontology

GOS: GOlgi SNARE

GQC: Golgi Quality Control

GWAS: Genome-Wide Association Study

HA: human influenza HemAgglutinin

HEK: Human Embryonic Kidney

hERG: human *Ether-à-go-go* Related Gene

HMG-CoA: 3-Hydroxy-3-Methyl-Glutaryl-Coenzyme A

HOG: High Osmolarity Glycerol response

HOPS: Homotypic fusion and Protein Sorting

HRD: HMG-coA Reductase Degradation

Hsp: Heat shock protein

ICP-MS: Inductively Coupled Plasma Mass Spectrometry

IgLD: Immunoglobulin-Like Domain

ILV: Intra-Lumenal Vesicle

KLHL: KeLtcH-Like

MG: Malachite Green

MVB: MultiVesicular Body

NCC: Sodium Chloride Cotransporter

NDFIP: NedD Four-Interacting Protein

NEDD: Neural precursor cell Expressed Developmentally Downregulated gene

NHA: Sodium-Hydrogen Antiporter

NHX: Sodium-Hydrogen eXchanger

NKCC: Sodium Potassium Chloride Cotransporter

NSAID: Non-Steroidal Anti-Inflammatory Drug

OST: OligoSaccharylTransferase

PAS: Per/Arnt/Sim

PDI: Protein Disulfide Isomerase

PEP: carboxyPEPtidase Y-deficient

PIB: PhosphatidyInositol-3-phosphate Binding

PGFR: Platelet-derived Growth Factor Receptor

PKA: Protein Kinase A

PMA: Plasma Membrane ATPase

P_o: open probability

POSH: Plenty Of SH3

Rab: Ras-related in brain

RCY: ReCYcling

rEAG: rat *Ether-À-go-go* related Gene

RFFL: RiFiFyLin

RING: Really Interesting New Gene

ROMK: Renal Outer Medullar Potassium Channel

RSC: Chromatin Structure Remodeling

RSP: Reverses Spt Phenotype

SCA: Single-Chain Antibody

SCS: Suppressor of Choline Sensitivity

SEC: SECretory

SGA: Synthetic Genetic Array

SGK: Serum and Glucocorticoid-regulated Kinase

SNARE: Soluble N-ethylmaleimide-sensitive factor Activating protein REceptor

SNF: Sucrose Non-Fermenting

SSA: Stress Seventy subfamily A

STE: STErile

SUR: SulfonylUrea Transporter

TAL: Thick Ascending Limb (of Loop of Henle)

TEF: Translation Elongation Factor

TEVC: Two-Electrode Voltage Clamp

TGN: *Trans*-Golgi Network

TIRF: Total Internal Reflection Fluorescence

TMD: TransMembrane Domain

TO: Thiazide Orange

TOK: Target Of Killer toxin

TRK: TRansport of Potassium

UPS: Ubiquitin Proteasome System

VNX: Vacuolar Na^+/H^+ eXchanger

VPS: Vacuolar Protein Sorting

Vpu: HIV protein U

WNK: With No Lysines

YPD: Yeast extract/Peptone/Dextrose

YPT: Yeast Protein Two

1.0 INTRODUCTION

In this section, I will describe the rationale, history, and future potential for using budding yeast to investigate potassium channels. This first section is adapted from a review article currently in revision at the journal *Genetics*. I will then describe how my dissertation research contributes to this legacy.

1.1 INVESTIGATING POTASSIUM CHANNELS IN YEAST

1.1.1 Potassium channel classes, activities, and structures

Potassium channels are ubiquitous in eukaryotes and prokaryotes and are the most diverse type of cation channel due to early evolutionary divergence (Loukin *et al.*, 2005). The most salient feature of potassium channels is their ability to discriminate K^+ from smaller cations such as Na^+ (MacKinnon, 2003). All potassium channels have four-fold symmetry around their central pore (MacKinnon, 1991). This is typically accomplished upon tetramerization of identical or homologous subunits, although some channels are dimers or monomers in which two or four pore-forming domains are fused in tandem. The paradigmatic feature of all potassium channels is the eight amino acid potassium selectivity motif, TXXTXG(Y/F)G. The alignment of the peptide backbone carbonyls of the selectivity motif mimic the hydration shell of a potassium (K^+) ion, thus favorably dehydrating K^+ ions while excluding ions with smaller van der Waals radii, such as Na^+ or Li^+ (Doyle *et al.*, 1998; Roux and MacKinnon, 1999).

Potassium channels are broadly classified based on the number of transmembrane domains (TMD): 6-TMD voltage-gated (K_v) channels and 2-TMD inward-rectifying (K_{ir}) channels (Miller, 2000).

In voltage-gated channels—also known as *Shaker*-type channels after the first such channel identified in *Drosophila melanogaster* (Tempel *et al.*, 1987)—the selectivity filter is situated between TMD5 and TMD6. In addition, TMD4 is distinguished by highly conserved arginine or lysine residues at every third or fourth position along the transmembrane helix, which are essential for sensing transmembrane voltage and channel opening upon membrane depolarization (Figure 1). Calcium-gated potassium channels (K_{Ca}) are also 6-TMD-containing channels and have diverged from K_v channels, though some (notably "big current" or "BK" channels) retain voltage sensitivity. As their name implies, they are activated upon binding intracellular Ca^{2+} through various mechanisms (Vergara *et al.*, 1998; Ghatta *et al.*, 2006).

Inward-rectifying channels have a simpler structure of two TMDs flanking the selectivity filter (Hibino *et al.*, 2010) (Figure 1). They are presumably the basal clade of potassium channels with widely distributed homologues in both prokaryotes and eukaryotes (Loukin *et al.*, 2005). Their bias for inward over outward currents (in apparent violation of the Nernst equation) occurs via transient block by intercellular divalent cations, such as Mg^{2+} and polyamines (Lu and MacKinnon, 1994). However, in mammalian physiological settings, K_{ir} channels rarely encounter sufficient voltage to allow potassium influx and are usually efflux channels. The classical mammalian K_{ir} channels ($K_{ir}2.x$) are constitutively active—*i.e.* they have a high open probability (P_o) and are regulated primarily by the amount of protein at the cell surface—while other classes have a low P_o until activated by G-proteins (*e.g.*, $K_{ir}3.x$) or intracellular nucleotides (*e.g.*, K_{ATP} or $K_{ir}6.x$) (Hibino *et al.*, 2010).

Mammalian cells also express tandem pore domain channels, or K_{2P} channels, which appear to be the product of a gene fusion event (Figure 1). K_{2P} channels are responsible for very small "leak" currents that are voltage insensitive and non-rectifying. However, K_{2P} channels can still be gated by a variety of stimuli, such as membrane stretching or deformation, heat, and pH (Enyedi and Czirják, 2010).

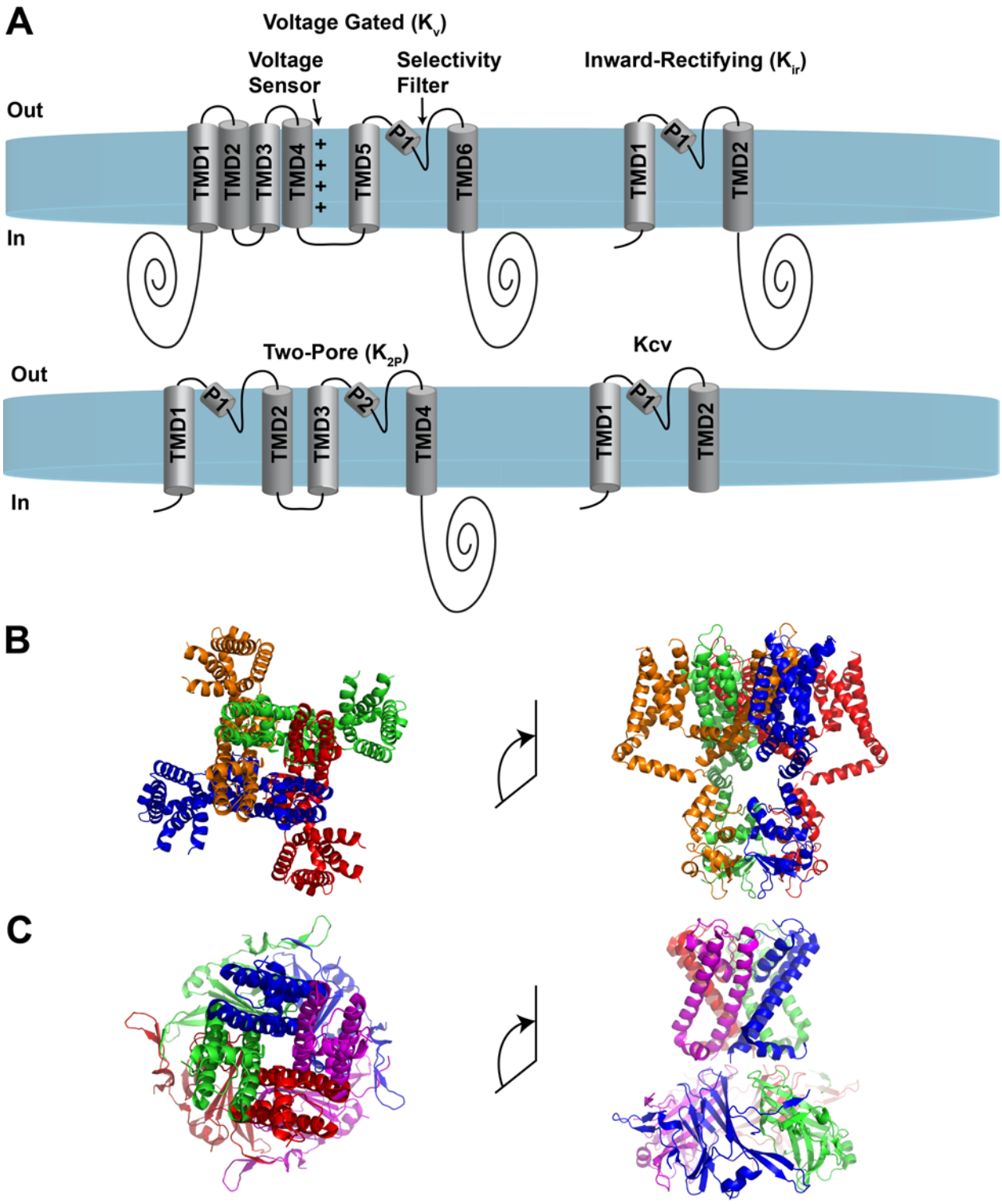

Figure 1: Topological and structural features of major potassium channel clades (A) Cartoon representation of the transmembrane topology and key functional features of several

subclasses of potassium channel monomers mentioned in this section. Note the universally conserved pore domain containing two TMDs, a pore (P) helix, and a selectivity filter. (B) Representative structures of mammalian *Shaker* (K_v1.2), a 6-TMD channel, and (C) bacterial KcsA, a 2-TMD channel, shown looking down the pore from the extracellular side (left images) and parallel to the membrane (right images). Both structures are homotetramers with individual polypeptides rendered in different colors. The *Shaker* structure is derived from PDB ID: 2A79 (Long *et al.*, 2005), and the KcsA structure is derived from PDB ID: 2WLM (Clarke *et al.*, 2010). All images were rendered in PyMol (v. 1.8.6).

Based on their activities, regulation, and distribution, potassium channels mediate a broad range of biological processes. For example, in humans they are involved in nerve conduction (Mathie and Veale, 2009), cardiac contraction (Sanguinetti and Tristani-Firouzi, 2006), hearing (Wangemann, 2006), maintenance of blood pressure (Wang *et al.*, 2010), immune responses (Cahalan *et al.*, 2001), and numerous other processes beyond the scope of this review. Moreover, polymorphisms in human potassium channels have been linked to dozens of genetic disorders affecting the nervous system, heart, kidneys, endocrine glands, and immune cells (see (Kim, 2014) for an extensive review of channelopathies). Unfortunately, investigating potassium channel activity, modulation, and biogenesis is often labor-intensive, especially in mammalian cells. The development of a rapid, genetically tractable model in which these studies can be conducted has significantly aided our understanding of potassium channel physiology.

1.1.2 Potassium channels and potassium homeostasis in *S. cerevisiae*

The budding yeast *Saccharomyces cerevisiae* presents several properties that make it an attractive system in which to probe the function of potassium channels. First, genetic transformations are famously facile in *S. cerevisiae* as compared to other commonly-studied organisms. Second, strain libraries have been developed in which every gene in the yeast genome

has been deleted, can be conditionally deactivated, or is present at reduced copy. Third, these unicellular eukaryotes can be propagated on either solid or in liquid growth medium, so yeast numbers are eminently scalable and the organism is amenable to high-throughput manipulations. Fourth, lab strains can be transitioned between the haploid and diploid state, allowing for genetic recombination and analyses of recessive and dominant phenotypes. Fifth, the resting membrane potential in *S. cerevisiae* is believed to be high relative to mammalian cells (see below), thus driving inward cation currents. Finally, despite nearly a billion years of evolutionary separation from humans, the vast majority of subcellular processes that animate yeast are conserved. Therefore, insights from yeast research are often analogous to the cell biology of multicellular eukaryotes.

Plasma membrane alkali metal transport in *S. cerevisiae* is adapted to efficiently import potassium and exclude sodium from the cytosol (for a detailed review, see (Ariño *et al.*, 2010)) (Figure 2). In brief, the electromotive force for potassium influx is generated by the electrogenic plasma membrane proton ATPase Pma1. Transmembrane potential in yeasts is believed to be quite high due to the activity of this proton transporter, but is notoriously difficult to measure directly with electrophysiological methods due to the high rigidity of the yeast cell wall (Vacata *et al.*, 1981; Volkov, 2015). Pma1 is the most abundant plasma membrane protein in yeast and consumes ~20% of cellular ATP (Morsomme *et al.*, 2000).

The Pma1-dependent transmembrane potential provides the electromotive force for potassium uptake through two high-efficiency channels, Trk1 and Trk2 (Figure 2). Trk1 was identified as the primary avenue for potassium influx (Gaber *et al.*, 1988; Ko and Gaber, 1991) and its structure is quite distinct from mammalian potassium channels. Most prominently, the pore-forming unit is a single polypeptide consisting of four 2-TMD units, which together form a fourfold symmetric pore. Under most growth conditions, Trk1 is responsible for nearly all potassium influx, but it is not essential. Yeast lacking *TRK1* (*trk1Δ*) have slightly increased potassium requirements that nevertheless fall within the bounds of ordinary laboratory growth medium. These yeast survive due to the presence of Trk2, which is a Trk1 paralogue with a lower affinity for potassium and far lower expression in wild-type yeast. In contrast, doubly mutated *trk1Δ trk2Δ* yeast have a drastically increased requirement for potassium supplementation in growth medium, usually ~100 mM. That these yeast are able to survive at all speaks to the presence of a very low-affinity potassium uptake system, termed “non-specific

cation channel 1" (Nsc1) (Bihler *et al.*, 1998). The gene encoding this putative channel is as yet unidentified, and in fact may not even exist because potassium may leak into *trk1Δ trk2Δ* cells through various nutrient transporters. Indeed, mutations in hexose or amino acid transporters are a common cause of phenotypic reversion in *trk1Δ trk2Δ* yeast (Ko *et al.*, 1993; Wright *et al.*, 1997; Liang *et al.*, 1998). This can be prevented by propagating *trk1Δ trk2Δ* cells on high potassium medium up until the time that key experiments are conducted (section 1.1.6). Nevertheless, *trk1Δ trk2Δ* cells are hyperpolarized and are sensitive to low pH (Ko and Gaber, 1991), to alkali metals other than potassium (Bertl *et al.*, 2003), and to a variety of toxic cations such as hygromycin B (Madrid *et al.*, 1998).

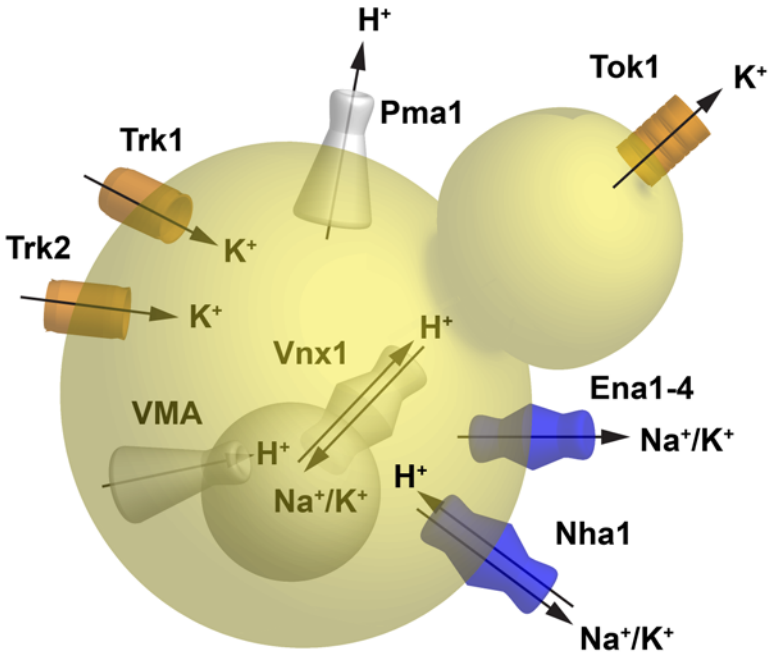

trk1Δ trk2Δ	Tolerates:	Sensitive to:
	-High K^+	-Low K^+
	-High pH	-Low pH
		-High Na^+/Li^+
		-High Cs^+
		-Toxic Cations

ena1-4Δ nha1Δ	Tolerates:	Sensitive to:
	-Low K^+	-High K^+
	-Low pH	-High pH
		-High Na^+/Li^+
		-High Cs^+

trk1Δ trk2Δ tok1Δ	Tolerates:	Sensitive to:
	-High K^+	-Low K^+
	-High Cs^+	-Low pH
	-High pH	-High Na^+/Li^+
		-Toxic Cations

Figure 2: Schematic of plasma membrane proton and alkali metal channels and transporters in *S. cerevisiae*. Native yeast channels and transporters mentioned in this text are shown here with representative ion currents. This figure has been adapted and simplified from previously published work (Ariño *et al.*, 2010). Select phenotypes of the potassium channel and transporter deletion strains mentioned in the text are shown to the right (Bañuelos *et al.*, 1998; Bertl *et al.*, 2003).

In addition to the Trk channels, *S. cerevisiae* express a voltage-gated outward-rectifying potassium channel, Tok1. Like K_v channels in animals, Tok1 opens upon membrane depolarization. However, Tok1 is neither essential nor does deletion of *TOK1* make *trk1Δ trk2Δ* yeast more sensitive to growth on low potassium medium; however, compared to *trk1Δ trk2Δ* yeast, the triple mutant strain exhibits increased tolerance to high cesium (Bertl *et al.*, 2003). In addition, whereas mammals lack Trk1 or Trk2 homologues, Tok1 is homologous to the vertebrate two-pore K_{2P} channels (Wolfe and Pearce, 2006). Therefore, select studies have utilized the *trk1Δ trk2Δ tok1Δ* potassium sensitive strain (section 1.1.7).

While potassium influx in yeast involves gradient-dependent passive transport through the Trk1 and Trk2 channels, potassium efflux under conditions of excess cytosolic potassium requires active transport. Yeast have two primary systems to expel excess alkali metals into the extracellular environment: the ENA (***e****xitus* ***na****tru*) uniporters and the Nha1 Na^+/H^+ antiporter (Figure 2). Although they primarily transport sodium, these systems are also able to export excess potassium (Bañuelos *et al.*, 1998). ENA uniporters are encoded as tandem repeats at a single locus on chromosome IV with high (~97%) conservation. The number of *ENA* isoforms varies among laboratory strains, with W3031-A having four copies and S288C having five. This may partially explain the observation that these two common laboratory workhorses differ in their tolerance to sodium and other cations (Petrezselyova *et al.*, 2010). Deletion of the *ENA* cluster renders yeast sensitive to both sodium and lithium. ENA expression is typically low but is strongly induced upon exposure to high sodium or lithium via the action of the osmoresponsive transcription factor Hog1 (Märquez and Serrano, 1996). In contrast, Nha1 is constitutively expressed at low levels and seems to play a housekeeping role in regulating intracellular potassium under low pH and in expelling the small quantities of Na^+ that enter through other transporters, such as the Na^+/PO_4^{3-} symporter Pho89 (Persson *et al.*, 1998). Both Nha1 and Ena1 promote growth in high K^+ medium, and a strain lacking both the *ENA* cluster (*ena1-4Δ*) and *NHA1* fail to propagate on high concentrations of potassium or any other alkali metal (Bañuelos *et al.*, 1998; Kinclová *et al.*, 2001).

Yeast are also capable of sequestering alkali metals in organelles, particularly the vacuole. Vnx1 is a vacuole-localized antiporter that can exchange vacuolar protons for cytosolic sodium or potassium (Cagnac *et al.*, 2007). Vnx1 likely plays an important role in detoxifying

the cytosol upon sodium stress as *vnx1Δ* yeast are sensitive to high sodium (Cagnac *et al.*, 2007) and the genomes of halotolerant fungi such as *Hortaea werneckii* contain multiple paralogues of *VNX1* (Plemenitaš *et al.*, 2016). While concentrating potassium in the vacuole can contribute to cellular turgor and help to balance the negative charge of vacuolar polyphosphate (Klionsky *et al.*, 1990), it is unclear whether the vacuole can function as a "strategic reserve" upon acute potassium starvation.

1.1.3 Discoveries with *trk1Δ trk2Δ* yeast

In the following subsections, I survey the many uses of *trk1Δ trk2Δ* yeast and then discuss several studies that have significantly aided our understanding of potassium channel function, regulation, biogenesis, and pharmacology. For the sake of brevity, I limit discussion to seminal studies, and the most recent findings. For further information, I direct the reader to the studies outlined in Table 1, which provides a more comprehensive list of discoveries in which exogenous potassium channels expressed in *trk1Δ trk2Δ* yeast played a key role.

Table 1: Select studies utilizing expression of an exogenous channel or transporter in *trk1Δtrk2Δ*, *trk1Δtrk2Δtok1*, or *ena1-4Δnha1Δ* yeast

Channel	Primary Method	Full Citation
$K_{2P}2.1$	Drug Screen	(Bagriantsev *et al.*, 2013)
$K_{ir}2.1$	Drug Screen	(Zaks-Makhina *et al.*, 2004)
$K_{ir}2.1$	Drug Screen	(Zaks-Makhina *et al.*, 2009)
$K_{ir}3.2$ (GIRK2)	Drug Screen	(Kawada *et al.*, 2016)
Akt1	Expression	(Sentenac *et al.*, 1992)
AKT2	Expression	(Cao *et al.*, 1995)
HIV-1 Vpu	Expression	(Herrero *et al.*, 2013)
Hkt1	Expression	(Schachtman and Schroeder, 1994)
Kat1	Expression	(Anderson *et al.*, 1992)
Kat1	Expression	(Schachtman *et al.*, 1992)
$K_{ir}2.1$	Expression	(Hasenbrink *et al.*, 2005)
$K_{ir}2.1$ (IRK1)	Expression	(Tang *et al.*, 1995)
$K_{ir}6.1/6.2$	Expression	(Graves and Tinker, 2000)

Table 1 (continued)		
K_v11.1 (hERG)	Expression	(Schwarzer *et al.*, 2008)
ORK1	Expression	(Goldstein *et al.*, 1996)
RhAG (not a Kchannel)	Expression	(André *et al.*, 2000)
SKD1,2 (Transporters)	Expression	(Perier *et al.*, 1994)
TcCat	Expression	(Jimenez and Docampo, 2012)
AKT1	Random Mutagenesis	(Ros *et al.*, 1999)
Hak5	Random Mutagenesis	(Alemán *et al.*, 2014)
HvHAK	Random Mutagenesis	(Mangano *et al.*, 2008)
Kat1	Random Mutagenesis	(Nakamura and Gaber, 2009)
Kat1	Random Mutagenesis	(Nakamura *et al.*, 1997)
Kat1	Random Mutagenesis	(Lai *et al.*, 2005)
KcsA	Random Mutagenesis	(Paynter *et al.*, 2008)
K_{ir}1.1 (ROMK)	Random Mutagenesis	(Paynter *et al.*, 2010)
K_{ir}2.1	Random Mutagenesis	(Cho *et al.*, 2000)
K_{ir}2.1	Random Mutagenesis	(Minor *et al.*, 1999)
K_{ir}3.2 (GIRK2)	Random Mutagenesis	(Yi *et al.*, 2001)
Ksv	Random Mutagenesis	(Chatelain *et al.*, 2009)
TRVP4	Random Mutagenesis	(Loukin *et al.*, 2010)
Kcv	Synthetic Biology	(Cosentino *et al.*, 2015)
K_{ir}1.1 (ROMK)	Synthetic Genetic Array	(Mackie *et al.*, 2018)
K_{ir}2.1	Synthetic Genetic Array	(Kolb *et al.*, 2014)
K_{ir}2.1	Trafficking assays	(Grishin *et al.*, 2006)
K_{ir}2.1 KCNK3 KCNK9	Trafficking assays	(Bernstein *et al.*, 2013)
K_{ir}3.2 (GIRK2)	Trafficking screening	(Bagriantsev *et al.*, 2014)
K_{ir}6.1	Trafficking assays	(Zerangue *et al.*, 1999)
Ksv	Trafficking assays	(Balss *et al.*, 2008)
K_{ir}1.1 (ROMK)	Trafficking assays	(O'Donnell *et al.*, 2017b)
K_{ir}2.1	Trafficking screening	(Shikano *et al.*, 2005)

1.1.4 Identification of uncharacterized potassium channels from cDNA libraries

The Gaber lab first noted the potential of exogenous potassium channels to substitute for the endogenous potassium uptake system in yeast (Ko and Gaber, 1991; Nakamura and Gaber, 1998), and numerous studies over the past two decades have exploited this phenotypic assay to identify novel classes of potassium channels from various organisms. By transforming cDNA

libraries into *trk1Δ trk2Δ* yeast and identifying clones that enable growth on low potassium media, researchers have identified new potassium channels rapidly and with minimal bias. This technique offers several advantages over traditional screens for new channels. In this case, cRNA libraries are injected into *Xenopus laevis* oocytes and then ion current is measured. This process must be reiterated several times with subdivided RNA pools. This labor-intensive protocol led to the identification of many potassium channels (see for example (Ho *et al.*, 1993)). In contrast, the yeast selection scheme is cheaper, there is no need for electrophysiology "rigs", and the isolation of positive clones does not require sequential subdivision of RNA pools and the isolation and amplification of unique clones because transformed yeast only express single clones. This technique has provided a particular boon for identifying potassium channels and transporters from the plant kingdom.

Potassium is a key macronutrient for plants that is absorbed from the soil through the root system and concentrated in cells to maintain cellular turgor. Because plants lack contractile tissues, potassium fluxes underpin various tropisms that allow them to respond to environmental stimuli (Dreyer and Uozumi, 2011). The first plant potassium channel, KAT1, was identified by coopting the *trk1Δ trk2Δ* growth phenotype on low potassium (Anderson *et al.*, 1992; Schachtman *et al.*, 1992). KAT1 is a *Shaker*-type voltage-gated channel with inward-rectifying properties, is highly expressed in guard cells, and its activation in response to hyperpolarization causes the stoma to swell and open. Dozens of subsequent studies have since identified previously unknown potassium channels and transporters in both model and crop plants, including AKT1, a strongly inward-rectifying potassium uptake channel in root hairs (Sentenac *et al.*, 1992; Hirsch *et al.*, 1998), as well as HKT, which was the first plant high-affinity potassium transporter identified (Schachtman and Schroeder, 1994) (see Table 1). Potassium transporters are functionally and morphologically distinct from potassium channels and as such fall outside the scope of this review, but they have also been extensively studied in yeast (see (Rodríguez-Navarro and Rubio, 2006) for review).

One limitation of this system bears mention. Full length K_v channels from animals are unable to rescue the growth of *trk1Δ trk2Δ* yeast on low potassium. This phenomenon arises due to the fact that mammalian K_v channels fail to open in the hyperpolarizing potential across the yeast membrane; in contrast, plant Kv channels open under these conditions, which is why KAT1 and other related channels could be isolated in yeast (Table 1). However, the K_v channel

rat *ether-à-go-go* Related Gene-1 (rEAG1) was able to restore growth in *trk1Δ trk2Δ* cells if the N-terminal 190 amino acids (*i.e.* the entire cytosolic N-terminal domain) were removed (Schwarzer *et al.*, 2008). This result, while potentially opening many doors for studying mammalian K_v channels in yeast, is puzzling as the N-terminal PAS domain of hERG, the human homologue of rEAG1, is necessary for channel activity in native systems (Gianulis and Trudeau, 2011). Fortunately, many mammalian K_{ir} channels function in *trk1Δ trk2Δ* and *ena1-4Δ nha1Δ* yeast: Of the 11 known human K_{ir} channels, 10 have been successfully expressed and are active in *trk1Δ trk2Δ* cells (D'Avanzo *et al.*, 2010). The first of these—and to date the most extensively studied—is the cardiac inward-rectifier $K_{ir}2.1$, which was originally called *IRK1* (Tang *et al.*, 1995) (see below).

New potassium channels can currently be predicted by *in silico* recognition of core features based on DNA sequence analysis. Nonetheless, *trk1Δ trk2Δ* yeast remain a valuable tool to validate the function of putative potassium channels detected in the ever-expanding collection of sequenced genomes. This approach is particularly useful for exotic potassium channels that lack the canonical potassium selectivity motif. Many of these non-canonical channels have been found in the genomes of viruses or intracellular parasites, such as *Trypanosoma cruzi* (Jimenez and Docampo, 2012).

Viroporins are small transmembrane proteins encoded in viral genomes that insert into the host cell plasma membrane, increase cell permeability, and play important roles in virion maturation and budding (Nieva *et al.*, 2012). Because they are exposed to the extracellular environment, viroporins are also attractive therapeutic targets. Expression of viroporins from various viral taxa in *trk1Δ trk2Δ* yeast established that these proteins function as potassium channels. Notable viroporins studied in this system include *Paramecium bursaria Chorella* virus-1 Kcv (Greiner *et al.*, 2011), human immunodeficiency virus-1 protein U (Vpu) (Herrero *et al.*, 2013), and porcine epidemic diarrhea virus ORF3 (Wang *et al.*, 2012a). Vpu lacks a canonical potassium selectivity motif, has a pentameric (rather than a tetrameric) pore structure, and only weakly selects potassium over other small monovalent cations, such as sodium and ammonium (Kukol and Arkin, 1999). In contrast, a potassium selectivity filter was predicted in Kcv based on its presence in a viral genome (Plugge *et al.*, 2000), even though Kcv is the smallest canonical potassium channel identified (each subunit is only 94 amino acids) and completely lacks a cytosolic C-terminal domain (Figure 1A) (Gazzarrini *et al.*, 2003).

1.1.5 Structure-function relationships via mutagenesis and genetic selection

Random mutagenesis has long been used as a rapid and nonbiased method to identify critical residues, motifs, and domains in ion channels. The approach may target specific regions, in which degenerate primer sets scramble a small segment of the coding sequence, or the entire coding sequence or a sizable portion thereof through error-prone PCR. Yeast are an ideal system for these studies as transformed yeast only uptake single clones, from which mutations can be quickly isolated and identified. In addition, homologous recombination can be used to join multiple linear DNA fragments, one of which can contain a mutagenized insert (created, for example, by PCR) and one that contains the expression plasmid, via direct transformation into recipient yeast strains (Weir and Keeney, 2014).

Targeted mutagenesis studies of KAT1 focused on the selectivity filter. The conserved "YG" site in the canonical selectivity filter TXXTXG**YG** was mutated to 400 possible combinations using a degenerate primer set (Nakamura *et al.,* 1997). While some conservative mutations of the tyrosine produced nominally functional channels with impaired selectivity (i.e., growth on low potassium in the absence of sodium), only the most conservative YG→FG mutation resulted in a fully selective channel that allowed growth of *trk1Δ trk2Δ* yeast on low potassium media in the presence of high sodium. When the residues flanking the selectivity motif were instead mutated, multiple mutations increased Na^+ exclusion, as evidenced by increased growth on low potassium as well as high sodium. Curiously, the mutations in the flanking region which led to increased Na^+ exclusion also allowed the transport of large toxic cations such as Cs^+ and triethylammonium (TEA) that normally block the channel. These data suggest that the entire pore region has evolved under dual selective pressure to exclude both larger and smaller cations than K^+ (Nakamura and Gaber, 2009).

While residues conferring selectivity are confined to a small but highly-conserved region in potassium channels, residues that regulate gating are often more broadly distributed. Jan and colleagues performed mutagenesis to determine the importance of the voltage-sensing TMD4 helix in relation to the pore forming domain in TMD5 in KAT1. Mutations in TMD5 that conferred a mild loss-of-function phenotype were isolated, and then random mutagenesis of TMD4 uncovered second-site suppressors, thus providing evidence of the close proximity of TMD4 and TMD5 particularly when the channel is in the open state (Lai *et al.,* 2005). Similar

studies from the same lab focused on identifying the gating mechanisms of mammalian K_{ir} channels. Specifically, TMD1 and TMD2 in $K_{ir}2.1$ were randomly mutagenized, and based on the relative tolerance of strains containing the mutated residues, the authors hypothesized that the TMDs of mammalian K_{ir} channels were more tightly associated than in bacterial Kcs channels based on structural work (Doyle *et al.*, 1998; Minor *et al.*, 1999).

Of the mammalian K_{ir} channels, $K_{ir}2.1$ is the most amenable to studies in *trk1Δ trk2Δ* yeast as it is highly expressed, traffics efficiently to the plasma membrane, and its open probability (P_o) is high (Minor *et al.*, 1999). In contrast, the G-protein-activated inward-rectifying potassium channel-2 (GIRK2, a.k.a. $K_{ir}3.2$) has a much lower P_o (~0.01). A random mutagenesis screen of the entire GIRK2 coding sequence identified five residues in the pore domain that are necessary for gating, and substitution at any of these positions increased the P_o independently of G-protein stimulation. The authors also identified a specific valine in TMD2 that plays a critical role during channel opening (Yi *et al.*, 2001).

1.1.6 Studies on potassium channel trafficking in the yeast model

The whole cell potassium conductance, which determines the potassium current for a given driving force, is the product of the single channel conductance, the open probability and the total number of channels at the surface membrane. Therefore, cells must tightly control the plasma membrane residence of ion channels by regulating synthesis, intramembrane trafficking, and degradation.

Like all classes of transmembrane proteins, potassium channels interface with the intramembrane trafficking machinery through specific amino acid motifs (Griffith, 2001). Most of these trafficking signals are short linear motifs, similar to “canonical” signals shared by a wide variety of membrane proteins, but they can also be found at the interface between two subunits (Ma *et al.*, 2011; Li *et al.*, 2016). ER-retention motifs are short linear motifs found on the cytosolic face of transmembrane proteins and promote retrograde transport from the Golgi apparatus to the endoplasmic reticulum (ER), thereby preventing cargo proteins from reaching the cell surface. One such motif is the di-arginine “RXR” motif that interacts directly with the coatamer (COPI) (Zuzarte *et al.*, 2009; Okamoto and Shikano, 2011) and becomes occluded as

the channel folds and assembles (Zerangue *et al.*, 1999). RXR was first characterized in $K_{ir}6.2$ and is present is many mammalian K_{ir} channels. Channels that lack this motif, such as $K_{ir}2.1$, are robustly trafficked to the plasma membrane in both yeast and mammalian cells (Grishin *et al.*, 2006). To identify novel ER exit/forward trafficking motifs that may override RXR, Shikano and colleagues fused a random peptide library to $K_{ir}2.1$-RXR and screened for increased channel activity in *trk1Δ trk2Δ* yeast. As a result of this analysis, the authors identified the "SWTY" motif as a 14-3-3 protein interactor (Shikano *et al.*, 2005). 14-3-3 proteins bind to phospho-serine/threonine motifs to regulate myriad processes (Muslin *et al.*, 1996; Kumar, 2017). In both yeast and multicellular eukaryotes, the -2 threonine of the "SWTY" motif must be phosphorylated to bind 14-3-3 proteins, and this phenomenon was demonstrated using both model substrates as well as naturally occurring proteins with SWTY-like sequences (Shikano *et al.*, 2005). In a similar study, novel modulators of GIRK2 ($K_{ir}3.2$) were identified by fusing either a peptide library that contained random 15 amino acid motifs flanked by a well-folded domain from *Staphylococcus aureus* protein Z, or a randomly mutagenized version of protein Z itself to either N- or C-terminus of GIRK2. This multi-pronged approach made for a more comprehensive screen by preventing bias against poorly folding peptides that are nonetheless strong positive regulators of GIRK2. As a result of this study, the authors identified a peptide that augments GIRK2 current by increasing plasma membrane residence (Bagriantsev *et al.*, 2014).

In contrast to the identification of embedded sequences that regulate potassium channel trafficking, genetic screens in yeast have also identified extragenic regulators of trafficking. This was accomplished through the use of synthetic genetic array (SGA) strategies (Tong and Boone, 2006) in which a genome-wide analysis can be performed to identify genes that when deleted alter the growth of potassium channel-expressing *trk1Δ trk2Δ* yeast on low potassium media (Figure 3). Based on the strength of the phenotype, the candidates can also be ranked.

The first instance in which an SGA was performed in yeast expressing a potassium channel used a targeted library of deletion strains lacking components associated with the early secretory pathway. The library was used to query yeast expressing a constitutively active GIRK variant ($K_{ir}3.2_{S177W}$) that increases Na^+ influx (Yi *et al.*, 2001). As a result of this phenotype, yeast growth was slowed on high sodium media. Therefore, isolated strains with increased growth on high sodium were hypothesized to lack a factor that promotes $K_{ir}3.2_{S117W}$ biosynthesis

and forward trafficking. The genes identified in this analysis were primarily involved in sphingolipid biosynthesis, which may facilitate channel opening at the plasma membrane (Epshtein *et al.*, 2009), and COPII vesicle cargo packing of GPI-anchored proteins, which may indirectly impact ER protein export. These data indicate a preeminent role of these pathways in K_{ir} channel biogenesis and function (Haass *et al.*, 2007).

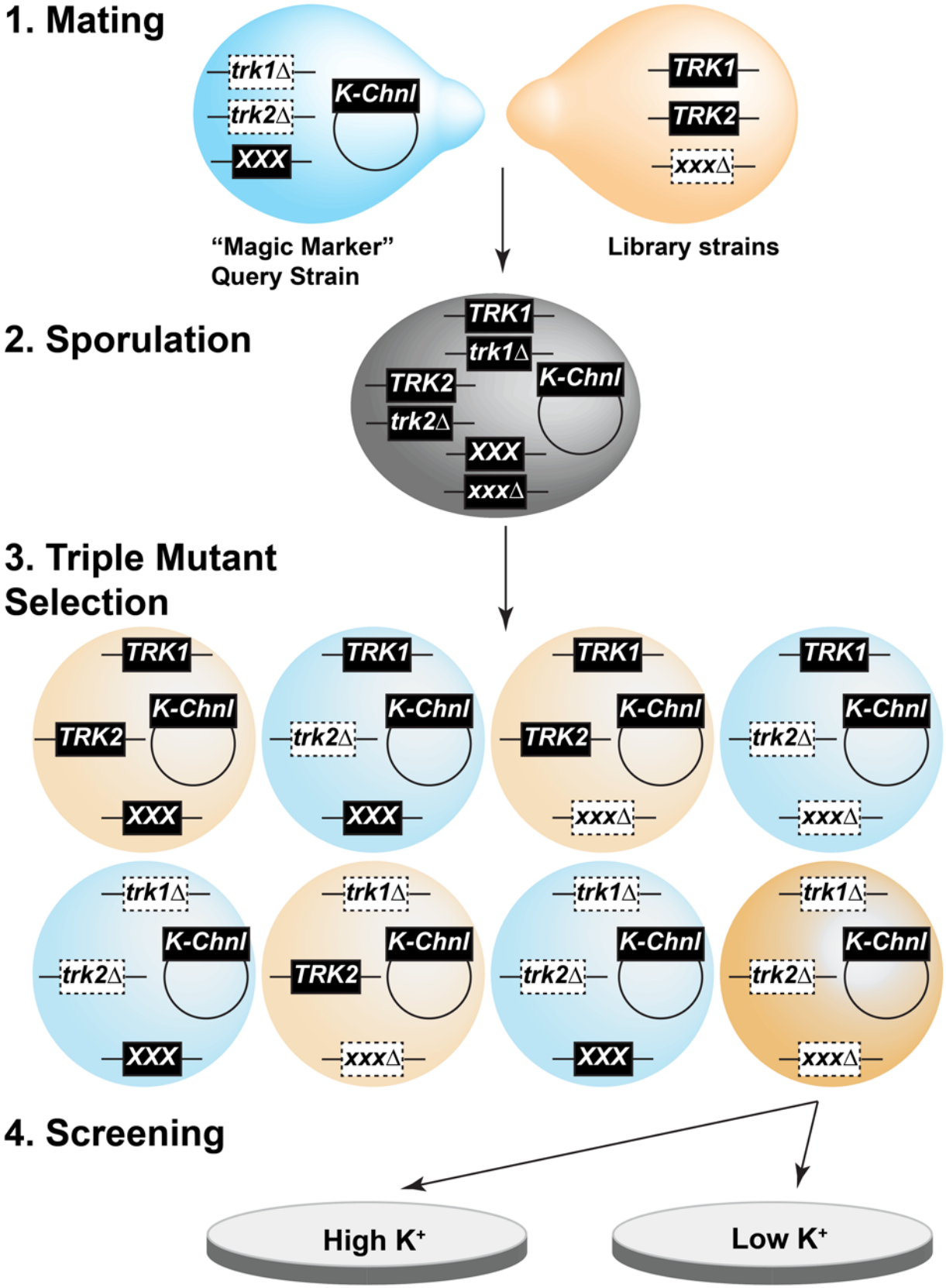
1. Mating
trk1Δ
trk2Δ
XXX
K-ChnI
TRK1
TRK2
xxxΔ
"Magic Marker"
Query Strain
Library strains
2. Sporulation
TRK1
trk1Δ
TRK2
trk2Δ
K-ChnI
XXX
xxxΔ
3. Triple Mutant
Selection
4. Screening
High K+
Low K+

Figure 3: Synthetic Genetic Array (SGA) technology to screen for potassium channel regulators (1) The "Magic Marker" yeast strain, which contains the *can1Δ* marker for dominant selection against diploid cells and *HIS3* under the control of the *STE2* promoter to select for *MAT**a*** haploids, is additionally deleted for *trk1Δ* and *trk2Δ.* This is strain is then transformed with a potassium channel ("*K-Chnl*") and mated to the yeast deletion library (*"xxxΔ*"). (2) Yeast colonies are transferred to selective media to propagate diploids, then onto low nitrogen media to induce sporulation. (3) Sporulated yeast are grown on a series of selective media to isolate *MAT**a*** haploid progeny harboring *trk1Δ trk2Δ* and the library hypomorph. All growth media in steps 1-3 should be supplemented with 100 mM K^+ to prevent intergenic suppression of potassium sensitivity. (4). Triple mutant ("*trk1Δ trk2Δ xxxΔ*") yeast are transferred to high and low potassium media and growth is assessed. See also Section 2.2.2.

Subsequent studies from the Brodsky lab have applied SGA to identify regulators of potassium channels with the entire non-essential gene library, which contains >5,000 gene knock-out strains. For this analysis, Dr. Alexander Kolb deleted *TRK1* and *TRK2* in the "magic-marker" SGA query strain (Tong and Boone, 2006), which resulted in slow growth on low potassium media. The strain was then transformed with a plasmid encoding $K_{ir}2.1$ and mated to each strain in the deletion collection. Yeast displaying increased growth on low potassium media were hypothesized to lack negative regulators of $K_{ir}2.1$. The result of this screen led to the isolation of yeast lacking genes encoding factors involved in vacuolar protein sorting (VPS) and several subunits of the endosomal complexes required for trafficking (ESCRT) (Kolb *et al.*, 2014). These data suggested that $K_{ir}2.1$, while primarily being targeted for destruction by the ER associated degradation (ERAD) pathway (see Section 1.2.2), is also routed to the vacuole for degradation; therefore, slowed vacuole-dependent degradation liberated additional $K_{ir}2.1$ channels at the plasma membrane, which facilitated growth on low potassium media. Consistent with this hypothesis, inhibition of the ESCRT pathway via knock-down strategies in human cells increased the steady-state pool of $K_{ir}2.1$. A second use of a yeast SGA to uncover regulators of potassium channel trafficking and stability is outlined in Chapter 2.

1.1.7 Pharmacological studies of potassium channels in yeast

As a large and functionally multifaceted class of proteins, potassium channels represent a wellspring of potential targets for new additions to the pharmacopoeia (Kaczorowski *et al.*, 2008; Wulff *et al.*, 2009). Drugs that regulate potassium channels have proved efficacious in clinical settings. For example, rosiglitazone, which stimulates insulin release from pancreatic β-cells through inhibition of K_{ATP} ($K_{ir}6.1$), has been used to treat diabetes and hypertension (Yu *et al.*, 2012), while retigabine, a potentiator of $K_v7.2/K_v7.3$ channels, has shown promise as an anti-epileptic (Ihara *et al.*, 2016). Conversely, the human *ether-à-go-go* related gene (hERG or $K_v11.1$) is a common nemesis of drug trials as it is inhibited by many structurally and functionally unrelated compounds due to its unusually promiscuous extracellular pore domain (Priest *et al.*, 2008). As hERG is critical for repolarization of the myocardium (*i.e.* the Q-T wave), hERG inhibition can lead to cardiac arrhythmia and sudden cardiac death. Therefore, there is an unmet need for drugs that target potassium channels that have been heretofore refractory to medicinal chemistry or that exhibit fewer side effects. To these ends, potassium channel pharmacology lends itself naturally to the *trk1Δ trk2Δ* system as molecules can be added directly to growth media to interact with the plasma membrane pool of potassium channels. As many of these compounds interact with the extracellular face of the channel pore, their efficacy is unlikely to be affected by *S. cerevisiae*'s well-known arsenal of multi-drug resistance ABC transporters.

In pioneering work, a library of >10,000 synthetic compounds was screened for their ability to inhibit $K_{ir}2.1$-mediated rescue of *trk1Δ trk2Δ* yeast as determined by the optical density of cultures in low potassium medium. From a list of preliminary hits, compounds were excluded that inhibited other potassium channels, such as GIRK2 or KAT1. Ultimately, a synthetic compound was found that blocked the ion conducting pore in $K_{ir}2.1$ and protected against potassium efflux-mediated caspase activation and apoptosis in primary cultured neurons (Zaks-Makhina *et al.*, 2004). A follow-up study using a natural products library identified gambogic acid as a potent and long-lasting inhibitor of $K_{ir}2.1$ that alters the interaction of the channel with the membrane microenvironment (Zaks-Makhina *et al.*, 2009). These screening techniques were then modified to find regulators of the mechano- and thermosensitive K_{2P} channel TREK-1 ($K_{2P}2.1$). K_{2P} channels are of broad interest in medicine due to their roles in pain, protection from

ischemia, migraine, and depression. By screening a library of >100,000 compounds in *trk1Δ trk2Δ* yeast that expressed TREK-1 and were grown in a variety of K^+ concentrations, one compound was identified that activates TREK-1 and its close relatives, but not more distantly related K_{2P} channels or other classes of potassium channels (Bagriantsev *et al.*, 2013).

In another successful application of this technology, the *KCNJ6* gene was used. *KCNJ6*, which encodes GIRK2 ($K_{ir}3.2$), is located on chromosome 21 in humans, and its duplication in trisomy-21 (Down syndrome) has been linked to cognitive impairment (Rachidi and Lopes, 2007). In a screen of >2000 compounds in GIRK-expressing *trk1Δ trk2Δ tok1Δ* yeast, proflavine and several derivatives were identified as voltage-dependent blockers of GIRK2 (Kawada *et al.*, 2016). It should be noted that the use of *trk1Δ trk2Δ tok1Δ* rather than *trk1Δ trk2Δ* allowed the authors to employ Cs^+ as a positive control for GIRK2 channel blockage. In each of the other drug screens a more pleiotropic positive control for cell death was used, such as SDS. In contrast, Cs^+ specifically targets the exogenously expressed potassium channels in *trk1Δ trk2Δ tok1Δ* yeast.

1.1.8 Synthetic biology and the future of potassium channel research in yeast

Potassium channels and other ion channels are critical to maintain homeostasis and allow for information transduction and stimuli response on much shorter timescales than any other biological process (Isacoff *et al.*, 2013). Due to their ion conducting properties and selectivity, potassium channels have attracted significant attention amongst synthetic biologists, who have endeavored to engineer novel gating mechanisms in potassium channels. Screens for neofunctionalized channels in yeast allow synthetic biologists to benefit from many of the same high-throughput molecular evolution techniques described thus far. For example, voltage sensitivity can be engineered into the Kcv channel upon fusion with a K_v-like voltage sensing domain from a phosphatase (Arrigoni *et al.*, 2013). More recently, a blue light activatable potassium channel was created by fusing the light-sensitive LOV2 module from an *Avena sativa* phototropin to the N-terminus of Kcv. Error-prone PCR mutagenesis was then used to identify clones that rescue growth of *trk1Δ trk2Δ* yeast on low potassium when activated by blue light.

The researchers then expressed this new potassium channel, termed blue light induced potassium channel-1 (BLINK1) in zebrafish embryos and found that their escape response reflex in response to touch was fully and reversibly inhibited upon exposure to blue light (Cosentino *et al.*, 2015). This study represents the first instance of an optogenetically controlled potassium channel and will enable the creation of transgenic animals expressing these photo-activatable potassium channels in specific neurons.

In the future, we envision continued use of the yeast screen for therapeutics, as many channel modulators lack desired specificity. Drugs are also needed for many other potassium channels, particularly those whose function increases the severity of various cancers (Huang and Jan, 2014). Moreover, we envision screens for modulators of mutated potassium channels for which treatments are currently lacking. For example, the expression of Bartter Syndrome mutant forms of ROMK, which are trapped in the early secretory pathway and degraded by ERAD (O'Donnell *et al.*, 2017a) (section 1.2.2), might respond to small molecule protein folding correctors. In fact, corrector molecules have proved to be efficacious treatments for other disease-causing mutated ion channels targeted for ERAD, such as CFTR (Van Goor *et al.*, 2011). A small molecule screen might uncover pharmacological chaperones which promote the folding of mutant ROMK and allow it to escape ERAD and other forms of protein quality control.

In sum, recent studies from multiple laboratories, spanning a wide breadth of disciplines, have demonstrated the continuing utility of a technique originally developed a quarter century ago. From the earliest identification of novel potassium channels before the genomic era to frontiers in molecular medicine and biotechnology, yeast screens have contributed significantly to our understanding of potassium channel biology. To date, a scan of the potassium channel literature demonstrates that most investigations have focused on a small group of channels—KAT1, $K_{ir}2.1$, GIRK—which are either isolated from highly studied model organisms or are intimately linked to human biology. However, this list barely scratches the surface of this diverse and ubiquitous class of biomolecules. In the upcoming decades, yeast-based assays will undoubtedly continue to serve in the vanguard of potassium channel science.

1.2 RATIONALE FOR STUDYING ROMK IN YEAST

The bulk of my research career at the University of Pittsburgh has been dedicated to elucidating the mechanisms involved in the cellular regulation of the renal outer medullary potassium (ROMK) channel ($K_{ir}1.1$). While many ion channels are believed to be partially regulated by protein quality control in both normal and diseases states, several biological and pragmatic considerations make ROMK an attractive system in which to answer these questions. Firstly, ROMK's physiological role of managing potassium concentrations in the extracellular fluid requires robust and rapid regulation, yet ROMK gating does not appear to be regulated since the channel has a constitutively high P_o (Choe *et al.*, 1999). In turn, transcriptional control is likely too slow to respond to the sudden spikes in extracellular potassium experienced upon consuming a high potassium meal. These considerations suggest the involvement of various post-translational avenues of regulation, but the exact mechanisms are still an area of active investigation. Secondly, polymorphisms in ROMK leading to a loss-of-function phenotype and cause an autosomal recessive condition known as Bartter Syndrome Type II. Furthermore, several of the disease-causing mutations lead to ROMK retention in the ER, hinting at the primacy of ER quality control in regulating the channel (Fallen *et al.*, 2009). Finally, ROMK is a mammalian K_{ir} channel, making it highly amenable to functional studies in yeast for the reasons enumerated in the preceding section. At its inception, my project built on the experimental designs and genetic toolkit constructed by a previous graduate student in the Brodsky lab, Dr. Alexander Kolb, to assay negative regulators of $K_{ir}2.1$ (Section 1.1.6) (Kolb *et al.*, 2014). As ROMK and $K_{ir}2.1$ are 42% identical, I reasoned that I could adapt these methods to study ROMK regulation in the yeast model.

1.2.1 The renal outer medullary potassium (ROMK) channel

While potassium is the most abundant cation in the human body, comprising about 0.4% of our total mass (Frausto da Silva and Williams, 2001), it is primarily sequestered intracellularly with extracellular concentrations maintained at ~4.5 mM in healthy individuals. It has long been understood that one of the primary functions of the mammalian kidney is to excrete excess

potassium following a high potassium meal. Accordingly, hyperkalemia is a major contributor to mortality and morbidity among individuals with chronic kidney disease (Einhorn *et al.*, 2009; Rodan, 2016).

ROMK was the first K_{ir} gene identified in mammals (Ho *et al.*, 1993) and is primarily expressed in two distinct distal segments of the nephron: the thick ascending limb (TAL) of the Loop of Henle and the cortical collecting duct (CCD). It is expressed as two nearly identical major isoforms via alternative splicing of the *KCNJ1* locus; ROMK1 has 19 more amino acids at its N-terminus than ROMK2. Although the functional consequences of alternative splicing are unclear, the two isoforms are expressed in different nephron segments and as such have divergent physiological roles (Figure 4). ROMK2 is constitutively expressed in the TAL, where it plays an important role in sodium balance and urinary concentration. In this segment, ROMK2 allows potassium to cycle so that sodium can be efficiently reabsorbed by the sodium/potassium/chloride cotransporter (NKCC2) (Welling and Ho, 2009). In contrast, ROMK1 is expressed more distally in the nephron in the CCD where it provides a means to secrete excess extracellular potassium into the pro-urine in response to changes in dietary intake. Accordingly, ROMK1 expression and activity in the CCD respond to a variety of regulatory stimuli (reviewed in Section 3.1.1) while ROMK2 expression and activity are maintained at a constant level.

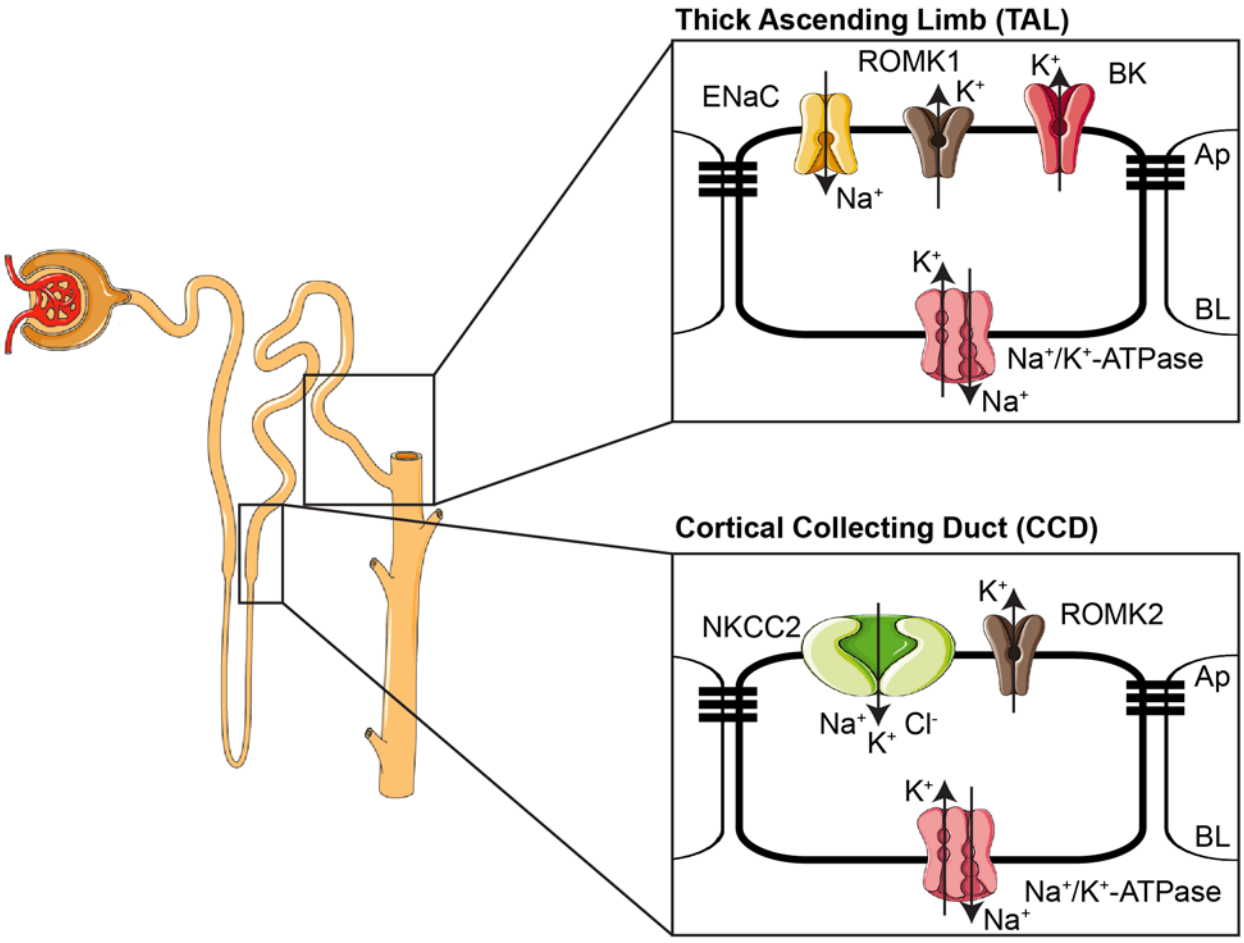

Figure 4: Major electrolyte channels and transporters in two segments of the distal nephron Polarized renal epithelium in the TAL and CCD is shown with cartoon representations of the primary ion channels and transporters mentioned in the text. The apical (Ap) surface faces the tubular lumen while the basolateral (BL) surface faces the extracellular fluid. All illustrations are taken from Servier Medical Art (https://creativecommons.org/licenses/by/3.0/legalcode).

ROMK is not essential, though ROMK$^{-/-}$ mice exhibit polyuria, natriuresis, and kaliuresis (Lu *et al.*, 2002). Potassium efflux from the distal nephron can also occur via BK channels. BK ($K_{Ca}1.1$) is expressed throughout the nephron and is upregulated in response to elevated aldosterone (Rieg *et al.*, 2007). BK currents are activated by increased tubular flow, which

explains why ROMK$^{-/-}$ mice exhibit kaliuresis. Although BK and ROMK are capable of compensating for each other when one channel is blocked or defective, it is believed that both contribute to potassium efflux in healthy kidneys (Rieg *et al.*, 2007).

As one of the most consequential cation channels in the renal epithelium, ROMK mediates two functions—constitutive reabsorption of sodium and selective excretion of potassium—critical to the survival of land animals (Rossier *et al.*, 2015). While potassium is abundant in many plant-based foods, over 90% of ingested potassium must be excreted in order to prevent fatal hyperkalemia (Rodan, 2016). Conversely, sodium is usually limiting in terrestrial environments, thus our kidneys have evolved to conserve sodium. Hypertensive patients have long been counselled to curb their sodium intake, however a study of over 100,000 individuals in 18 countries found that blood pressure is most strongly correlated not with gross sodium intake but rather with the ratio of sodium to potassium in the diet (Mente *et al.*, 2014).

As mentioned in Section 1.1.1, mutations in potassium channels give rise to a range of human diseases, and ROMK is no exception. As of this writing, over 50 loss-of-function mutations in ROMK—distributed evenly throughout the primary sequence—have been linked to the autosomal recessive disease Type II Bartter syndrome. The Bartter syndromes are a group of diseases caused by mutations in various components of the sodium reabsorption system in the distal nephron (Fremont and Chan, 2012), in which ROMK2 plays a critical role (see above). In addition to hyponatremia, Type II Bartter Syndrome is also characterized by potassium misregulation due to the central role of ROMK1 in mediating potassium efflux. Type II Bartter syndrome typically presents prenatally as polyhydramnios and can be diagnosed in neonates as polyuria, hypercalciuria, and hyperkalemia (Simon *et al.*, 1996a; Bhat *et al.*, 2012; Fremont and Chan, 2012). The initial acute hyperkalemia progresses to chronic hypokalemia due to the compensatory effects of flow-activated BK channels. Type II Bartter syndrome patients typically experience growth and developmental defects due to the pleiotropic effects of chronic electrolyte imbalance. Assuming that a competent diagnosis is made early in life, some of these symptoms may be alleviated with dietary potassium supplementation and non-steroidal anti-inflammatory (NSAID) drugs; however hypercalciuria leads to nephrocalcinosis in many patients which invariably leads to renal failure (Puricelli *et al.*, 2010). Very few Type II Bartter syndrome patients survive past adolescence due to persistent hypotension and eventual renal failure (Shaer, 2001).

Type II Bartter syndrome is an exceptionally rare disease, estimated at roughly $1:10^6$ births, but since Bartter-associated polyhydramnios often leads to premature birth and subsequent infant mortality, the real number of cases is probably higher. An analysis of the sequenced genomes from the third cohort of the Framingham Heart Study (FHS) shows that known Bartter polymorphisms have a prevalence of 1:670 (all heterozygous) and correlate with reduced blood pressure that nonetheless falls well within the optimum range for healthy individuals (Ji *et al.,* 2008). Similar findings were reported for NKCC2 and the sodium chloride cotransporter (NCC): the targets, respectively, of the diuretics furosemide and thiazides. It is hypothesized that as this cohort ages, carriers of Bartter mutations will experience reduced mortality and morbidity due to hypertension-related conditions such as congestive heart failure and stroke.

The vital role of ROMK in regulating sodium reabsorption and therefore blood pressure, makes it an attractive target for novel antihypertensive therapeutics. Such drugs would theoretically not cause potassium-wasting as an off-target effect as is seen with furosemide and thiazides. Dr. Jerod Denton's research group at Vanderbilt University has identified novel ROMK channel blockers—VU590 and VU591—that appear to act by direct occlusion of the channel pore (Bhave *et al.,* 2011; Kharade *et al.,* 2017). A group at Merck Pharmaceuticals has also reported on a ROMK inhibitor that is structurally unrelated to the VU compounds, but seems to interact with the same residues in ROMK. As predicted, this compound induces potassium-sparing diuresis in a rat model (Tang *et al.,* 2016).

Overall, ROMK is central to our understanding of two diseases: one of which is devastating to newborn children and yet rare enough that many pediatricians will never see a case, and the other is the largest current burden on global health as measured by total disability-adjusted life-years (DALYs) lost (Murray and Lopez, 2013). In addition to its medical relevance, ROMK presented an attractive study system for studies in yeast since several lines of evidence suggested that cellular protein quality control pathways are employed to regulate ROMK in both normal and disease states.

1.2.2 Disease-causing ROMK mutants are delivered to the ERAD pathway

A study in *Xenopus laevis* oocytes and HEK293 cells examined 20 Type II Bartter Syndrome-causing mutations and found that 14 mutations (i.e. ~75%) abrogate channel export from the ER rather than directly affecting channel conductance (Peters *et al.*, 2003). In collaboration with Dr. Brighid O'Donnell, I hypothesized that many of these mutations compromise ROMK folding or tetramerization, which would trap the channels in the ER and target them for ERAD. Yeast and multicellular eukaryotes utilize ERAD to recognize and degrade misfolded proteins in both the ER lumen and the ER membrane (Vembar and Brodsky, 2008). As the ER lumen lacks a major degradative protease, the AAA+ ATPase Cdc48/p97 retrotranslocates substrates to the cytosol for degradation in the proteasome (Ye *et al.*, 2001; Jarosch *et al.*, 2002; Rabinovich *et al.*, 2002; Bodnar and Rapoport, 2017). Mutations in proteins that enter the secretory pathway, including several classes of ion channels, have been linked to several genetic diseases, many of which arise from protein misfolding and targeting for ERAD (Guerriero and Brodsky, 2012).

We chose to focus on four mutations which had been shown to cause ER-retention in the C-terminal β-sandwich immunoglobulin-like domain (IgLD) (Fallen *et al.*, 2009; Fang *et al.*, 2010). In addition, we hypothesized that mutations in the IgLD would be more likely to cause misfolding and subsequent ERAD. As the IgLD is the only β-sheet rich domain in ROMK, it likely represents a kinetic barrier to polypeptide folding (Fallen *et al.*, 2009; Beerten *et al.*, 2012). Mutations in cytosolic β-rich domains such as IgLDs are particularly deleterious for protein folding (De Angelis *et al.*, 2002; Randles *et al.*, 2006; Metzger and Michaelis, 2009), and my colleague in the Brodsky Lab, Dr. G. Michael Preston, has recently shown that destabilizing mutations in a β-rich domain of a model ERAD substrate increase its aggregation propensity (Preston *et al.*, 2018)

Working initially in the yeast model, Dr. Brighid O'Donnell and I found that four Bartter Syndrome mutations in the ROMK IgLD cause loss of function in *trk1Δ trk2Δ* yeast and that this phenotype was correlated with increased ERAD of the mutant proteins. We recapitulated increased ERAD of ROMK IgLD mutants in HEK 293 cells, thus establishing Bartter Syndrome Type II as an ERAD-linked channelopathy (O'Donnell *et al.*, 2017b). Through this study, and in agreement with prior studies from Dr. Paul Welling's group (Schwalbe *et al.*, 1998; Ortega *et al.*, 2000), we noted that wild-type ROMK is not appreciably degraded by ERAD in mammalian

cells. Therefore, it follows that the wild-type channel most likely relies instead on post-ER quality control for regulation and quality control.

1.2.3 Protein quality control in the secretory pathway

To understand the mechanisms of post-ER quality control, it is helpful to briefly summarize how eukaryotic cells traffic proteins from one organelle to another. The secretory and endocytic pathway quality control steps are visually represented in Figure 5.

The composition of the eukaryotic plasma membrane is controlled by the compensatory actions of the secretory and endocytic pathways. The genetic components of the secretory pathway were first identified using yeast forward genetics (Novick *et al.*, 1980) and have been elucidated in great mechanistic detail in subsequent decades (see (Schekman, 2010) for historical perspective). In brief, nascent polypeptides enter the secretory pathway through the ER translocon (Deshaies and Schekman, 1987; Stirling *et al.*, 1992). Those that are correctly folded, assembled, and modified are exported from the ER to the Golgi apparatus in COPII-coated vesicles (Zanetti *et al.*, 2012) and eventually unite to form a *cis*-Golgi cisterna. Secretory proteins receive further modifications as Golgi cisternae mature, eventually becoming concentrated and encapsulated into uncoated secretory vesicles in the *trans*-Golgi network (TGN) (Matsuura-Tokita *et al.*, 2006; Glick and Luini, 2011). These secretory vesicles then bud from the TGN and fuse with the plasma membrane. Coated vesicles also bud from the TGN and are transported to endosomes, allowing delivery of endosome or lysosome/vacuole resident proteins from the Golgi (Kienzle and von Blume, 2014). Note that this description represents a generalized portrayal of the secretory pathway, and drastic variations exist among different organisms and cell types. For example, neuronal dendrites are capable of routing secretory cargo through recycling endosomes, circumventing the Golgi altogether (Jensen *et al.*, 2014; Bowen *et al.*, 2017).

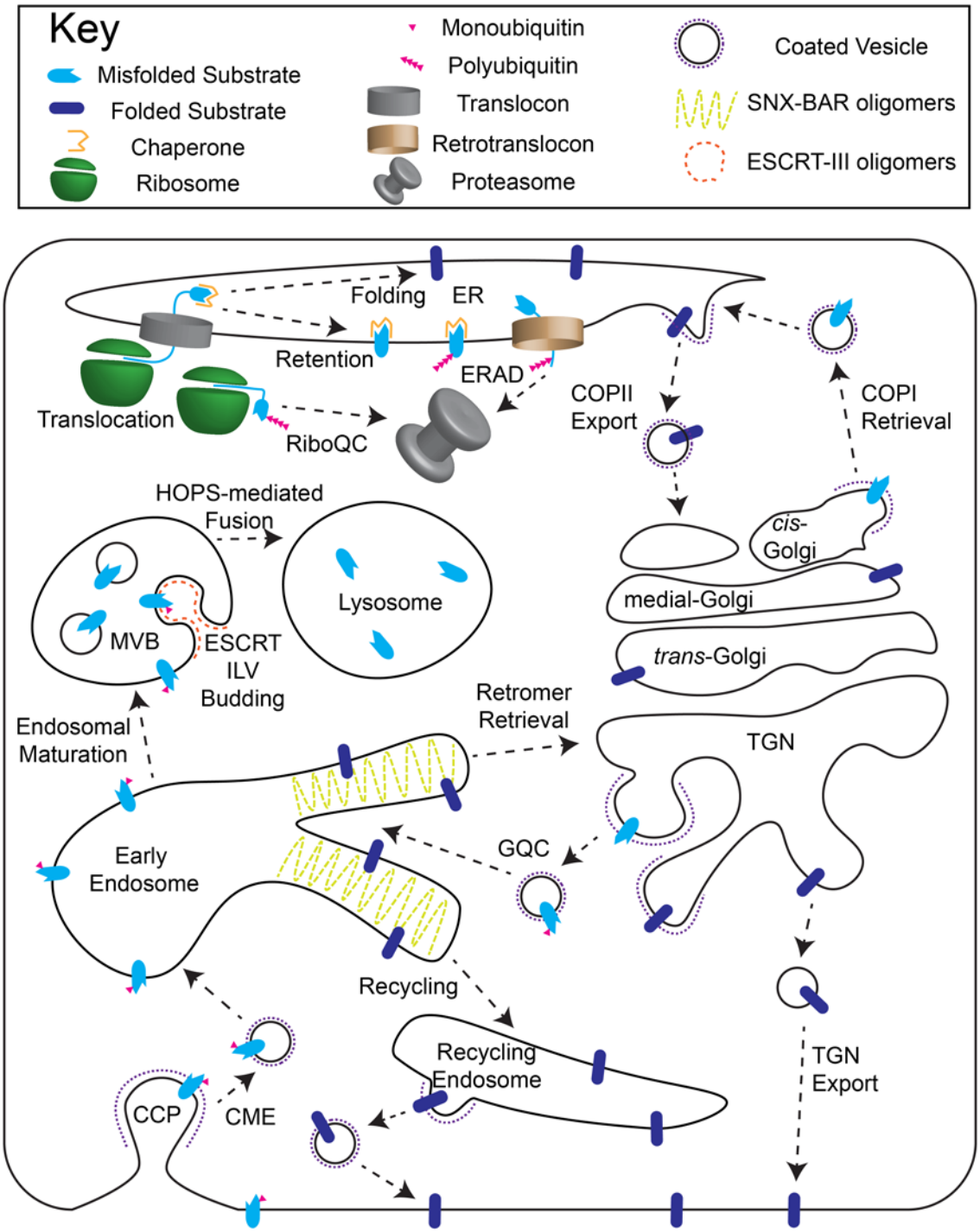

Figure 5: Quality control in the secretory and endocytic pathways. Cartoon representation of the secretory and endocytic pathways and their quality control branches in a generalized eukaryotic cell. Note that in *S. cerevisiae*, the Golgi cisternae do not form a cohesive stack as they do in mammalian cells. Also, yeast and other fungi have vacuoles in place of lysosomes.

Abbreviations: CCP—Clathrin Coated Pit, CME—Clathrin Mediated Endocytosis, COP—Coat Protein, ERAD—ER Associated Degradation, ESCRT—EndoSomal Complexes Required for Trafficking, GQC—Golgi Quality Control, ILV—IntraLumenal Vesicle, MVB—Multi-Vesicular Body, RiboQC—Ribosomal Quality Control, SNX—Sorting NeXin, TGN—*trans* Golgi Network.

The endocytic pathway retrieves proteins and membrane components from the plasma membrane and is broadly divided into clathrin-mediated (CME) (Pearse, 2000; McMahon and Boucrot, 2011) and clathrin-independent (CIE) endocytosis. Clathrin assembles spontaneously into a proteinaceous cage on the cytosolic side of a vesicle. Sites of endocytosis are readily visible in electron micrographs as electron-dense clathrin-coated pits (CCPs) (Ungewickell and Branton, 1981; Smith *et al.*, 1998) and a variety of scaffolding proteins will recruit transmembrane cargo to CCPs as a prelude to endocytosis. Endocytic vesicles eventually coalesce to form early endosomes. Proteins in these structures have three possible fates: recycling to the Golgi apparatus through sorting into SNX-BAR-sculped membrane tubules that branch off from early endosomes (Burd and Cullen, 2014; McNally *et al.*, 2017), direct recycling to the plasma membrane through specialized recycling endosomes (Grant and Donaldson, 2009; van Weering and Cullen, 2014), or degradation in the lysosome/vacuole (see below).

Although the diversity of factors which control protein trafficking may seem dizzying, all intramembrane trafficking follows a tidy set of principles that are conserved among pathways and among organisms:

1. Sites of vesicle budding are highly selective for particular substrates. Cargo selection machinery can recognize genetically encoded consensus sorting motifs as well as post-translational modifications such as ubiquitination or glycosylation.
2. Processes which bend membranes into pits or tubules occur through spontaneous protein oligomerization. However, membrane scission and vesicle uncoating require energy input in the form of ATP or GTP hydrolysis.

3. The membranes of various organelles are distinct and can be readily discriminated from each other by trafficking machinery to ensure that cargo is delivered to the correct destination. The Rab family of small GTPases plays a central role in this process.
4. Vesicle fusion to destination organelles is a two-step process. First, vesicles are loosely bound to their target membrane by multi-protein complexes known as tethers. Once the vesicle and target membrane are in close proximity, membrane fusion is mediated by the spontaneous multimerization of SNARE proteins, one on the vesicle membrane and three on the target (Ungar and Hughson, 2003).

Eukaryotes utilize three major quality control pathways: the ubiquitin-proteasome system (UPS), delivery to membrane-bound proteolytic organelles, such as the fungal vacuole or metazoan lysosome, and autophagy. All quality control pathways must select certain substrates for degradation and spare others. This enables cells to modulate their proteome in response to stress or stimuli and to eliminate misfolded proteins before they can damage the cell. Quality control pathways must also keep proteases sequestered from bulk cellular proteins and shuttle substrates destined for degradation to these sites of proteolysis. The common thread uniting all degradative pathways is ubiquitin. With very few exceptions, protein quality control pathways utilize ubiquitin as a tag for substrates destined for degradation (Kraft *et al.*, 2010; Shields and Piper, 2011; MacGurn *et al.*, 2012; Preston and Brodsky, 2017).

Proteins that transit the secretory pathway encounter quality control pathways at various stages in their maturation. Quality control begins with translation as nascent polypeptides can be co-translationally ubiquitinated in response to cellular stress, defective mRNA, or stalled translocation into the ER (Bengtson and Joazeiro, 2010; Brandman *et al.*, 2012; von der Malsburg *et al.*, 2015). Similarly, defective translocation into the ER can trigger cleavage of partially translocated proteins by the ER-resident protease Ste24 (Ast *et al.*, 2015).

ER quality control (ERQC) is built on the twin pillars of retaining incompletely folded substrates and degrading those that cannot achieve their native fold. The ER lumen is rich in chaperones and lectins that help newly synthesized proteins fold. Chaperone-bound proteins that have not assumed their native fold are excluded from COPII export vesicles (Ellgaard *et al.*, 1999). The ER lectins calnexin and calreticulin act as a kinetic brake by preventing ER export until the process of trimming and modifying core glycans is complete. Chaperone binding is also required to initiate ERAD. Therefore, secretory proteins that spend more time bound to

chaperones are more likely to be targeted for degradation (Vembar and Brodsky, 2008). ERAD is the preeminent quality control pathway in the early secretory pathway and the last opportunity to engage the UPS. ERAD is capable of degrading substrates that are misfolded (Xie *et al.*, 2009), that are improperly glycosylated (Bhamidipati *et al.*, 2005; Szathmary *et al.*, 2005) or lipidated (Fisher *et al.*, 2011), or that have not assembled into a functional complex (Mueller *et al.*, 2015). A number of metabolically controlled "wild type" proteins are also targeted for ERAD including proteins with broad relevance to human health such as HMG-CoA reductase—the rate-limiting enzyme in cholesterol biosynsthesis and the target of statin drugs—and apolipoprotein B (ApoB): the principal proteinaceous component of low-density lipoproteins and chylomicrons (Hampton and Rine, 1994; Zhou *et al.*, 1998).

While ribosomal QC and ERAD converge on the cytosolic proteasome, post-ER quality control converges on proteolytic compartments: the lysosome in animals and the vacuole in plants and fungi. Substrates that escape ERQC in COPII can be retrieved to the ER via Golgi-derived COPI-coated vesicles (Geva and Schuldiner, 2014; Briant *et al.*, 2017). In addition, the Golgi can reroute defective or unneeded plasma membrane-destined cargo to the lysosome/vacuole for degradation (Arvan *et al.*, 2002; Dobzinski *et al.*, 2015). As a means of disposing of misfolded proteins, Golgi quality control (GQC) is far more prominent in yeast than in metazoans, as the mechanisms of ER-retention are less stringent in yeast. Indeed, improperly folded proteins can "leak" into the Golgi, particularly under conditions of ER stress (Spear and Ng, 2003). Rerouting from the Golgi to the lysosome/vacuole also allows cells to respond to environmental stimuli by degrading plasma membrane proteins, such as nutrient transporters, that are no longer needed (Scott *et al.*, 2004).

Quality control at the plasma membrane depends on endocytosis to deliver substrates for lysosomal/vacuolar degradation. Endocytosis is often stimulated by substrate ubiquitination (Bonifacino and Weissman, 1998; Hicke and Dunn, 2003) that may result from direct interaction between E3 ligases with client proteins or may involve an intermediate scaffolding protein (Lin *et al.*, 2008). There is some evidence that the endocytic machinery is able to detect plasma membrane protein misfolding or aggregation and therefore constitutes a *bona fide* quality control mechanism (Arvan *et al.*, 2002; MacGurn, 2014). For example, a disease-associated misfolding mutation in CFTR causes rapid ubiquitin-dependent endocytosis of the channel when cells are shifted to a non-permissive temperature (Okiyoneda *et al.*, 2010).

Endocytic vesicles fuse to form organelles called early endosomes or sorting endosomes. Substrate ubiquitination can occur at endosomes and both E3 ligases and adaptor proteins are known to be localized to endosomes (Shin *et al.*, 2001; Kim *et al.*, 2006; Mund and Pelham, 2009; Evangelinos *et al.*, 2016). Early endosomes have both vacuolar and tubular subdomains. In general, tubular endosomal domains are associated with cargo recycling while vacuolar subdomains are associated with degradation (van Weering and Cullen, 2014). It is believed that recycling from early endosomes is the default pathway for most cargo proteins and that only ubiquitinated cargo is sorted for degradation (Grant and Donaldson, 2009).

Delivery of cargo from early endosomes to late endosomes proceeds via a process of homotypic fusion mediated by the class-C vacuole-endosome transport (CORVET) complex. This transition is marked by increased acidification of the endosomal lumen, increased size due to homotypic fusion, and an exchange of Rab5 for Rab7. Late endosomes are also called multi-vesicular bodies due to the intralumenal budding of vesicles containing cargo destined for vacuolar/lysosomal degradation. The budding of these intralumenal vesicles (ILVs) is directed by the endosomal sorting complexes required for trafficking (ESCRTs). ESCRT differs from all other vesiculation and tubulation machinery discussed thus far as it induces concave rather than convex membrane curvature, however it follows a similar set of principles. ESCRT-0 is a soluble recognition factor that binds ubiquitinated substrates and directs assembly of the downstream complexes. ESCRT-I and ESCRT-II sequentially assemble on the late endosomal membrane by binding endosome-enriched phospholipid phosphatidylinositol-3-phosphate (PI3P). This leads to the recruitment of additional ubiquitinated substrates as well as ESCRT-III. The ESCRT-III subunits then oligomerize and bind membranes, inducing negative curvature and ILV invagination. Finally, an ATPase, Vps4, constricts the inward-budding vesicle and eventually directs membrane scission (Babst, 2005; Henne *et al.*, 2013). Vps4-mediated ILV scission is the final nail in the coffin for an ESCRT client as MVBs eventually fuse with the lysosome/vacuole through the action of the homotypic fusion and protein transport complex (HOPS) (Plemel *et al.*, 2011).

1.2.4 Goals of dissertation research

Unlike gated ion channels such as GIRK2 ($K_{ir}3.2$), which have a low P_o until activation by their effector (Yi *et al.*, 2001), ROMK has an invariably high P_o of ~0.9 under normal physiological conditions (Choe *et al.*, 1999). Therefore, as is the case for $K_{ir}2.1$ (Section 1.1.6), cells must rely on the protein trafficking pathways described above in order to fine tune gross potassium currents mediated by ROMK. At the onset of this work, no studies had attempted to identify and rank genetic factors that regulate ROMK in a systemic and genome-wide manner. In addition to providing a comprehensive picture of the ROMK genetic interaction network, this study aimed to identify key ROMK regulators that may be potential targets for novel therapeutics for Type II Bartter syndrome or hypertension.

Given the ability to perform genome-wide screens for K_{ir} channel effectors in yeast, I decided to perform a yeast SGA screen (Kolb *et al.*, 2014) (Section 1.1.6) in order to better define the ROMK trafficking pathway. I then conducted follow-up experiments in the yeast system as most major protein quality control and membrane trafficking pathways in human cells were first discovered in yeast (Robinson *et al.*, 1988; Kaiser and Schekman, 1990; Tsukada and Ohsumi, 1993; McCracken *et al.*, 1996; Xie and Varshavsky, 1999). In order to confirm the relevance of key findings in a more physiologically relevant system, I ultimately recapitulated select experiments in mammalian cells in culture. Based on these efforts, I discovered that the endosomal sorting pathways regulate ROMK residence at the plasma membrane in both yeast and mammalian cells.

2.0 THE ENDOSOMAL SORTING FACTORS ESCRT AND CORVET SUPPRESS PLASMA MEMBRANE RESIDENCE OF THE RENAL OUTER MEDULLARY POTASSIUM CHANNEL (ROMK)

The contents of this chapter are adapted from two recently published articles appearing in the *Journal of Biological Chemistry* (O'Donnell *et al.*, 2017b; Mackie *et al.*, 2018). The figures and text have been edited for clarity and flow.

2.1 INTRODUCTION

Protein quality control allows cells in all organisms to survive proteotoxic stresses and fine-tune their proteome in response to environmental changes (Balchin *et al.*, 2016). Significant recent work has elucidated in great detail how protein quality control pathways operate in the cytoplasm and in the endoplasmic reticulum (ER) (Ellgaard *et al.*, 2016; Gottschling and Nyström, 2017; Preston and Brodsky, 2017). Common to both pathways is the delivery of substrates to the cytoplasmic proteasome, which selectively degrades ubiquitinated and misfolded protein substrates (Schmidt and Finley, 2014). In addition, proteins that reside in the ER or in the ER membrane must be removed from this compartment and delivered to the proteasome. The selection, delivery, and degradation of misfolded proteins in this compartment proceeds through the ER associated degradation (ERAD) pathway. Quality control "decisions" that operate at later steps in the secretory pathway, such as in the Golgi apparatus, the endosome, and the plasma membrane, have also been identified in eukaryotic cells (Arvan *et al.*, 2002; Geva and Schuldiner, 2014; MacGurn, 2014). However, the relative influence of each system on specific client proteins is rarely investigated.

One critical class of proteins that transit the secretory pathway—and that might be subject to more than one quality control checkpoint—are ion channels. Even under ideal circumstances, ion channels may possess unfavorable folding kinetics or are thermodynamically unstable because of dynamic structural transitions, and/or because charged and hydrophilic residues reside within their transmembrane domains (Gajewski *et al.*, 2011). Long-range interactions between channel domains or even between channel subunits further compromise folding efficiency (Lukacs and Verkman, 2012). Perhaps not surprisingly, genetic mutations that exacerbate protein misfolding result in degradation by cellular protein quality control pathways, including ERAD and the late secretory quality control pathways, (section 1.2.3) (Young, 2014). For example, the Cystic Fibrosis Transmembrane Conductance Regulator (CFTR) requires approximately 30 minutes from the onset of translation to reach its native conformation, during which ~70% of the wild-type channel is recognized as being misfolded and is targeted for ERAD (Lukacs *et al.*, 1994; Ward and Kopito, 1994). The predominant cystic fibrosis-causing allele, ΔF508, interferes with the assembly of a soluble domain that engages a transmembrane domain-containing segment (Mendoza *et al.*, 2012; Rabeh *et al.*, 2012) so essentially all of the mutant protein is degraded by ERAD. Moreover, even if the mutant is released to the plasma membrane, either through the application of chemical chaperones or by low temperature incubation, it is more rapidly endocytosed than the wild type protein and destroyed in the lysosome via plasma membrane quality control (Sharma *et al.*, 2004; Okiyoneda *et al.*, 2010, 2018). Furthermore, ΔF508-containing aggregates have been detected in cells, which may be selected for degradation in the lysosome via the autophagic pathway (Luciani *et al.*, 2010). Studies of multimeric ion channels, such as the voltage-gated potassium channel human *Ether-à-go-go* Related Gene (hERG), have found that subunit assembly can also present an energetic barrier during ion channel maturation (Li *et al.*, 2017). In addition, hERG mutants associated with long Q-T syndrome are degraded by ERAD in a chaperone- and proteasome-dependent manner (Gong *et al.*, 2005; Anderson *et al.*, 2006; Wang *et al.*, 2012b). Together, these data emphasize the inefficient nature of ion channel biogenesis and indicate that genetic, disease-causing mutations can interfere with protein folding in the secretory pathway.

In addition to CFTR and hERG, the impact of cellular quality control mechanisms in the regulation of other disease-associated ion channels has also been investigated (Anderson *et al.*, 2006; Hirota *et al.*, 2008; Gao *et al.*, 2012, 2013; Buck *et al.*, 2013; Donnelly *et al.*, 2013; Iwai *et*

al., 2013; Kolb *et al.*, 2014; Young, 2014; Seaayfan *et al.*, 2016). However, the rules that govern the quality control of diverse ion channels remain poorly defined. I propose that a continued investigation into the mechanisms underlying the biogenesis and degradation of ion channels will help uncover these rules and define how associated "channelopathies" might be treated.

To this end, I initiated studies on the homo-tetrameric Renal Outer Medullary Potassium (ROMK) channel, also known as $K_{ir}1.1$. ROMK is the primary potassium efflux channel in the thick ascending limb and distal nephron (Zhou *et al.*, 1994) and is expressed as two major isoforms with divergent physiological roles. ROMK2 is primarily expressed in the thick ascending limb of the loop of Henle and is responsible for potassium cycling coupled to sodium and chloride reabsorption through the sodium potassium chloride cotransporter, NKCC2. In contrast, bulk potassium secretion via ROMK1 occurs in the late distal convoluted tubule, connecting tubule, and cortical collecting duct, and ROMK1 expression is increased in response to dietary potassium intake (Wang *et al.*, 1990; Frindt *et al.*, 2009). Under physiological conditions, both ROMK isoforms have a high open probability (P_o) of ~0.9 (Ho *et al.*, 1993; Leung, 2000), so channel expression must be tightly regulated due to its vital role in regulating serum potassium levels. Indeed, ROMK function is thought to be regulated primarily through the homeostatic control of protein trafficking (Zeng *et al.*, 2002; Fang *et al.*, 2009; Lin *et al.*, 2009; Welling and Ho, 2009). In addition, mutations that deplete ROMK from the plasma membrane cause an autosomal recessive salt-wasting disorder known as Type II Bartter syndrome (Simon *et al.*, 1996b). Interestingly, individuals heterozygous for a Type II Bartter mutant allele exhibit resistance to hypertension, most likely because of decreased NKCC2-mediated reabsorption of sodium (Ji *et al.*, 2008). Of the >50 identified Bartter syndrome-associated mutations in ROMK, many appear to affect ROMK trafficking or post translational modification when ectopically expressed in *Xenopus laevis* oocytes (Peters *et al.*, 2003). To date, therapies for Bartter syndrome are not curative and patients require lifelong multi-drug treatments and potassium supplementation. Thus, a deeper understanding of the trafficking and degradative machineries that shepherd ROMK to and from the plasma membrane is necessary to devise effective treatments for type II Bartter syndrome.

In this study, I used the *trk1Δ trk2Δ* yeast to define the relative contributions of protein trafficking and two distinct quality control pathways on ROMK stability and plasma membrane residence. I conducted an SGA screen to monitor growth on low potassium as a readout for

genes that increase ROMK function at the plasma membrane. By screening the yeast non-essential deletion collection (Giaever *et al.*, 2002), I identified two complexes with established roles in post-endocytic trafficking that regulate the plasma membrane levels of ROMK: the endosomal complexes required for trafficking (ESCRT) and the class-C core vacuole/endosome tethering (CORVET) complex. I then confirmed the biological relevance of these complexes by silencing select ESCRT and CORVET homologs in human cells. These data provided the first genome-wide analysis of factors that control ROMK biogenesis, and my work may lead to the identification of components that, in principle, could be therapeutically modulated to treat disorders associated with ROMK function.

2.2 MATERIALS AND METHODS

2.2.1 Yeast strain construction, growth conditions, and plasmid construction

All strains were grown at 30°C unless indicated otherwise. Temperature sensitive strains were propagated at room temperature prior to temperature shift. Standard procedures were followed for propagation and transformation of yeast (Adams and Kaiser, 1998). Importantly, SC medium used in this study contained 1 g/L monosodium glutamate instead of ammonium sulfate as the primary nitrogen source as ammonium sulfate interferes with the efficacy of aminoglycoside antibiotics and was buffered with MES to a pH of ~4.5 (Kolb *et al.*, 2014). For serial dilution growth assays, 200 µl cultures were grown overnight with agitation in 96-well dishes in selective liquid medium supplemented with 100 mM KCl and covered with a Breathe-Easy polyurethane membrane (Sigma-Aldrich, St. Louis, MO) to prevent evaporation. Once all cultures reached stationary phase, they were serially diluted 1:5 five times to fill a grid in a standard 96-well plate. Droplets from each dilution were then transferred to SC-Leu solid medium supplemented with 100, 25, 10, and 0 mM KCl using a 48-pin manifold (Sigma-Aldrich, St. Louis, MO). These plates were incubated for 4 days and imaged on days two, three, and four using a BioRad (Hercules, CA) Image Station. Medium to which no potassium was added ("0 mM") has been estimated to contain 7-10 mM potassium (Nakamura and Gaber, 1998).

Table 2: Yeast strains used in this study

Strain	Relevant Phenotype	Source
trk1Δ trk2Δ (YAK01)	*MATα his3Δ leu2Δ ura3Δ trk1Δ::URA3 trk2Δ::NATMX can1Δ::STE2pr-HIS3*	(Kolb *et al.*, 2014)
trk1Δ trk2Δ vps23Δ	*MATa his3Δ leu2Δ ura3Δ trk1Δ::URA3 trk2Δ::NATMX can1Δ::STE2pr-HIS3 vps23Δ::KANMX*	(Kolb *et al.*, 2014)
BY4742 (PEP4 or *CDC48*)	*MATα his3Δ leu2Δ ura3Δ*	Invitrogen
pep4Δ	*MATα his3Δ leu2Δ ura3Δ pep4Δ::KANMX*	Invitrogen
cdc48-2	*MATα his3Δ, leu2Δ, ura3Δ, cdc48-2::KANMX*	(Moir *et al.*, 1982)
HRD1 DOA10	*MATα ade2, his3, leu2, ura3, trp1*	(Pagant *et al.*, 2007)
hrd1Δ doa10Δ	*MATα ade2 his3 leu2 ura3 trp1 hrd1::KANMX DOA10::KANMX*	(Pagant *et al.*, 2007)
SSA1	*MATα his3-11,15 leu2-3,112, ura3-52 trp1- Δ1, lys2, ssa2- 1(LEU2), ssa3-1(TRP1), ssa4- 2(LYS2)*	(Becker *et al.*, 1996)
ssa1-45	MATα, his3-11,15, leu2-3,112, ura3-52, trp1-Δ1, lys2, ssa1-45, ssa2-1(LEU), ssa3-1(TRP1), ssa4-2(LYS2)	(Becker *et al.*, 1996)
trk1Δ trk2Δ vps3Δ	*MATα his3Δ leu2Δ ura3Δ trk1Δ::URA3 trk2Δ::NATMX vps3Δ::KANMX*	This study
trk1Δ trk2Δ vps8Δ	*MATα his3Δ leu2Δ ura3Δ trk1Δ::URA3 trk2Δ::NATMX vps8Δ::KANMX*	This study
trk1Δ trk2Δ vps27Δ	*MATa his3Δ leu2Δ ura3Δ trk1Δ::URA3 trk2Δ::NATMX vps27Δ::KANMX*	(Kolb *et al.*, 2014)
trk1Δ trk2Δ vps36Δ	*MATα his3Δ leu2Δ ura3Δ trk1Δ::URA3 trk2Δ::NATMX vps36Δ::KANMX*	This study
trk1Δ trk2Δ vps20Δ	*MATα his3Δ leu2Δ ura3Δ trk1Δ::URA3 trk2Δ::NATMX vps20Δ::KANMX*	This study
trk1Δ trk2Δ snf7Δ	*MATα his3Δ leu2Δ ura3Δ trk1Δ::URA3 trk2Δ::NATMX snf7Δ::KANMX*	This study
trk1Δ trk2Δ end3Δ	*MATα his3Δ leu2Δ ura3Δ trk1Δ::URA3 trk2Δ::NATMX end3Δ::KANMX*	This study
trk1Δ trk2Δ pep12Δ	*MATα his3Δ leu2Δ ura3Δ trk1Δ::URA3 trk2Δ::NATMX pep12Δ::KANMX*	This study
trk1Δ trk2Δ gos1Δ	*MATα his3Δ leu2Δ ura3Δ trk1Δ::URA3 trk2Δ::NATMX can1Δ::STE2pr-HIS3 gos1Δ::KANMX*	This study
trk1Δ trk2Δ bsd2Δ	*MATα his3Δ leu2Δ ura3Δ trk1Δ::URA3 trk2Δ::NATMX bsd2Δ::KANMX*	This study
trk1Δ trk2Δ vps5Δ	*MATα his3Δ leu2Δ ura3Δ trk1Δ::URA3 trk2Δ::NATMX vps5Δ::KANMX*	This study

Table 2 (continued)		
trk1Δ trk2Δ vps35Δ	*MATα his3Δ leu2Δ ura3Δ trk1Δ::URA3 trk2Δ::NATMX vps35Δ::KANMX*	(Kolb *et al.*, 2014)
RSP5	*MATa his3 lys2 trp1 ura3 prc1::TRP1 rsp5::HIS3 leu2::RSP5:LEU2 bar1::HIS3*	(Dunn and Hicke, 2001)
rsp5-2	*MATa his3 lys2 trp1 ura3 prc1::TRP1 rsp5::HIS3 leu2::rsp5-2:LEU2 bar1::HIS3*	(Dunn and Hicke, 2001)
trk1Δ trk2Δ vps23 Δnhx1Δ	*MATα his3Δ leu2Δ ura3Δ trk1Δ::URA3 trk2Δ::NATMX vps23Δ::KANMX nhx1Δ::KANMX*	This study
trk1Δ trk2Δ vps23Δ vps5Δ	*MATα his3Δ leu2Δ ura3Δ trk1Δ::URA3 trk2Δ::NATMX vps23Δ::KANMX vps5Δ::KANMX*	This study
trk1Δ trk2Δ vps23Δ rcy1Δ	*MATα his3Δ leu2Δ ura3Δ trk1Δ::URA3 trk2Δ::NATMX vps23Δ::KANMX rcy1Δ::KANMX*	This study
Snf7-RFP	*MATα his3Δ1 leu2Δ0 lys2Δ0 ura3Δ0 Snf7-RFP::KANMX*	(Huh *et al.*, 2003)

Rat ROMK1 was tagged with an HA epitope in the extracellular loop as previously reported (Yoo *et al.*, 2003), and the S44D and K80M mutations were introduced as recently described (O'Donnell *et al.*, 2017b). All yeast ROMK expression in this study utilized the strong constitutive *TEF1* promoter and the *CYC1* terminator (Mumberg *et al.*, 1995). The manually curated *trk1Δ trk2Δ xxxΔ* strains originating from this study were made using standard mating, sporulation, and tetrad dissection techniques (Adams and Kaiser, 1998). The genotypes of all parental strains originating from the Yeast Knockout Collection were confirmed by colony PCR prior to mating with YAK01 using the primers indicated in Table 3.

The Venus-ROMK$_{K80M}$ expression vector was made by subcloning the gene encoding ROMK2 into the mVenusC1 (Koushik *et al.*, 2006) expression vector with the restriction enzymes Kpn1 and Acc1. PCR amplification and site-directed mutagenesis were then used to make the Lys→Met mutation analogous to K80M in ROMK1 and to flank Vn-ROMK with XmaI and XhoI restriction sites. These enzymes were then used to subclone Vn-ROMK into the yeast expression vector pRS415.

Table 3: Oligonucleotides used in this study

Name	Purpose	Sequence (5'-3')
KanB	Confirm all strains deleted with KANMX	ctgcagcgaggagccgtaat
Vps3_Ext_Fwd	Confirm deletion of *VPS3*	gacagagaatctaggctgtc
Vps3_Int_Rev	Confirm deletion of *VPS3*	tgaggtgaggattcgctatc
Vps8_Ext_Fwd	Confirm deletion of *VPS8*	ggtgtagggagttatggtgg
Vps8_Int_Rev	Confirm deletion of *VPS8*	aagttgtccatgagactacgg
Vps36_Ext_Fwd	Confirm deletion of *VPS36*	ggcgtagcgacatattaagaag
Vps36_Int_Rev	Confirm deletion of *VPS36*	cgcacttttaccaagttcatc
Vps20_Ext_Fwd	Confirm deletion of *VPS20*	gacttggaataacctgtggg
Vps20_Int_Rev	Confirm deletion of *VPS20*	acttctaggatcgccctatc
Snf7_Ext_Fwd	Confirm deletion of *SNF7*	gacaacgatggagttccgtaac
Snf7_Int_Rev	Confirm deletion of *SNF7*	cgccattactttattgcccttcg
Pep12_Ext_Fwd	Confirm deletion of *PEP12*	ccctttctcacacagtggcatc
Pep12_Int_Rev	Confirm deletion of *PEP12*	ctatctttgccacagatctc
Gos1_Ext_Fwd	Confirm deletion of *GOS1*	gctccgaatgtgcatttcacag
Gos1_Int_Rev	Confirm deletion of *GOS1*	gattacatcctgtctctggcc
Bsd2_Ext_Fwd	Confirm deletion of *BSD2*	ccggagatgtaaataaccgtgg
Bsd2_Int_Rev	Confirm deletion of *BSD2*	tgcttccctcgtcctctatg
Vps5_Ext_Fwd	Confirm deletion of *VPS5*	cggaagttgtccgctaagaac
Vps5_Int_Rev	Confirm deletion of *VPS5*	gtctttccattctggcgcac
Nhx1_Ext_Fwd	Confirm deletion of *NXH1*	ctagctactctaagataaagggc
Nhx1_Int_Rev	Confirm deletion of *NHX1*	cttgattcaactcgtacccac
Vps23_Ext_Fwd	Confirm deletion of *VPS23*	ggacgcgcagagagttagta
Vps23_Int_Rev	Confirm deletion of *VPS23*	gtcagagtgcgtaaataccc
Venus_BamHI_Fwd	Construction of pRS415 Vn-ROMK$_{K80M}$ plasmid	catcatggatccatggtgagcaagggcgagga
ROMK_SmaI_Rev	Construction of pRS415 Vn-ROMK$_{K80M}$ plasmid	catcatcccgggttacattttggtgtcatctgtttca
YangP1	Construction of pRS415-Vn-ROMK$_{K80M}$ plasmid	gctggacctgaaatggaggtacatgatgaccgtgttcatcac
YangP2	Construction of pRS415-Vn-ROMK$_{K80M}$ plasmid	gaaggctgtgatgaacacggtcatcatgtacctccatttcag
TSG101 siRNA 1	Silencing *TSG101*transcript	CCAAAUACUUCCUACAUGCdtdt
TSG101 siRNA 2	Silencing *TSG101*transcript	CCGUUUAGAUCAAGAAGUAdtdt
HGS siRNA 1	Silencing *HGS* transcript	GAACCCACACGUCGCCUUGdtdt
HGS siRNA 2	Silencing *HGS* transcript	GAGGUAAACGUCCGUAACAdtdt
VPS8 siRNA 1	Silencing *VPS8* transcript	GCAUCUUCACCUAUACUAUdtdt
VPS8 siRNA 2	Silencing *VPS8* transcript	GCACUUUGGUUUCCGUUAUdtdt

2.2.2 Synthetic genetic array screening conditions

All screening procedures and media recipes were adapted from protocols published by the Boone lab (Tong and Boone, 2006), utilized the *trk1Δ trk2Δ* strain, and contained a plasmid designed for ROMK1$_{S44D+K80M}$ expression (see above). All yeast manipulations utilized a metal 96-pin manifold (V&P Scientific, San Diego, CA) except for the final transfer onto permissive and selective medium, which used a disposable plastic 96-pin manifold. Briefly, the query strain (YAK01) transformed with the ROMK1$_{S44D+K80M}$ expression vector was mated with the MAT**a** deletion collection (Invitrogen) on YPD plates grown overnight at room temperature. Diploids were selected with SC-Leu containing 200 µg/L G418 (Research Products International, Mount Prospect, IL), 100 µg/L clonNAT (Werner BioAgents, Jena, Germany), and 100 mM KCl to maintain potassium sensitivity and hinder the appearance of suppressor mutations. These plates were incubated for 2 days. The diploids were then sporulated onto nitrogen-deficient medium for 5 days at room temperature, and the tetrads were transferred onto SC medium lacking leucine, arginine, histidine, and uracil but containing 200 µg/L G418, 100 µg/L clonNAT, and 50 µg/L L-canavanine (Sigma-Aldrich) in order to select for desired spores and against unsporulated diploids and undesired spores. Cells on this selective medium were incubated for 2 days, and this step was repeated two times but with 1 day incubations. Finally, the array of triple mutant haploid MAT**a** cells lacking *TRK1, TRK2,* and one other unique non-essential gene were transferred to SC-Leu supplemented with 100 mM KCl and SC-Leu with no additional KCl ("0 mM" potassium). Growth on these plates was assessed by imaging them after 12, 24, and 36 hr using the white light setting on a BioRad image station. Rescreening of hits was performed as described above, but with the additional step of transferring the array of triple mutant haploids into 100 µl of liquid SC-Leu medium supplemented with 100 mM KCl in a 96-well dish after the third selection step. These cultures were grown to saturation overnight, then droplets of liquid culture were transferred onto 0 mM and 100 mM KCl SC-Leu solid medium with the 96-pin manifold.

2.2.3 Cycloheximide chase analysis

Yeast cultures transformed with human potassium channels expressed under the control of the *TEF1* were grown overnight to saturation, diluted into 5 ml of SC-Leu at an OD_{600} of 0.25, and grown to mid-log phase, which I define as an OD_{600} of 0.7-1.3. Cultures were treated with 150 µg/mL of cycloheximide (Sigma-Aldrich) and incubated with agitation in a 37˚C waterbath unless otherwise specified. A total of 1 ml aliquots of culture were withdrawn at the indicated times and immediately harvested and flash frozen in liquid nitrogen. Aliquots were processed and analyzed for Western blot analysis as described below. For cycloheximide chase analyses of the temperature-sensitive *cdc48*-2 strain, all cultures were incubated at 39˚C for 120 min prior to cycloheximide addition. For cycloheximide chase analyses of the temperature-sensitive *ssa1-45* and *rsp5-2* strains, all cultures were incubated at 37˚C for 60 min or 39°C for 75 min respectively prior to cycloheximide addition.

Cycloheximide chase studies in HEK cells were performed 20-24 hrs after induction with doxycycline. Cells were pretreated with either 10 µM leupeptin (Sigma-Aldrich), 5 µM MG-132 (EMD Millipore, Billerica, MA) or vehicle for 1 hr before the addition of cycloheximide (50 µg/ml), and then cells were chased in the presence or absence of the protein degradation inhibitors for 1- 3 hrs. Cell lysates, collected every hour after addition of cycloheximide, were resolved by SDS-PAGE and probed in Western blots with ROMK antibodies (R79 Serum (Wade *et al.*, 2011)).

2.2.4 Analysis of ROMK residence

To perform a sucrose gradient analysis of ROMK residence, yeast cultures transformed with plasmids encoding the indicated channels were grown overnight to saturation, diluted into 200 mL of SC-Leu to an initial OD_{600} of 0.25, and then allowed to grow to mid-log phase. A total of 150 OD_{600} of cells were harvested and lysed with glass beads in a solution containing 10% sucrose, 10 mM Tris pH 7.6, 1 mM DTT, 1 mM PMSF) (Sigma), 1 µg/mL leupeptin (Sigma), 0.5 µg/mL pepstatin A (Sigma), and 10 mM EDTA (Roberg *et al.*, 1997). The entire volume of the clarified lysate was then layered on top of a sucrose gradient with 1.5 ml of 30% sucrose, 1.5

ml of 40% sucrose, 2.5 ml of 50% sucrose, 1.5 ml of 60% sucrose, 1.5 ml of 65% sucrose, and 2.5 ml of 70% sucrose in the same buffer. The gradients were centrifuged in a Beckman L8-70M ultracentrifuge (Beckman-Coulter, Pasadena, CA) at 28,500g for 18.5 hrs. The gradient was then divided into 24 fractions, which were analyzed by SDS-PAGE and Western blot (see below).

Prior to microscopy, all strains were grown to mid-log phase in SC-Leu media or in SC-Leu-His for strains co-transformed with Scs2-mCh. Cells were placed on a 35 mm, poly-D-lysine-coated dish (MatTek, Ashland, MA) and imaged with a Nikon (Tokyo) Eclipse Ti inverted microscope equipped with epifluorescence, an Apo100 x objective (NA 1.45) and an Orca Flash 4.0 cMOS (Hamamatsu, Bridgewater, NJ) camera. NIS-Elements software (Nikon) was used to control the imaging parameters, and all images within an experiment were captured used identical acquisition settings. Post-acquisition processing was conducted using ImageJ (National Institutes of Health). To stain the vacuolar membrane, cells were incubated with 300 μM of the FM4-64 dye (Thermo Fisher) for at least 30 min, which allows for FM4-64 bound to lipid at the cell surface to traffic to the vacuolar-limiting membrane (Vida and Emr, 1995), and were washed prior to imaging. All images were acquired at room temperature.

2.2.5 Inductively Coupled Plasma Mass Spectrometry (ICP-MS)

Yeast cultures transformed with a vector control or a vector engineered for the expression of distinct human potassium channels were grown overnight to saturation, diluted into 7 ml of SC-Leu medium containing either 100 mM or 10 mM KCl at an OD_{600} of 0.2, and allowed to grow for 8 hrs. Approximately 3.0 OD_{600} of cells were harvested by vacuum filtration onto 1.2 μm pore glass fiber membrane filters (EMD Millipore). Next, the cells were washed with 1 μM EDTA and with double distilled water before they were dissolved in 30% trace metal grade HNO_3 (Fisher) at 65^{o}C overnight. Solutions were clarified by centrifugation at 20,000g for 10 min to remove any solid debris and diluted with 2% sub-boil distilled HNO_3 prior to analysis on a Perkin Elmer (Waltham, MA) NexION 300x ICP-MS. All elemental concentrations were determined using a 5-point calibration curve. An internal standard of beryllium, germanium, and thallium was added to all samples to assess signal strength and instrument drift. A 2% nitric acid blank was run every seven samples to assess signal memory effects. All biological replicates

were run in technical duplicate and the technical replicates are the average of 3 replicate measurements from the ICP-MS.

2.2.6 HEK293 cell culture and siRNA knockdown

All cells were propagated at 37˚C in a 5% CO_2 humidified incubator. Cells were passaged every 3-4 days using standard methods. All experiments were conducted after seven or fewer passages. T-REx-HEK-293 ROMK cells were a generous gift from the laboratory of Dr. Jerod Denton (Fallen *et al.*, 2009), and the original T-REx-HEK 293 cells were purchased from Invitrogen. Upon receipt, they were tested for mycoplasma using a PCR-based kit (ATCC, Manassas, VA) and found to be negative. T-REx-HEK-293 ROMK cells were propagated in high-glucose DMEM (Sigma Life Sciences) supplemented with 10% Fetal Bovine Serum, 5 µg/ml Blasticidin S, and 250 µg/ml Hygromycin B to maintain selection for the integrated tetracycline-inducible ROMK cassette (Raphemot *et al.*, 2013). To induce ROMK expression, cells were treated with 2 µg/ml tetracycline for at least 24 hrs. siRNA silencing was achieved with 1.5 µg/ml Lipofectamine RNAiMax (ThermoFisher) transfection reagent and 10 nM RNA duplex (GE Life Sciences, Marlborough MA) (sequences are indicated in Supplementary Table 3). Lipofectamine and RNA were incubated separately in 0.25 ml pre-warmed OptiMEM (ThermoFisher) for 5 min, mixed at a 1:1 volumetric ratio, incubated for another 5 min, and then added to cells. After 24 hrs, culture media was changed and the transfection protocol was repeated a second time.

2.2.7 HEK293 cell surface biotinylation

Prior to biotinylation, cells at 80-90% confluency were treated with 125 µg/ml cycloheximide for 2 hrs to increase the cell surface concentration of ROMK. The cells were washed 3 times with Dulbecco's Phosphate Buffered Saline (DPBS), then treated with 0.3 mg/ml EZ-Link Sulfo-NHS Biotin (Thermo-Fisher) for 1 hr. Excess biotin was quenched by washing the cells with 100 mM glycine in DPBS 3 times, the cells were lysed in HEENG buffer (20 mM HEPES pH=7.6, 1 mM EDTA, 1 mM EGTA, 25 mM NaCl, 10% glycerol) containing 1% Triton TX-100 and cOmplete,

Mini, EDTA free protease inhibitors (Roche Diagnostics, Mannheim, Germany) for 1 hr, and the mixture was centrifuged for 5 min at maximum speed to remove any insoluble material. Soluble protein concentrations were assessed with a Pierce BCA Protein Assay Kit (Thermo-Fisher) per the manufacturer's instructions. For each condition, 300 µg of protein was added to 30 µl of Pierce NeutrAvidin Agarose (Thermo-Fisher) beads, brought to a total volume of 1 ml, and incubated overnight. Beads were then triple washed with DPBS and treated with 1X SDS-PAGE sample buffer for 1 hr at room temperature prior to SDS-PAGE and Western blot analysis (see below). All steps of this protocol were conducted at 4˚C.

2.2.8 Western blot analysis

To assay protein expression in yeast, equivalent OD_{600} cultures at mid-log growth phase were lysed in 300 mM NaOH, 1 mM 2-mercaptoethanol, 1 mM PMSF (Sigma), 1 µg/mL leupeptin (Sigma), and 0.5 µg/mL pepstatin A (Sigma). Total protein was precipitated from lysate with 5% trichloroacetic acid (TCA), resuspended in SDS-PAGE sample buffer, incubated for at least 1 hr at room temperature, and analyzed by SDS-PAGE (Zhang *et al.*, 2001). Steady-state levels of protein in HEK293 cells were analyzed by dissolving 30 µg of protein from clarified lysate in SDS-PAGE sample buffer, incubating for at least 1 hr, and analyzing by SDS-PAGE.

All Western blots were developed with the SuperSignal West enhanced chemiluminescence kit (Thermo-Fisher) per the manufacturer's instructions. Chemiluminescence images were obtained on a BioRad image station. Quantitation of signal intensity was performed by measuring integrated pixel density in ImageJ (National Institutes of Health). Relevant antibody information is supplied in Table 4.

Table 4: Antibodies used in this study

Target	**Species of Origin**	**Source**	**Catalog #**	**Lot # (If Available)**
Hemagglutinin (HA) HRP-conjugated	Donkey	Roche	12013819001	23551600
G6PD	Rabbit	Sigma-Aldrich	A9521	n/a
Sec61	Rabbit	(Stirling *et al.*, 1992)	n/a	n/a
Pma1	Mouse	Abcam (Cambridge, UK)	ab4645	40B7
GFP	Mouse	Roche	11814460001	14442000
ROMK	Rabbit	(Wade *et al.*, 2011)	n/a	n/a
Hsp90	Mouse	Enzo Life Sciences, Farmingdale, NY	ADI-SPA-830-D	01101340
ATP1A	Mouse	Santa Cruz Biotechnology, Dallas, TX	C464.6	sc-21712
TSG101	Mouse	GeneTex, Irvine, CA	GTX70255	4A10
HGS	Mouse	Abcam	ab56468	n/a
VPS8	Rabbit	Proteintech, Rosemont, IL	15079-1-AP	n/a
β-actin	Mouse	Abcam,	ab6276	n/a
Rabbit IgG (HRP-conjugated)	Goat	Cell Signaling Technology, Beverly, MA	7074S	26
Mouse IgG (HRP-conjugated)	Goat	Cell Signaling Technology, Beverly, MA	7076S	29

2.3 RESULTS

2.3.1 Identification of a ROMK variant suitable for SGA

Initial attempts to express ROMK1 in *trk1Δ trk2Δ* yeast failed to reveal growth rescue on low potassium media (Figure 6A). This contrasts with the strong rescue phenotype observed in yeast expressing the inwardly rectifying channel $K_{ir}2.1$, which shares 42% sequence identity with ROMK1. To remedy this problem, I modified ROMK1 with two point mutations which I hypothesized would potentiate it in yeast. First, ROMK1 contains an intracellular acid-sensitive gate, which keeps the channel closed under conditions of cellular acidification (Rapedius *et al.*, 2007a). All K_{ir} channels are acid-gated to some degree, but only in ROMK, $K_{ir}4.x$, and $K_{ir}5.1$ does the IC_{50} fall within a physiologically relevant range (Paynter *et al.*, 2010). . I hypothesized that this pH gate closes ROMK because the yeast cytosol is acidic (pH 5.5–6.8), particularly in stationary phase cultures growing on solid agar medium (Paynter *et al.*, 2010). Therefore, Lys-80, which is crucial for pH gating (Rapedius *et al.*, 2007a) was mutated to Met (K80M). Second, ROMK1 is retained in the ER of mammalian cells due to the presence of multiple RXR motifs at both the N- and C-terminal domains. Aldosterone-regulated phosphorylation at Ser-44 by SGK-1 overrides ER retention, promoting anterograde traffic (Yoo *et al.*, 2005). To favor ER exit in yeast, Ser-44 was mutated to Asp (S44D).

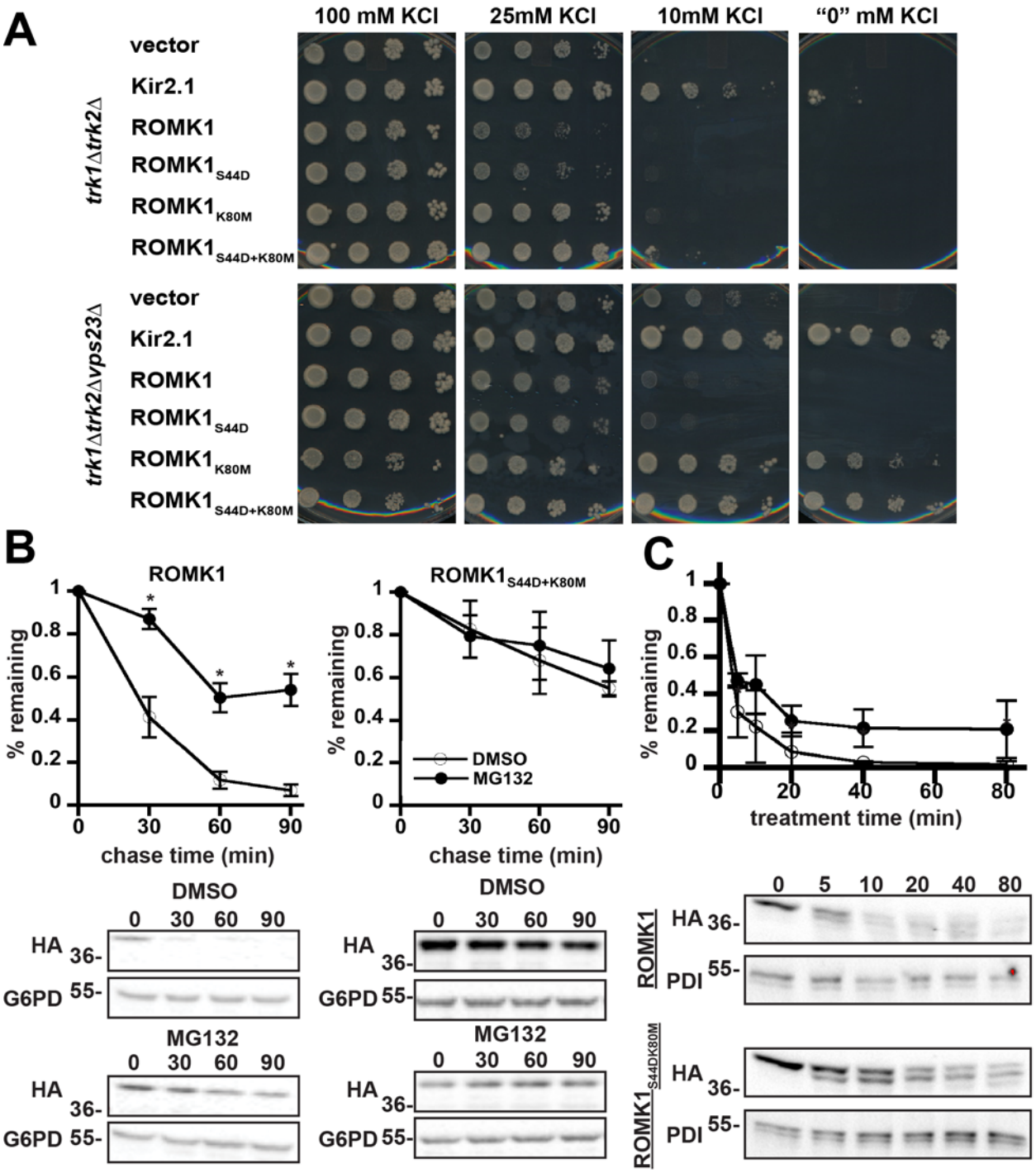

Figure 6: The S44D and K80M mutations in ROMK improve its function and stability. A. Yeast containing an empty expression vector or plasmids engineered for the expression of Kir2.1, wild-type ROMK, or the S44D and K80M mutations alone or in combination were spotted onto SC medium containing the indicated added concentration of KCl. B. Yeast

expressing wild-type ROMK or ROMK1$_{S44D+K80M}$ were treated with either 100 µM MG132 (closed circles) or with an equal volume of DMSO (open circles) for 30 min before the addition of cycloheximide. ROMK expression was assessed by Western Blot and data were normalized to the initial timepoint. Representative blots are shown and all blots were stripped and reprobed for glucose-6-phosphate dehydrogenase (G6PD) as a loading control. Data represent the means of six independent experiments from two independent yeast transformations. C. ER-enriched microsomes prepared from wild-type yeast expressing wild-type ROMK1 or ROMK1$_{S44D+K80M}$ were treated with 10 µg/ml Proteinase K for the indicated times. Representative blots are shown, and protein disulfide isomerase (PDI) was used as a loading control. Data represent the means of four independent experiments. Error bars show standard errors of the mean, *indicates a significant ($p<0.05$) difference as assessed by Student's t-test.

Vectors engineered for the constitutive expression of ROMK1, each of the single mutants, and the double mutant were constructed and introduced into *trk1Δ trk2Δ* yeast as well as into a strain that Dr. Alexander Kolb had previously identified as deficient in a negative regulator of Kir2.1, *trk1Δ trk2Δ vps23Δ* (Kolb *et al.*, 2014) (section 1.1.6). As shown in Figure 6A, ROMK1$_{S44D+K80M}$ rescued the growth of cells on low potassium almost as well as Kir2.1. Although the ROMK1$_{S44D}$ species displayed only minimal growth rescue, this mutation augmented growth when combined with the K80M mutation. Importantly, the expression of any of these species did not retard the growth of *trk1Δ trk2Δ* yeast (data not shown). Therefore, I chose to use the double mutant (ROMK1$_{S44D+K80M}$) for subsequent experiments. All K_{ir} channels in this study were expressed under the control of the *TEF1* promoter on a low-copy plasmid as prior research with K_{ir}2.1 has found that this expression scheme produces optimal low potassium growth rescue in *trk1Δ trk2Δ* yeast (Kolb *et al.*, 2014).

Cycloheximide chase analysis revealed that ROMK1$_{S44D+K80M}$ was more resistant to proteasomal degradation than ROMK1, as the degradation rate was affected less when ROMK1$_{S44D+K80M}$ expressing cells versus ROMK1-expressing cells were treated with the proteasome inhibitor MG132 (Fig. 4B). Based on its effects on channel gating, I reasoned that the K80M mutation might stabilize the channel by favoring its open conformation. To test this

hypothesis, ER-derived microsomes were prepared from yeast expressing wild type ROMK1 and ROMK1$_{S44D+K80M}$. As proposed, I discovered that ROMK1$_{S44D+K80M}$ was more resistant to *in vitro* degradation by ProteinaseK as compared to the wild type channel (Figure 6C). Dr. Brighid O'Donnell, a University of Pittsburgh Medical Center (UPMC) neonatology fellow, would take advantage of the fact that ROMK1$_{S44D+K80M}$ is refractory to proteasomal degradation. Specifically, she was able to use this construct as a control for investigating the role of select Type II Bartter syndrome mutations in targeting ROMK for ERAD (O'Donnell *et al.*, 2017a, 2017b) (section 1.2.2).

I next tested the two alternatively spliced isoforms in the kidney, ROMK1 and ROMK2, which are identical except for a 19-amino acid residue N-terminal extension in ROMK1. To date, no biophysical differences between the channels have been identified, though they have divergent physiological roles (Welling and Ho, 2009) (section 1.2.1). Curiously, ROMK2$_{S44D+K80M}$ did not rescue the growth of *trk1Δ trk2Δ vps23Δ* yeast on low potassium media as effectively as ROMK1$_{S44D+K80M}$ (Figure 7A), despite somewhat higher steady-state expression levels of ROMK2$_{S44D+K80M}$ compared to ROMK1$_{S44D+K80M}$ (Figure 8). Notably, the degree of rescue mediated by ROMK1$_{S44D+K80M}$ was similar to that of K_{ir}2.1, which was used in a previous screen from the lab (Kolb *et al.*, 2014). Hence, ROMK1$_{S44D+K80M}$ was used for the remainder of the work outlined in this chapter. Furthermore, I predicted that the ROMK1$_{S44D+K80M}$ protein could be used to conduct an SGA analysis, which could provide for the first time a whole genomic profile of the factors that negatively regulate ROMK trafficking.

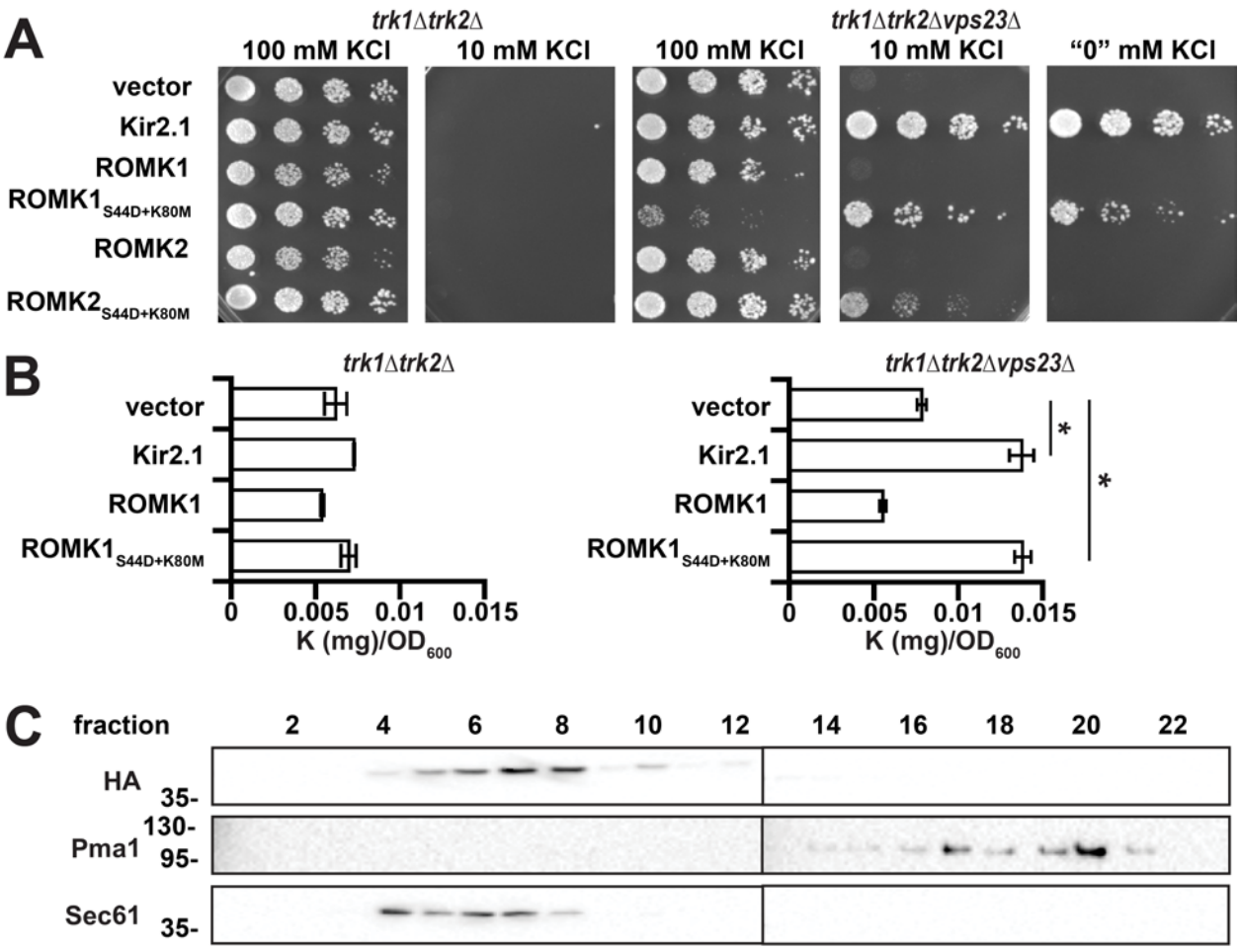

Figure 7: ROMK1$_{S44D+K80M}$ increases potassium uptake. A. Yeast strains with the indicated genotypes transformed with an empty expression vector control or vectors engineered to express Kir2.1, wild-type ROMK1, or ROMK1$_{S44D+K80M}$ were serially diluted onto medium supplemented with the indicated amounts of KCl. B. Intracellular potassium levels, as measured by ICP-MS, were assessed using equivalent amounts of yeast containing an empty vector or expressing Kir2.1, wild-type ROMK1, or ROMK1$_{S44D+K80M}$. Cells were cultured for 8 hrs in liquid media containing either 100 mM or 10 mM KCl. Data show the means of 3 biological replicates. Error bars show standard deviations, *indicates $p<0.05$ (Student's t-test). C. Western blots of sucrose gradient fractions showing migration of HA-tagged ROMK1$_{S44D+K80M}$ containing microsomes in wild-type yeast. Pma1 marks the plasma membrane-derived fractions while Sec61 marks ER-derived fractions.

In order to confirm that $K_{ir}2.1$ and $ROMK1_{S44D+K80M}$ directly increase the amount of intracellular potassium in *trk1Δ trk2Δ* yeast, I prepared extracts from yeast cells expressing these proteins, as well as from those containing a vector control, and subjected the extracts to Inductively Coupled Plasma Mass Spectrometry (ICP-MS) with the assistance of Dr. Daniel Bain of the University of Pittsburgh Department of Geology and Environmental Science. This method allows for precise measurement of the metallic elemental composition of a biological sample. I first noted that the level of intracellular potassium in *trk1Δ trk2Δ* yeast expressing $ROMK1_{S44D+K80M}$ was not statistically different from the vector control after approximately 8 hrs of culture in medium containing 10 mM potassium (Figure 7B, left graph). These data are consistent with the inability of this strain to grow better than the vector control in the same medium (Figure 7A). However, both $K_{ir}2.1$ and $ROMK1_{S44D+K80M}$ expression increased intracellular potassium more than twofold compared to the vector control in *trk1Δ trk2Δ vps23Δ* cells (Figure 7B, right graph), consistent with Vps23 acting as a negative regulator of ROMK.

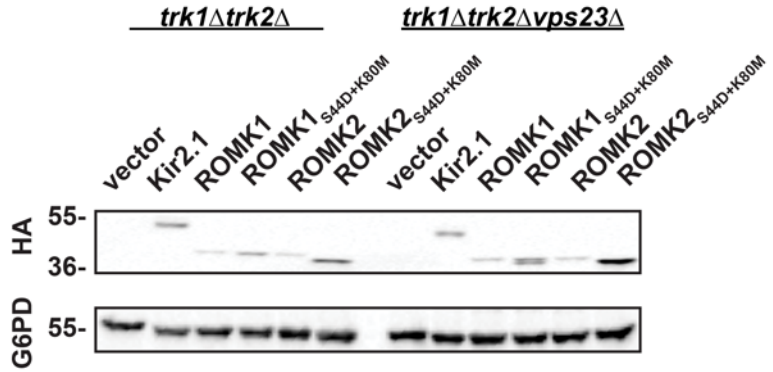

Figure 8: Expression of the ROMK1 and ROMK2 variants in yeast. Western blots of lysate from yeast of the indicated genotype and expressing the indicated HA-tagged potassium channels or containing an empty vector control were probed with an anti-HA antibody. All blots were stripped and reprobed for glucose-6-phosphate dehydrogenase (G6PD) as a loading control.

Prior studies established that *trk1Δ trk2Δ* yeast are sensitive to the toxic cations hygromycin B (an aminoglycoside antibiotic), spermine, and tetramethylammonium (Barreto *et*

al., 2011). This phenotype arises from increased cellular uptake of the toxins in *trk1Δ trk2Δ* yeast because the membrane is hyperpolarized when potassium entry is limited. Therefore, I examined growth on medium containing hygromycin B. Consistent with data in Figure 7A, $K_{ir}2.1$ or $ROMK1_{S44D+K80M}$ expression enhanced *trk1Δ trk2Δ vps23Δ* yeast growth on medium supplemented with hygromycin B (Figure 9). Together, these results indicate that $ROMK1_{S44D+K80M}$ functions as a potassium transporter in yeast, allowing for sufficient import of this cation to support growth on low potassium medium.

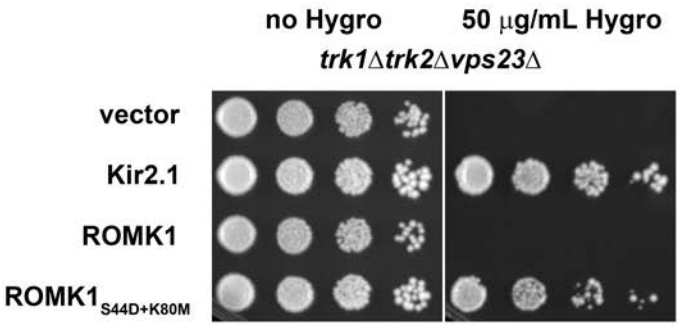

Figure 9: $ROMK1_{S44D+K80M}$ expression increases resistance to the toxic cation Hygromycin B. Yeast strains with the indicated genotype transformed with an empty expression vector control or vectors engineered to express Kir2.1, wild-type ROMK1, or $ROMK1_{S44D+K80M}$ were serially diluted onto growth medium supplemented with the indicated amounts of Hygromycin B (Hygro).

When examined under steady-state conditions in mammalian cells, ROMK primarily resides in the ER (Peters *et al.*, 2003; Welling and Ho, 2009). Similarly, I found that the majority of $ROMK1_{S44D+K80M}$ co-migrated with the ER-resident protein Sec61 when lysates from a wild-type yeast strain isogenic to *trk1Δ trk2Δ* and its derivatives (BY4742) were subjected to subcellular fractionation by sucrose gradient sedimentation analysis (Figure 7C). ROMK appeared to be absent in the Pma1-containing plasma membrane fractions. Based on the clear increase in intracellular potassium and the phenotypic data presented above, these results suggest that $ROMK1_{S44D+K80M}$ growth rescue on low potassium medium requires only small amounts of

protein at the plasma membrane that are undetectable using this approach. This conclusion is consistent with data from Dr. Alexander Kolb, indicating that very low levels of $K_{ir}2.1$ plasma membrane residence are sufficient for growth rescue under these steady-state conditions (Kolb *et al.*, 2014).

2.3.2 ROMK1$_{S44D+K80M}$ is primarily degraded by the vacuole and not by ERAD in yeast

ER-associated degradation (ERAD) is one of the first lines of defense against the accumulation of misfolded proteins in the secretory pathway (section 1.2.2). As neither ROMK1 nor ROMK1$_{S44D+K80M}$ was completely stable when the proteasome was inhibited with the proteasome inhibitor MG132 (Figure 6B), I hypothesized that a sub-population of ROMK is degraded in the vacuole, which serves as the degradative compartment for post-ER quality control in yeast (MacGurn *et al.*, 2012). To determine whether the vacuole contributes directly to ROMK degradation, both wild-type ROMK1 and ROMK1$_{S44D+K80M}$ were expressed in a yeast strain lacking Pep4, which activates proteases in the vacuole by cleaving their immature forms (Woolford *et al.*, 1986), as well as in an isogenic wild-type strain. I then analyzed their relative degradation profiles in a cycloheximide chase assay. As shown in Figure 10, both ROMK variants were significantly stabilized in *pep4Δ* yeast. However, while ROMK1 was only partially stabilized (Figure 10A), consistent with targeting to the ERAD pathway, ROMK1$_{S44D+K80M}$ was almost completely stable within the 90-minute timescale of the chase (Figure 10B). These data also emphasized the overall heightened stability of the ROMK1$_{S44D+K80M}$ protein as compared to wild type ROMK1 (O'Donnell *et al.*, 2017b).

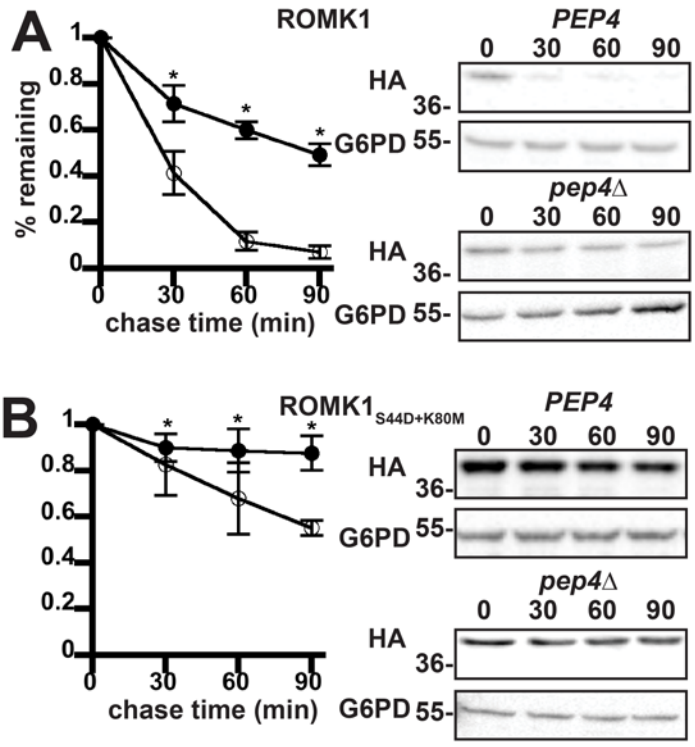

Figure 10: ROMK1 and ROMK1$_{S44D+K80M}$ are degraded to varying degrees by the vacuole in yeast. Yeast cultures expressing HA-tagged versions of either (A) ROMK1 or (B) ROMK1$_{S44D+K80M}$ grown to mid-logarithmic phase were dosed with cycloheximide and aliquots were withdrawn at 0, 30, 60, and 90 min. A yeast strain lacking the master vacuolar protease (*pep4*Δ, filled circles) or an isogenic wild-type (*PEP4*, open circles) expressing the proteins were shifted from room temperature to 37^{O}C 30 min before addition of cycloheximide. ROMK expression was assessed by Western Blot and data were normalized to the initial timepoint. Representative blots are shown and all blots were stripped and reprobed for glucose-6-phosphate dehydrogenase (G6PD) as a loading control. Data represent the means of six independent experiments from two independent yeast transformations. Error bars show standard errors of the mean, *indicates a significant ($p<0.05$) difference as assessed by Student's t-test.

I next examined the relative efficiencies with which wild-type ROMK1 and the ROMK1$_{S44D+K80M}$ isoform are degraded by ERAD. During ERAD, misfolded protein substrates are recognized by molecular chaperones such as Hsp70 and ubiquitinated by E3 ubiquitin ligases that are ER associated (Ellgaard *et al.*, 2016; Gottschling and Nyström, 2017). After the acquisition of a polyubiquitin tag, the ERAD substrate is retrotranslocated from the ER in an ATP-dependent process that utilizes the AAA-ATPase, Cdc48 (in yeast) or p97 (in mammals). I found that wild-type ROMK1 behaves like a canonical yeast ERAD substrate as it was significantly stabilized when Cdc48 was inactivated, when the genes encoding two ER-localized E3 ubiquitin ligases in yeast, Hrd1 and Doa10, were deleted, or when the cytosolic Hsp70 Ssa1 was disabled (Figure 11A,C,E). However, ROMK1$_{S44D+K80M}$ is consistently more stable, and the relative amount of degradation is affected less or not at all by ablation of these ERAD components (Figure 11B,D,F). Therefore, I propose that the degradation of wild-type ROMK1 is dominated by ERAD whereas the degradation of ROMK1$_{S44D+K80M}$ is dominated by post-ER quality control. Therefore, ROMK1$_{S44D+K80M}$ represents a novel “tool” with which to decipher how the post-ER quality control machinery regulates channel levels.

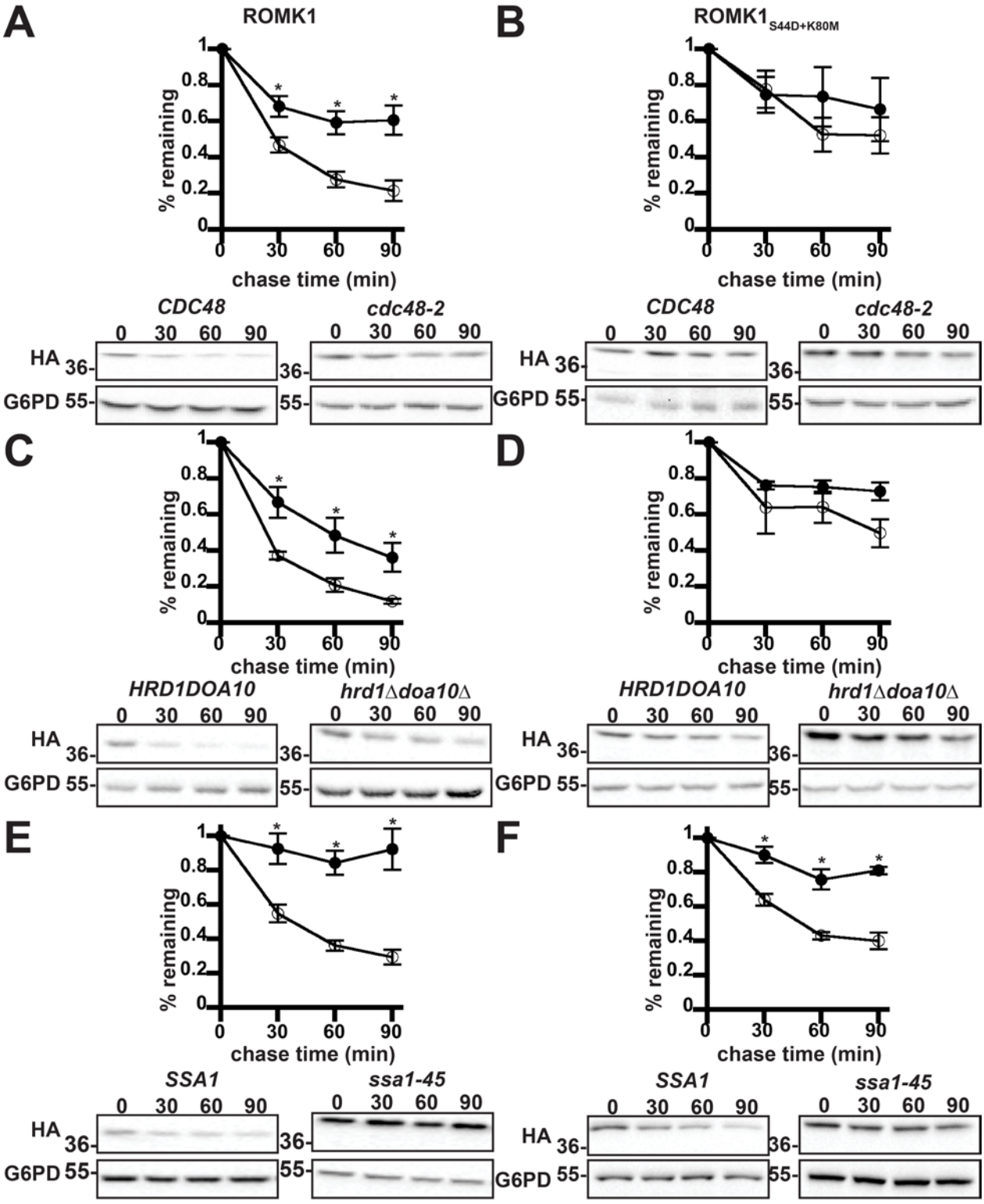

Figure 11: ROMK1 is degraded by the ERAD pathway to a greater extent than ROMK1$_{S44D+K80M}$ in yeast. Yeast cultures expressing HA-tagged versions of either (A,C,E)

ROMK1 or (B,D,F) ROMK1$_{S44D+K80M}$ grown to mid-logarithmic phase were dosed with cycloheximide and aliquots were withdrawn at 0, 30, 60, and 90 minutes. Yeast strains containing either a temperature sensitive mutation in the gene encoding Cdc48 (*cdc48-2*, filled circles) or lacking the mutant allele (*CDC48*, open circles) expressing (A) wild-type ROMK1 or (B) ROMK1$_{S44D+K80M}$ were shifted from room temperature to 39°C for 60 min before addition of cycloheximide. A yeast strain lacking the ER-resident E3 ubiquitin ligases (*hrd1Δ doa10Δ*, filled circles) or an isogenic wild-type strain (*HRD1 DOA10*, open circles) expressing (C) wild-type ROMK1 or (D) ROMK1$_{S44D+K80M}$ were shifted from room temperature to 37°C 30 min before addition of cycloheximide. Yeast strains lacking four cytosolic isoforms of Hsp70 (Ssa1, Ssa2, Ssa3, and Ssa4) and containing either a temperature sensitive mutation of Ssa1 (*ssa1-45*, filled circles) or an isogenic wild-type allele (*SSA1*, open circles) and expressing (E) wild-type ROMK1 or (F) ROMK1$_{S44D+K80M}$ were shifted from room temperature to 37°C 30 min before addition of cycloheximide. For all experiments, ROMK expression was assessed by Western Blot and normalized to the initial timepoint. Representative images are shown and all blots were stripped and reprobed for glucose-6-phosphate dehydrogenase (G6PD) as a loading control. Data represent the means of six independent experiments from two independent yeast transformations. Error bars show standard errors of the mean and *indicates a significant ($p<0.05$) difference as assessed by Student's t-test.

2.3.3 SGA for ROMK1 effectors implicates late secretory pathway protein degradation

Since ROMK1$_{S44D+K80M}$ rescues potassium sensitivity in *trk1Δ trk2Δ vps23Δ* yeast and appears to do so by increasing intracellular potassium (Figure 7A,B), I next conducted a whole-genome screen for other factors that negatively regulate ROMK residence and activity at the plasma membrane. To this end, ROMK1$_{S44D+K80M}$-expressing *trk1Δ trk2Δ* yeast were mated with the non-essential yeast deletion collection and arrays of triple mutant progeny (i.e., those that were deleted for *TRK1*, *TRK2*, and a non-essential gene; see Experimental Procedures) were generated (Figure 3). Potential negative effectors were identified by comparing growth on high (100 mM)

versus low (“0” mM) potassium medium, in which the only available potassium derives from trace amounts in the media components (Nakamura and Gaber, 1998). Strain growth was ranked by z-score (number of standard deviations from the plate mean) to correct for variance among agar plates. The initial screen revealed 40 very strong hits (z-score >3), 228 strong hits (z-score >2), and 519 weak hits (z-score >1) from the nearly 5,000 strains screened (Appendix D). The confirmed negative regulator of ROMK, *VPS23* (Figures 5A,6A), was among the very strong hits from the screen. I then re-arrayed select parental strains representing the 228 strong and very strong hits into fresh 96-well plates and performed the screen a second time to eliminate false positives. For the purposes of this study, I also eliminated from consideration genes known to sensitize yeast to toxic cations, such as members of the RSC chromatin remodeling complex (Barreto *et al.*, 2011). GO-term analysis of the 40 confirmed strongest hits indicated a positive ($p<0.05$) enrichment for the terms “endosomal transport”, “late endosome to vacuole transport”, and “vacuolar transport”, each of which are components of the late secretory trafficking and quality control machineries (Table 5). Other genes associated with these pathways were also represented among the strong (z-score >2) and weak (z-score >1) hits.

Table 5: Gene ontology (GO) term analysis of very strong hits (z-score >3) isolated from initial screen. Gene ontology (GO) term analysis of very strong hits (z-score >3) isolated from initial screen listed in increasing order of p-value from most significant (<0.001) to least significant (<0.05).

GO Term	**Genes**
ATP-dependent chromatin remodeling	*SWC5, SWR1, RSC1, RSC2, BDF1, NPL6*
Nucleosome organization	*SWC5, SWR1, RSC1, RSC2, BDF1, NPL6*
Chromatin remodeling	*SWC5, SWR1, RSC1, RSC2, BDF1, NPL6*
Histone Exchange	*SWC5, SWR1, BDF2*
DNA-templated transcription, elongation	*RSC1, RSC2, NPL6, NPL3, RPA49*
Protein-DNA complex subunit organization	*SWC5, SWR1, RSC1, RSC2, BDF1, NPL6*
Chromatin disassembly	*RSC1, RSC2, NPL6*
Protein-DNA complex disassembly	*RSC1, RSC2, NPL6*
Endosomal transport	*VPS8, VPS23, YPT7, VPS20, VPS21*
Late endosome to vacuole transport	*VPS8, VPS23, VPS20, VPS21*
Vacuolar transport	*VPS8, VPS23, VPS64, YPT7, VPS20, VPS21*

Next, to further increase my confidence in select hits, I reconstructed several of the triple mutant strains *de novo* by manually mating *trk1Δ trk2Δ* with the appropriate strain from the deletion collection, inducing sporulation, micro-dissecting the resultant tetrads, and selecting triple knock-out progeny (Table 6, underlined). This step was necessary to correct for false positives from the original list of screen hits and to build a trustworthy set of strains for subsequent experiments. Select strains that were absent from the original screen were included in this curated list as they are well-characterized components of the endosome-to-vacuole sorting pathway and genetically interact with the isolated hits (Table 6). The parental strains from the deletion collection corresponding to those in this curated list were also confirmed by PCR (see Table 3 for oligonucleotides used for this experiment). The reconstructed strains were then transformed with a vector control or the $K_{ir}2.1$, ROMK1, or $ROMK1_{S44D+K80M}$ expression vectors. Transformants were serially diluted onto a range of potassium supplemented media, and yeast expressing $ROMK1_{S44D+K80M}$ that grew better on low ("0" or 10 mM) concentrations of potassium relative to the vector control were considered to be verified negative regulators of ROMK (Figures 12,13). Importantly, the relative amounts of Kir2.1, ROMK1, and $ROMK1_{S44D+K80M}$ in these strains did not reflect the degree to which growth was rescued (Figure 14), suggesting that the primary effect of the mutants was on protein residence at the plasma membrane and not only on changes in global protein levels.

Table 6: Endosomal transport genes considered for further investigation in this study. Genes are arranged by functional classification. Genes in boldface were identified in the screen, while those in normal type were selected as known interactors with identified genes. Underlined genes were selected for *de novo* strain reconstruction.

Family	**Function**	**Genes**
CORVET	Tether Early Endosomes	*VPS3*, ***VPS8***, *VPS18, VAM6, VPS11, VPS16*
HOPS	Tether Late Endosomes	*VPS39, VPS41, VPS18, VAM6, VPS11, VPS16*
Table 6 (continued)		

ESCRT-0	Bind Ubiquitinated Cargo	***VPS27***, *HSE1*
ESCRT-I	Recruit Cargo to ILVs	***VPS23***, *VPS28, VPS37, MVB12*
ESCRT-II	Recruit Cargo to ILVs	*VPS22, VPS25,* ***VPS36***
ESCRT-III	Invaginate ILVs	*VPS2,* ***VPS20****, VPS24, SNF7*
Vps4C	Sever ILVs	***VPS4****, VPS60, VTA1*
Retromer	Return Cargo to Golgi	***VPS5****, VPS17, VPS26, VPS29, VPS35*
Rsp5 Adaptors	Promote Ubiquitination	***SSH4,*** *BSD2, EAR1*
SNAREs	Fuse Membranes	***TVP15, TVP23****, TGL6, VAM7, PEP12,* ***GOS1***
Rab GTPases and cofactors	Identify Endosomal Sub-Populations	***VPS21****,* ***YPT7****, YPT10,* ***MSB3****, MSB4, VPS9, BTS2*

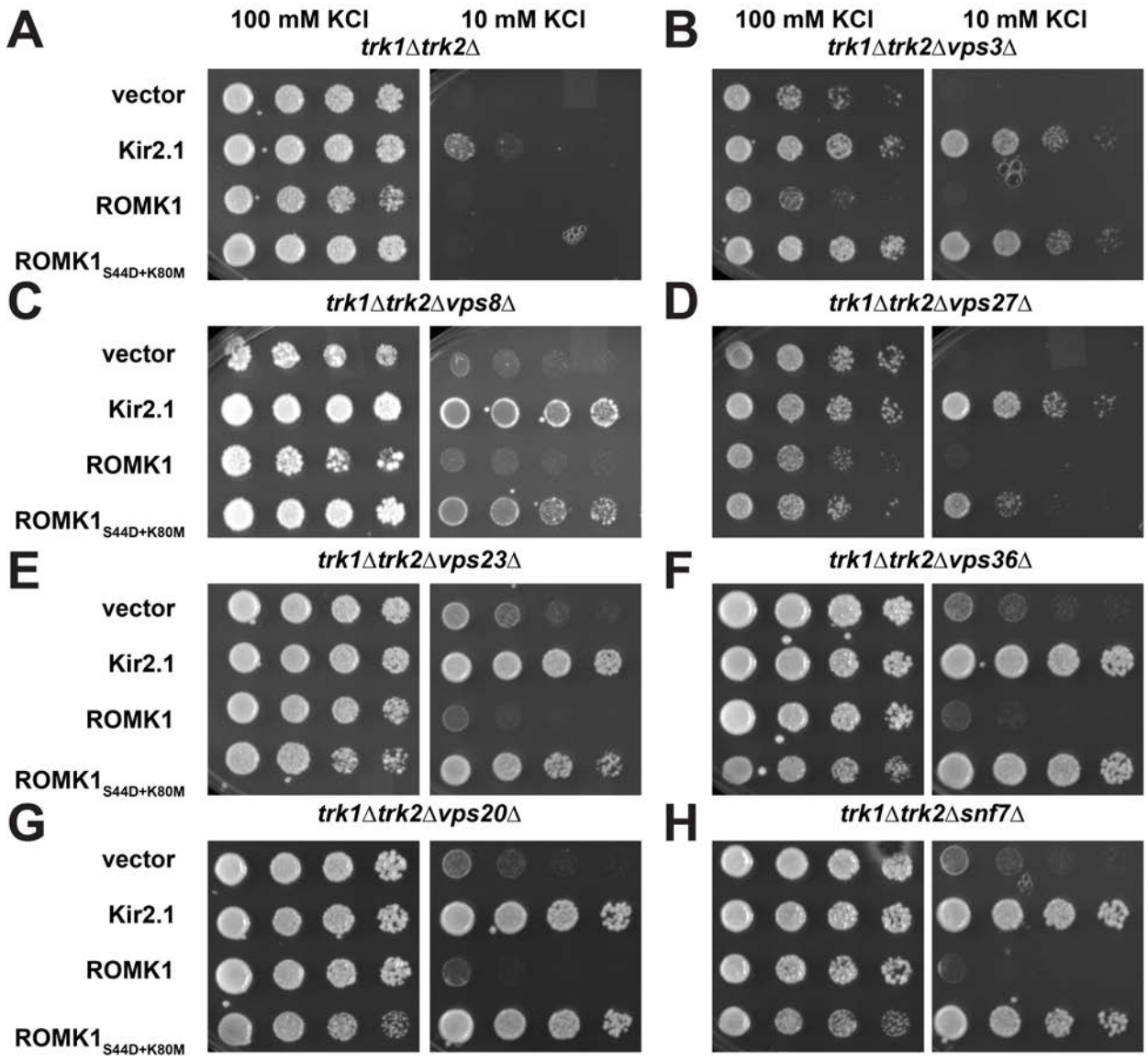

Figure 12: The deletion of genes encoding select ESCRT and CORVET components improves the growth of potassium sensitive yeast expressing ROMK1$_{S44D+K80M}$. Yeast strains with the indicated genotypes transformed with an empty expression vector control or vectors engineered to express Kir2.1, wild-type ROMK1, or ROMK1$_{S44D+K80M}$ were serially diluted onto medium supplemented with the indicated amounts of KCl. All strains in this figure were identified in the high-throughput SGA screen and then reconstructed *de novo*. All experiments were performed in duplicate, and representative serial dilutions are shown.

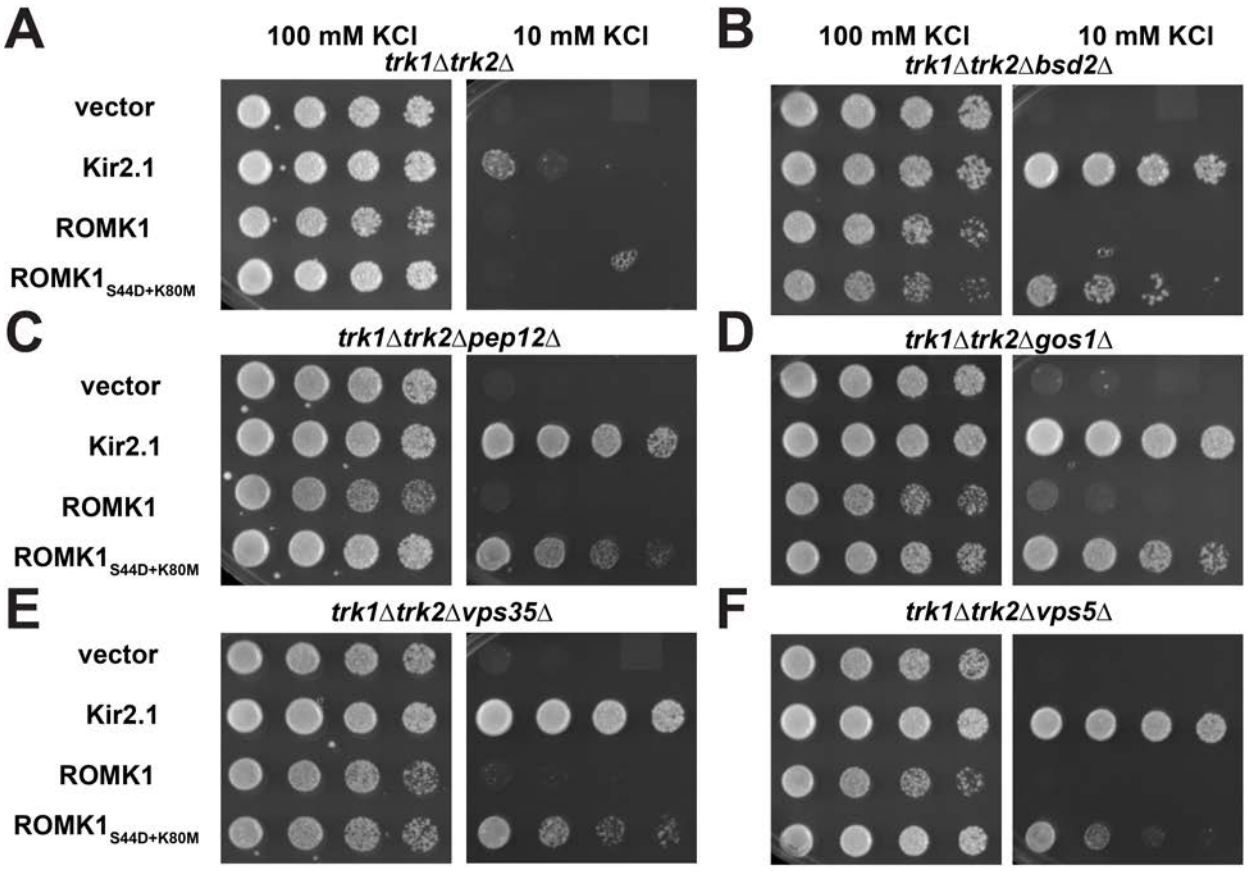

Figure 13: Deletion of genes encoding other endosomal sorting components improves the growth of potassium sensitive yeast expressing ROMK1$_{S44D+K80M}$. Yeast strains with the indicated genotypes transformed with an empty expression vector control or vectors engineered to express Kir2.1, wild-type ROMK1, or ROMK1$_{S44D+K80M}$ were serially diluted onto medium supplemented with the indicated amounts of KCl. All strains in this figure were identified in the high-throughput SGA screen and then reconstructed de novo. All experiments were performed in duplicate, and representative assays are shown.

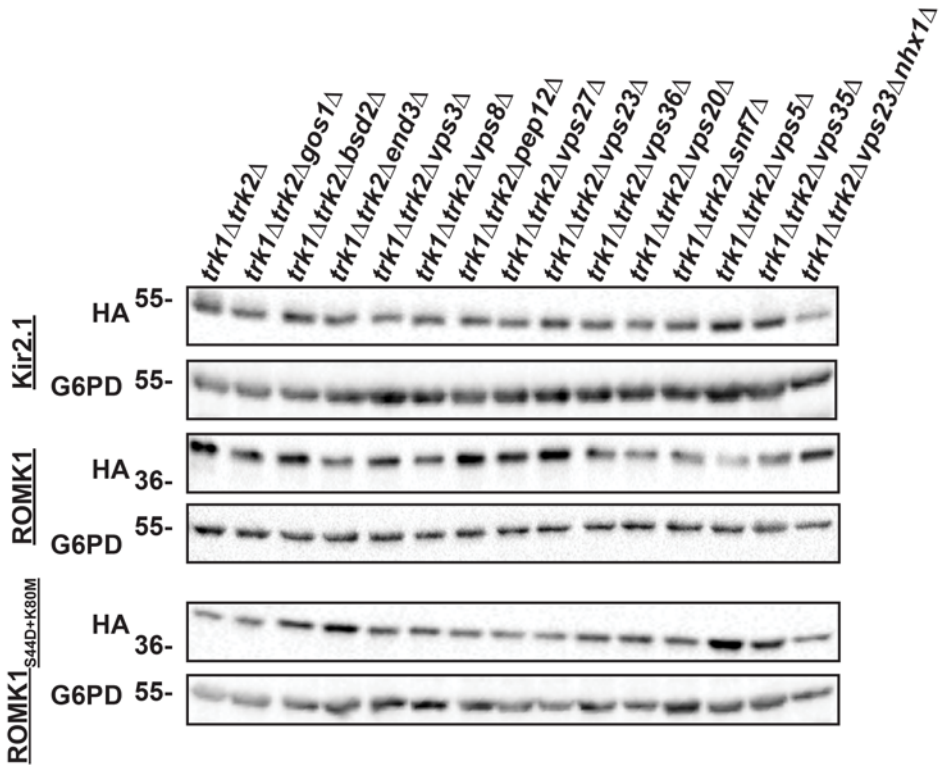

Figure 14: Expression of human potassium channels in the indicated hits from the SGA screen. Western blots were performed with lysates from yeast with the indicated genotypes and expressing the indicated potassium channels. Both Kir2.1 and the ROMK variants are HA-tagged. All blots were stripped and reprobed for glucose-6-phosphate dehydrogenase (G6PD) as a loading control.

To bolster my confidence that the rescue of growth on low potassium medium correlates with an increase in ROMK plasma membrane residency, I next conducted sucrose gradient analysis on fractionated membranes derived from *end3Δ* potassium sensitive yeast and an isogenic wild-type strain. In the *end3Δ* background, which is endocytosis deficient, a small amount of ROMK1$_{S44D+K80M}$ appears to comigrate with the plasma membrane marker Pma1 (Figure 15B "long exposure"). A signal corresponding to the plasma membrane was not evident when lysates from wild-type cells were examined (Figure 15A). Thus, even though the amount of the protein at the plasma membrane is quite low, ROMK1$_{S44D+K80M}$ promotes robust rescue of potassium sensitive growth in *end3Δ* yeast (Figure 15C,D). This phenomenon most likely arises from the high P_o reported for ROMK (Ho *et al.*, 1993; Leung, 2000) coupled with the presumably high transmembrane voltage in *S. cerevisiae*.

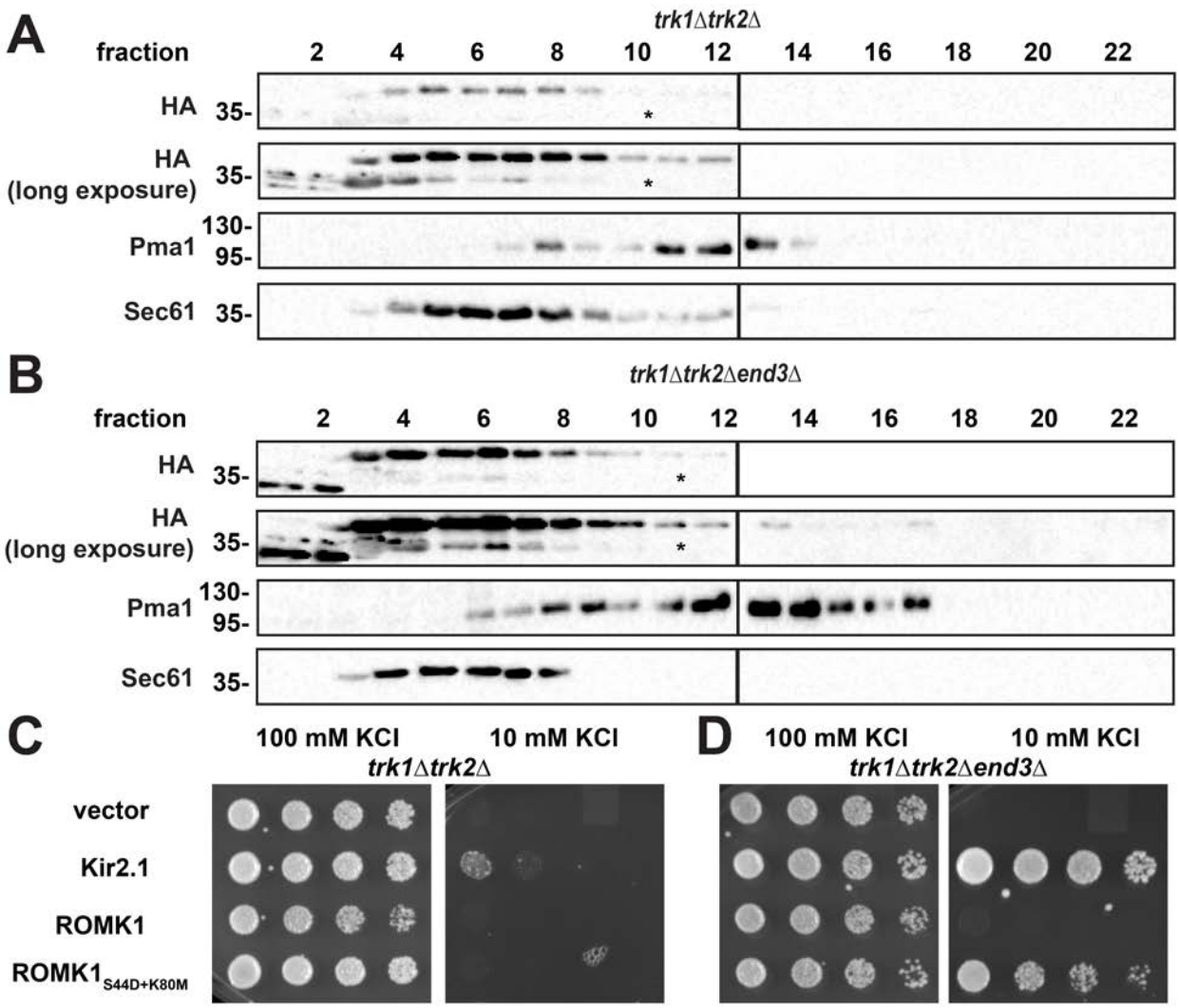

Figure 15: Deletion of endocytosis component End3 allows for ROMK plasma membrane residency. Western blots of sucrose gradient fractions showing migration of HA-tagged ROMK1$_{S44D+K80M}$ in *trk1Δ trk2Δ* (A) and *trk1Δ trk2Δ end3Δ* (B) yeast. Two exposures of the HA immunoblot are shown. * indicates an uncharacterized band that is likely a degradation product. Pma1 marks the plasma membrane-derived fractions while Sec61 marks ER-derived fractions. Note the population of ROMK that resides in fractions 13-17 that comigrates with Pma1. (C,D) Yeast strains with the indicated genotypes transformed with an empty expression vector control or vectors engineered to express Kir2.1, wild-type ROMK1, or ROMK1$_{S44D+K80M}$ were serially diluted onto medium supplemented with the indicated amounts of KCl. All strains in this figure were identified in the high-throughput SGA screen and then reconstructed de novo. All

experiments were performed in duplicate, and representative assays are shown. Note: panel C is identical to Figure 12A.

Vps8, a subunit of the CORVET complex, was identified as one of the strongest hits from the initial screen (Table 6, Figure 12). The CORVET complex is a heterohexamer involved in tethering vesicles containing Vps21, which is the yeast Rab5 homolog, prior to early endosome biogenesis (Balderhaar *et al.*, 2013). CORVET shares four out of six subunits with the HOPS complex, which performs a similar role as CORVET. However, HOPS instead functions with vesicles containing Ypt7, which is the yeast Rab7 homolog, to promote fusion of multi-vesicular bodies (MVBs) with the vacuole (Plemel *et al.*, 2011; Kingsbury *et al.*, 2014). Components of both complexes are conserved from yeast to man (Pols *et al.*, 2013; Lachmann *et al.*, 2014; Perini *et al.*, 2014). Therefore, to determine whether CORVET and/or HOPS functioned as novel, negative regulators of ROMK, both unique and shared CORVET and HOPS knockout strains were generated in the *trk1Δ trk2Δ* background. I discovered that only deletion of the CORVET-specific subunits Vps3 and Vps8 improved the growth of in *trk1Δ trk2Δ* yeast expressing ROMK1$_{S44D+K80M}$ (Figure 12B-C). In contrast, deletion of the HOPS-specific subunits Vps39 and Vps41 and shared subunits Vps11, Vps16, Vps18, and Vps33 had no or little effect on growth (data not shown). A model to explain these data is provided in the section 2.4.

Several other strong hits, as measured by the degree of growth rescue on low potassium, included strains lacking the ubiquitin-binding subunits of the four ESCRT complexes: Vps27 (ESCRT-0), Vps23 (ESCRT-I), Vps36 (ESCRT-II), and Vps20 (ESCRT-III) (Figure 7D-H). The ESCRT subcomplexes act sequentially to recruit ubiquitinated endocytic and Golgi-derived cargo into the MVB degradation pathway (Babst, 2005) (section 1.2.3). ESCRT targeting is primarily mediated by the cytoplasmic E3 ubiquitin ligase Rsp5 in yeast and the homologous Nedd4 ligases in mammals (Stringer and Piper, 2011; Henne *et al.*, 2013). Therefore, I hypothesized that disabling Rsp5 would stabilize ROMK1$_{S44D+K80M}$ to a greater degree than ROMK1 since the degradation of ROMK1$_{S44D+K80M}$ was exclusively Pep4-dependent (Figure 10). As anticipated, ROMK1$_{S44D+K80M}$ was completely stable in yeast containing the temperature-sensitive *rsp5-2* allele (Figure 16Figure 16B). The lack of any Rsp5-dependence on wild-type

ROMK1 degradation (Figure 16A) likely reflects the predominant contribution of ERAD to the disposal of this channel (Figures 6B, 11A,C,E).

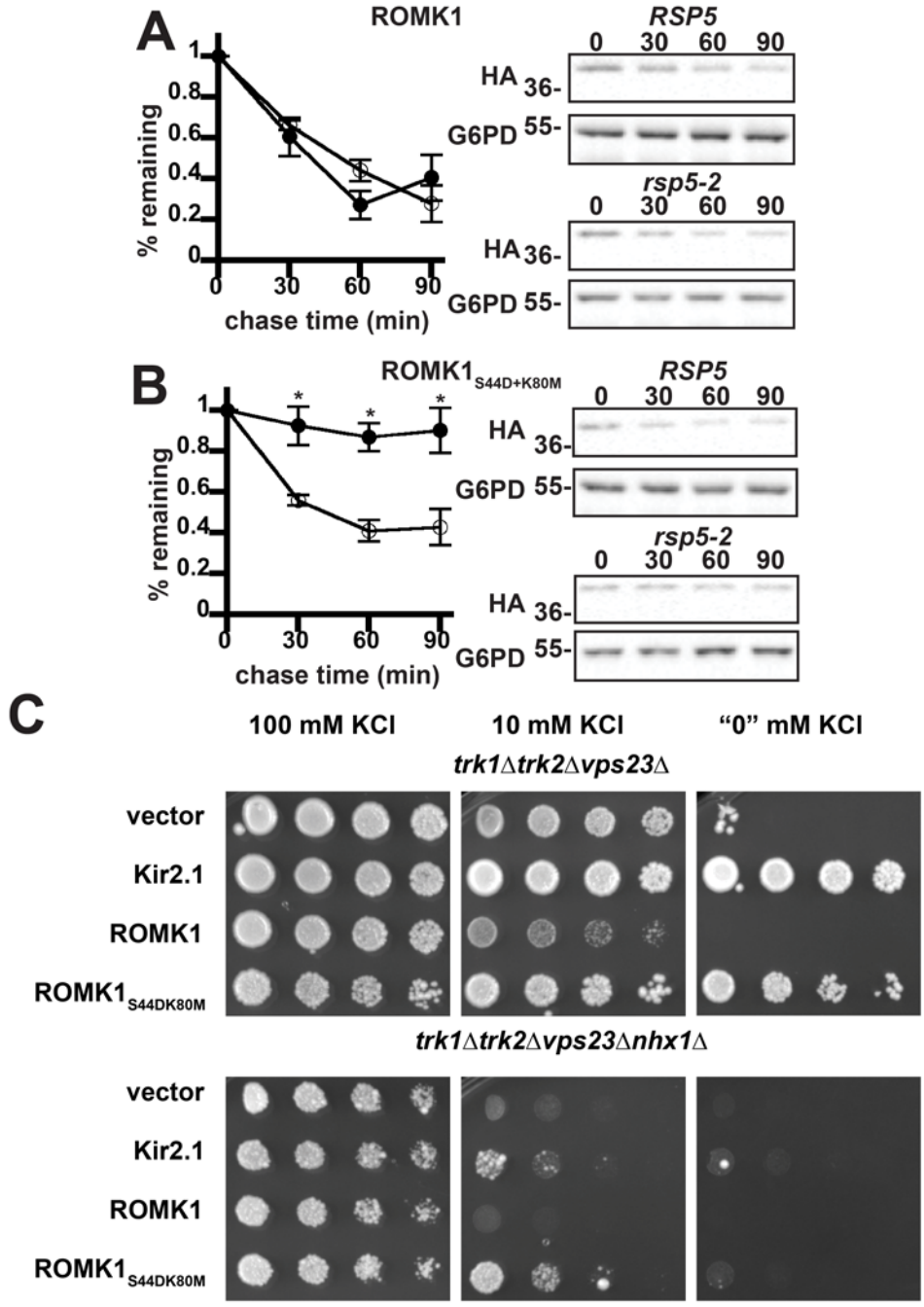

Figure 16: Rsp5 promotes the degradation of ROMK1$_{S44D+K80M}$ and Nhx1 promotes recycling of ROMK. Yeast cultures expressing HA-tagged versions of either (A) ROMK1 or (B) ROMK1$_{S44D+K80M}$ grown to mid-logarithmic phase were dosed with cycloheximide and aliquots were withdrawn at 0, 30, 60, and 90 minutes. Yeast strains containing either a temperature sensitive mutation in the gene encoding Rsp5 (*rsp5-2*, filled circles) or wild-type

yeast (*RSP5*, open circles) expressing ROMK were shifted from room temperature to 39°C 75 min before addition of cycloheximide. ROMK expression was assessed by Western Blot and normalized to the initial timepoint. Representative blots are shown and all blots were stripped and reprobed for glucose-6-phosphate dehydrogenase (G6PD) as a loading control. Data represent the means of four independent experiments. Error bars show standard errors of the mean and *indicates a significant ($p<0.05$) difference as assessed by Student's t-test. (C). Yeast strains with the indicated genotypes transformed with an empty expression vector control or vectors engineered to express Kir2.1, wild-type ROMK1, or ROMK1S44D+K80M were serially diluted onto medium supplemented with the indicated amounts of KCl. All experiments were performed in duplicate, and a representative assay is shown.

How is ROMK activity enhanced in yeast lacking ESCRT, CORVET, or other endosomal sorting genes? Early endosomes are crucial branch points from which cargo may be trafficked in a retrograde fashion to the Golgi apparatus through the action of the Retromer and GARP complexes, sorted into intralumenal vesicles by ESCRT, or recycled directly to the plasma membrane. Direct recycling is known to occur in yeast, though the precise mechanisms are not completely understood (MacDonald and Piper, 2016). I hypothesized that perturbations in ESCRT and other pro-degradation factors shift the dynamic equilibrium of the endosomal population of ROMK toward increased recycling. To test this hypothesis, I crossed my reconstructed *trk1Δ trk2Δ vps23Δ* strain with *nhx1Δ* yeast, which lack a sodium-proton exchanger involved in endosome acidification and cargo recycling (Kojima *et al.*, 2012). As expected, the *NHX1* deletion ablated ROMK-mediated growth on low potassium medium in the *trk1Δtrk2Δvps23Δ* background (Figure 16Figure 16C), suggesting that the increase in ROMK activity when ESCRT is perturbed arises from increased recycling.

As the contribution of Nhx1 during cargo recycling is indirect, I sought to replicate this analysis with components of known protein recycling pathways in the cell. I chose Vps5, a BAR-domain containing subunit of the Retromer subcomplex that induces the formation of tubular structures for endosome-to-Golgi recycling (Burd and Cullen, 2014), and Rcy1, a factor presumed to act upstream of most Vps proteins (Wiederkehr *et al.*, 2000). Surprisingly, deletion

of neither *VPS5* (Figure 17A) nor *RCY1* (Figure 17B) in the *trk1Δ trk2Δ vps23Δ* background ablated ROMK1$_{S44D+K80M}$ activity. These data suggest that ROMK recycling occurs through redundant pathways.

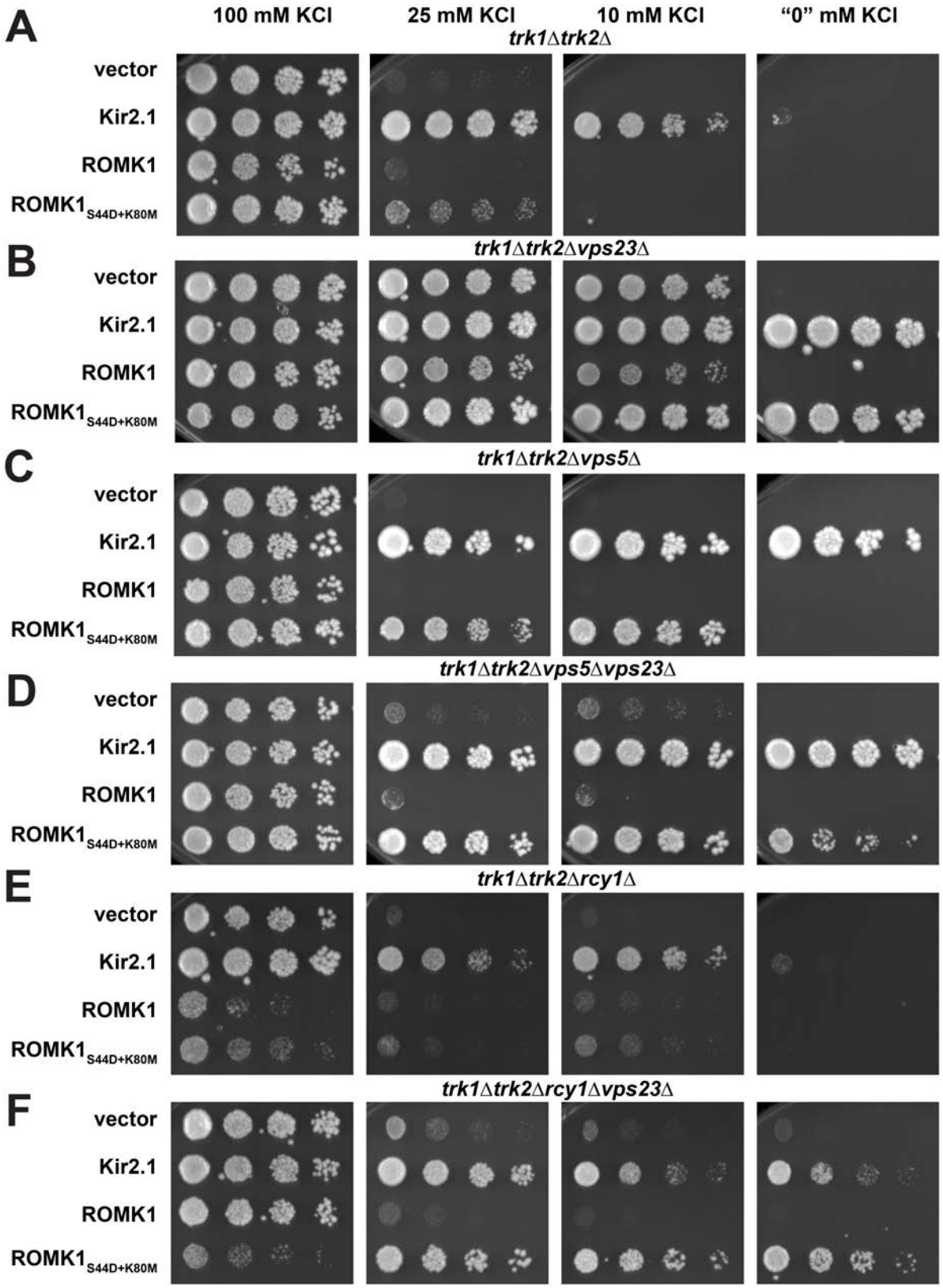
A
100 mM KCl
25 mM KCl
10 mM KCl
"0" mM KCl
trk1Δtrk2Δ
vector
Kir2.1
ROMK1
ROMK1S44D+K80M
B
trk1Δtrk2Δvps23Δ
C
trk1Δtrk2Δvps5Δ
D
trk1Δtrk2Δvps5Δvps23Δ
E
trk1Δtrk2Δrcy1Δ
F
trk1Δtrk2Δrcy1Δvps23Δ

Figure 17: Deletion of Vps5 or Rcy1 does not abrogate enhanced growth of ESCRT-deficient potassium sensitive yeast expressing ROMK1$_{S44D+K80M}$. Yeast strains with the indicated genotypes transformed with an empty expression vector control or vectors engineered to express Kir2.1, wild-type ROMK1, or ROMK1$_{S44D+K80M}$ were serially diluted onto medium supplemented with the indicated amounts of KCl. Images were captured after three days of growth at 30°C All experiments were performed in duplicate, and representative assays are shown.

2.3.4 ROMK vacuolar targeting is impeded in yeast deficient in ESCRT components

Having shown that ROMK1$_{S44D+K80M}$ is ERAD-resistant and is regulated by ESCRT and CORVET, I next asked whether ROMK subcellular localization is altered in strains lacking genes encoding select members of these complexes. To this end, I expressed Venus-tagged ROMK$_{K80M}$ (Vn-ROMK) in an ESCRT (*snf7Δ*) and CORVET (*vps8Δ*) deficient yeast strain, in the *pep4Δ* mutant, and in an isogenic wild -type strain (*BY4742*). In wild-type yeast, Vn-ROMK partially colocalized with both an mCherry-tagged ER-resident marker, Scs2-mCh (Zhou *et al.*, 2014), and the dye FM4-64 (Vida and Emr, 1995), which binds lipids on the cell surface, passes through the endocytic pathway, and accumulates on the vacuolar limiting membrane (Figure 18A,B). These results are consistent with passage of the protein through the secretory pathway and into a pre-degradative compartment. In agreement with dual localization, an immunoblot of lysate from wild-type yeast with an antibody that detects GFP derivatives, such as Venus, shows both full-length Vn-ROMK (predicted molecular mass of ~70 kDa) and the free Venus species (predicted molecular mass of ~28 kDa) (Figure 18C). The free Venus species arises from the fact that the fluorescent protein tag is refractory to vacuolar proteolysis (Guiney *et al.*, 2016), so once the Vn-ROMK channel enters a proteolytic compartment the fusion protein is only partially digested. Consistent with this view, Vn-ROMK-derived fluorescence accumulated primarily in the vacuole in *pep4Δ* yeast (Figure 18A,B), and the free Venus species was absent when vacuolar proteases were inactivated (Figure 18C). These data are also consistent with my observation that ROMK1$_{S44D+K80M}$ degradation is primarily vacuolar (Figure 10B).

In the *snf7Δ* ESCRT mutant, Vn-ROMK fluorescence shifts from the ER and vacuole to a large punctum that is adjacent to, but not contiguous with, the vacuolar limiting membrane (Figure 18A,B, see white arrows). This localization pattern is consistent with a substrate that is unable to enter intraluminal vesicles and therefore accumulates on the surface of the prevacuolar compartment due to the loss of ESCRT activity in this background (Stringer and Piper, 2011). Furthermore, the free Venus species is again absent in immunoblot analyses of *snf7Δ* lysates (Figure 18C). Interestingly, a species of ~36 kDa is instead present in this background and not in the isogenic wild-type. The appearance of this band, only in ESCRT mutants, could be due to proteolytic clipping by proteases within the prevacuolar compartment, as its observed molecular weight coincides with a predicted cleavage site between the first and second transmembrane domains of ROMK (data not shown). The fluorescence of Vn-ROMK in other ESCRT mutants (e.g., *vps23Δ* and *vps36Δ*) showed a nearly identical phenotype to *snf7Δ* (data not shown). Finally, to confirm that the Vn-ROMK-enriched puncta in *snf7Δ* cells represents the prevacuolar compartment, I expressed Vn-ROMK in a strain expressing an mCherry-tagged version of the Snf7 protein and found that Vn-ROMK and Snf7-RFP colocalize (Figure 18D, white arrows). It was previously observed that the RFP tag interferes with Snf7 function (Huh *et al.*, 2003), causing a dominant negative phenotype similar to the genetic null (Figure 18C, compare lanes 7 and 10). Therefore, the expression of Snf7-RFP serves both as a marker of the prevacuolar compartment and as an inhibitor of trafficking beyond this compartment.

I also examined localization and Vn-ROMK processing in the *vps8Δ* CORVET mutant. In this strain, Vn-ROMK is primarily present in the ER with little to no vacuolar signal (Figure 18A,B). Furthermore, although the free Venus species accumulates in this background, its levels are reduced relative to the isogenic wild-type strain (Figure 18C). In some *vps8Δ* cells, I observed Vn-ROMK accumulating in small puncta near the outer margin of the cell (Figure 18B, white arrows). These results are in accordance with reduced vacuolar delivery in the *vps8Δ* strain and are in line with localization patterns observed for native yeast substrates in this genetic background (Luo and Chang, 2000).

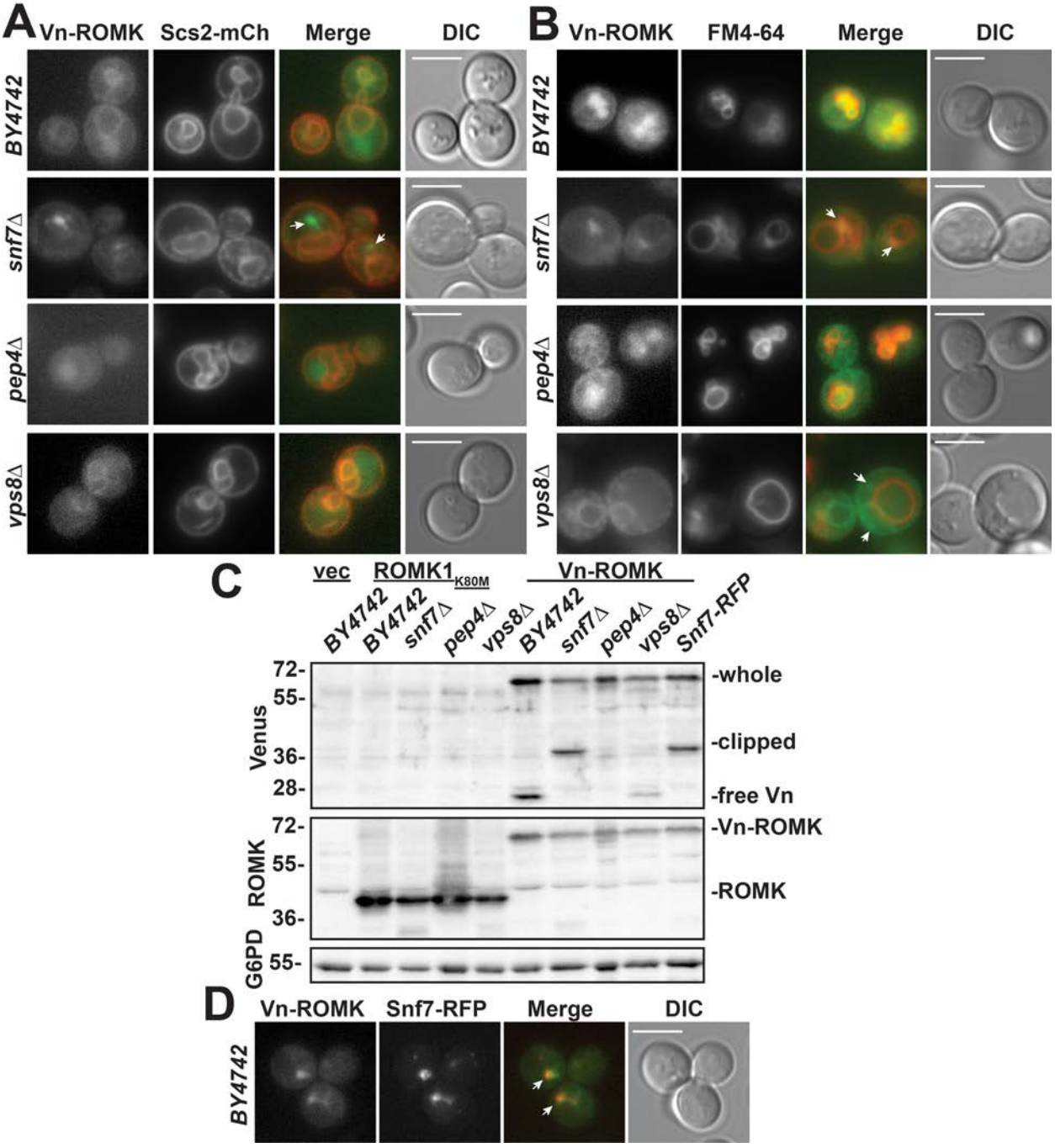

Figure 18: Venus-tagged ROMK$_{K80M}$ (Vn-ROMK) vacuolar trafficking is arrested in ESCRT-deficient yeast and reduced in CORVET-deficient yeast. Epifluorescence live cell images of the indicated yeast strains co-expressing Venus-ROMK$_{K80M}$ (Vn-ROMK) and the ER-resident protein Scs2-mCherry (Scs2-mCh). B. Epifluorescence live cell images of the indicated yeast strains expressing Vn-ROMK are shown and were treated with the styryl dye FM4-64 for

at least 30 min prior to imaging in order to stain the endosomal and vacuolar membranes. C. Western blot analysis of lysates from yeast of the indicated genetic backgrounds expressing Vn-ROMK or untagged ROMK1$_{K80M}$, or containing an empty expression vector was performed using the indicated antibodies. The Venus epitope migrates as three bands: full length Vn-ROMK (whole), a partially degraded species (clipped), and free Venus (free-Vn). The blot was stripped and reprobed with an antibody against the ROMK C-terminus to show the relative expression of untagged ROMK1$_{K80M}$ (ROMK) and Vn-ROMK. All unlabeled bands are due to non-specific antibody binding (compare to lane 1 "vec"). G6PD is also shown as a loading control. D. Epifluorescence live cell images of yeast co-expressing Vn-ROMK and Snf7-RFP. For all images, a direct interference contrast (DIC) image is shown at right. The white scale bar measures 5 μm. White arrows indicate features of interest as described in the text.

2.3.5 ESCRT and CORVET deplete ROMK from the plasma membrane in HEK293 cells

Given that components in the trafficking and degradation machineries in the late secretory pathway are conserved between yeast and humans, I next asked whether depleting the levels of select components that function in this pathway increases the steady-state distribution of ROMK at the plasma membrane in human cells. To answer this question, I reduced the levels of HGS (sole homologue of yeast Vps27), TSG101 (sole homologue of Vps23), and VPS8 (sole homologue of Vps8) in HEK293 cells that stably express wild-type ROMK1 under the control of an inducible promoter. Next, ROMK at the plasma membrane was biotinylated, captured on beads, and quantified via Western blot with anti-ROMK antibodies. Robust suppression of TSG101, HGS, and VPS8 protein levels was achieved by siRNAs-mediated knockdown. Moreover, silencing each of these components increased the steady-state levels of ROMK1 at the plasma membrane (Figure 19A). I noted that both immature and mature glycosylated ROMK were biotinylated, as previously reported (Fallen *et al.*, 2009), and that is likely a consequence of ROMK overexpression in these cells. As controls for this experiment, I found that the Na^+/K^+ ATPase α-subunit, ATP1A, was also biotinylated, but its cell surface expression was unchanged upon knockdown of the ESCRT or CORVET subunits (Figure 19A). In turn, the abundant cytosolic protein, Hsp90, was not biotinylated. Similar results were obtained when this

experiment was repeated with a second set of siRNA oligonucleotides (data not shown). As in yeast, ROMK1 residence in this cell line is primarily intracellular with only a small subpopulation resident at the plasma membrane. This is evidenced by the low ratio of biotinylated protein to total relative to that of ATP1A (Figure 19A). Accordingly, I was unable to visualize a plasma membrane population of ROMK via immunofluorescence microscopy as the protein appeared primarily confined to the ER (data not shown).

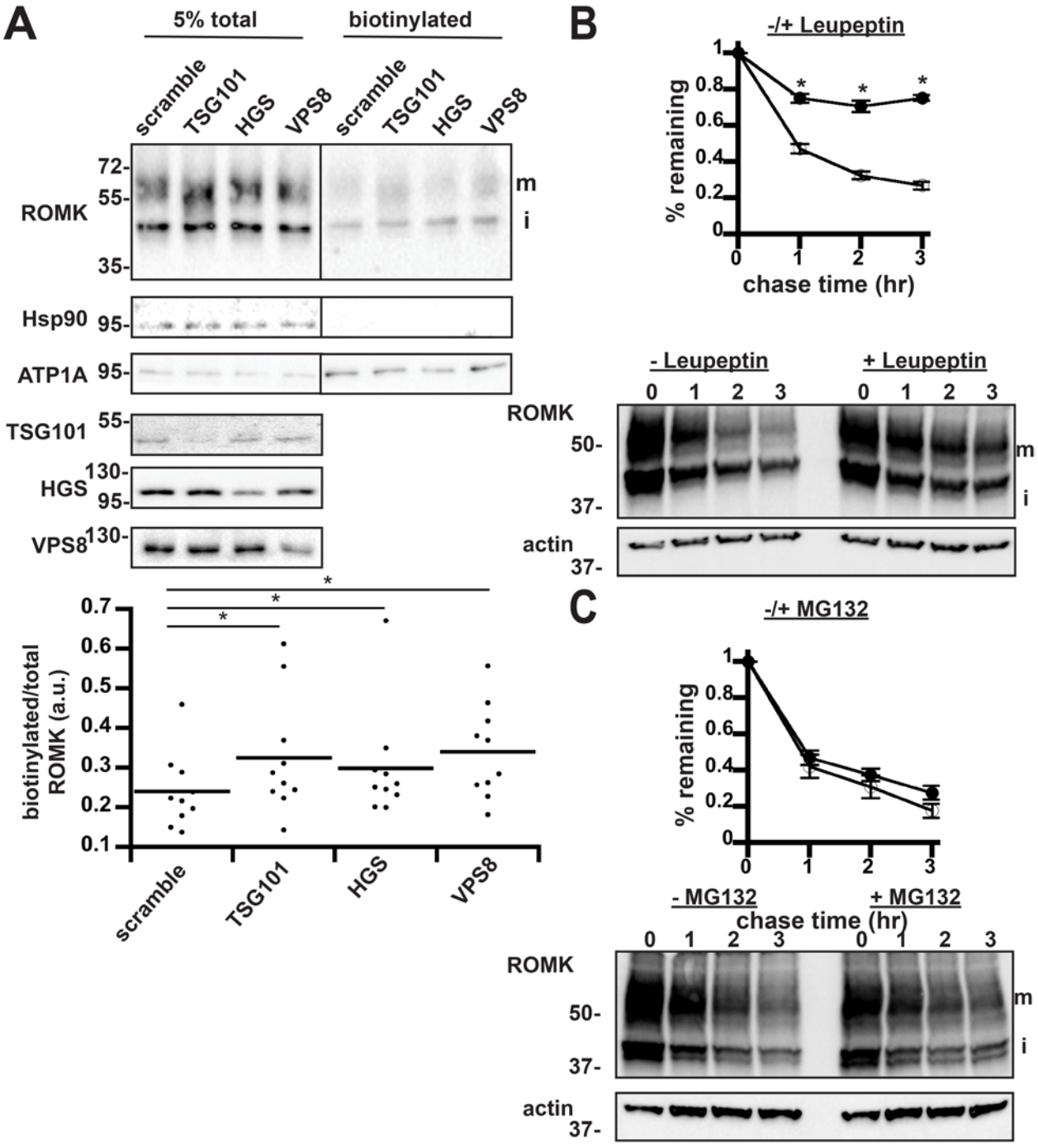

Figure 19: Depletion of select ESCRT and CORVET components increases ROMK surface expression in HEK293 cells. A. Lysates from HEK293 cells expressing ROMK under the control of the doxycycline-inducible "T-REx" promoter were examined by anti-ROMK immunoblot *in toto* (left) or were surface biotinylated and precipitated with NeutAvidin beads (right). ROMK migrates as two bands: an (i) immature ER-glycosylated band at ~45 kDa and

(m) a larger maturely glycosylated species of ~55-65 kDa (75). All blots were stripped and reprobed for cytosolic Hsp90 and plasma membrane-enriched ATP1A to show accurate loading and selective biotinylation of only cell surface proteins. An empty lane between the total and biotinylated samples was cropped out as indicated by the line. Quantitation of change in cell surface ROMK normalized to total protein for each replicate is shown below. Cell lysates from all siRNA-targeted factors were blotted on separate membranes to show efficient knockdown. Silencing for nine experimental replicates led to a decrease of 63 ± 4.7% for TSG101, 71 ± 4.3% for HGS, and 55 ± 5.1% for VPS8. *indicates $p<0.05$ (Student's t-test). B,C. HEK293 cells expressing ROMK under the control of the doxycycline-inducible "T-REx" promoter were pretreated with the lysosomal protease inhibitor Leupeptin (B) or MG132 (C) (closed circles), or vehicle (open circles) for 1 hour prior to cycloheximide addition. Samples were harvested at the indicated times. ROMK expression was assessed by Western Blot and normalized to the initial timepoint. For this figure, only the upper mature band (m) was quantitated. Representative blots are shown and all blots were stripped and reprobed for actin as a loading control. Data represent the means of three independent experiments. Error bars show standard errors of the mean and *indicates a significant ($p<0.05$) difference as assessed by Student's t-test.

To examine if ROMK1 was primarily degraded in the lysosome in HEK293 cells, I then performed a cycloheximide chase analysis in the presence or absence of the lysosomal protease inhibitor, leupeptin in collaboration with Dr. Paul Welling and Bo-Young Kim of the University of Maryland Medical School, Baltimore. As shown in Figure 19B, the addition of leupeptin reduced the rate of ROMK1 degradation relative to the vehicle control. However, treatment with MG132 had no observable effect on ROMK stability (Figure 19C), indicating that ERAD played a minimal role in degrading ROMK1 in HEK293 cells. These effects were observed for both the mature (m) and immature (i) ROMK species (data not shown). It is important to emphasize that wild type ROMK1 was used in these experiments since the ROMK1$_{S44D+K80M}$ derivative was only needed in yeast to overcome defects in its trafficking/regulation (also see Section 2.4, below). Nevertheless, these data indicate that ROMK1 degradation in mammalian cells is primarily lysosomal and also utilizes the ESCRT and CORVET complexes to deplete ROMK

from the cell surface. Thus, the yeast-based expression system identified evolutionarily conserved trafficking components that influence the biogenesis of human potassium channels in a human kidney-derived cell line.

2.4 DISCUSSION

Surface expression of the ROMK channel in the distal nephron is physiologically downregulated in states of dietary potassium deprivation by clathrin-dependent endocytosis to safeguard against deleterious potassium loss and to maintain potassium homeostasis (Zeng *et al.*, 2002; Al-Qusairi *et al.*, 2017). My studies identify components of the trafficking machinery that may underlie a highly regulated pathway that determines whether internalized channels recycle to the surface or are targeted for degradation in the lysosome. Indeed, my genetic screen in yeast revealed that trafficking components involved in endosomal sorting and trafficking act as negative regulators of ROMK. Particularly noteworthy ROMK regulators included the CORVET subunits Vps3 and Vps8, the ESCRT subunits Vps27, Vps23, Vps36, Vps20, and Snf7. Knockdown of the sole human homologues of Vps23, Vps27, and Vps8 increased density of ROMK at the plasma membrane of HEK293 cells, indicating that negative regulators identified in the yeast screen are also relevant in human cells (Figure 19A).

To explain how inhibition of ESCRT and CORVET genetic components increases ROMK plasma membrane residency, I propose the following model (Figure 20). Deletion or silencing of ESCRT, CORVET, and other endosomal sorting factors shifts the equilibrium of cargo sorting at early endosomes to favor increased recycling of ROMK to the plasma membrane. Evidence for this model is provided by the abrogation of ROMK function in a yeast strain lacking both an ESCRT component and a recycling component (Figure 16Figure 16C). It is likely that deletion or silencing of different components produces the same phenotype through different mechanisms, as divergent recycling pathways originate from different endosomal populations (van Weering and Cullen, 2014; MacDonald and Piper, 2016). Indeed, the subcellular localization of Venus-tagged ROMK differs dramatically between yeast strains lacking ESCRT and CORVET components (Figure 18), despite similar ROMK function in these

strains (Figure 12). With the exception of the *end3Δ* strain, increased ROMK activity is unlikely due to non-specific inhibition of endocytosis, as deletion of ESCRT and CORVET components do not perturb the rate of endocytosis (Luo and Chang, 2000; Wiederkehr *et al.*, 2001).

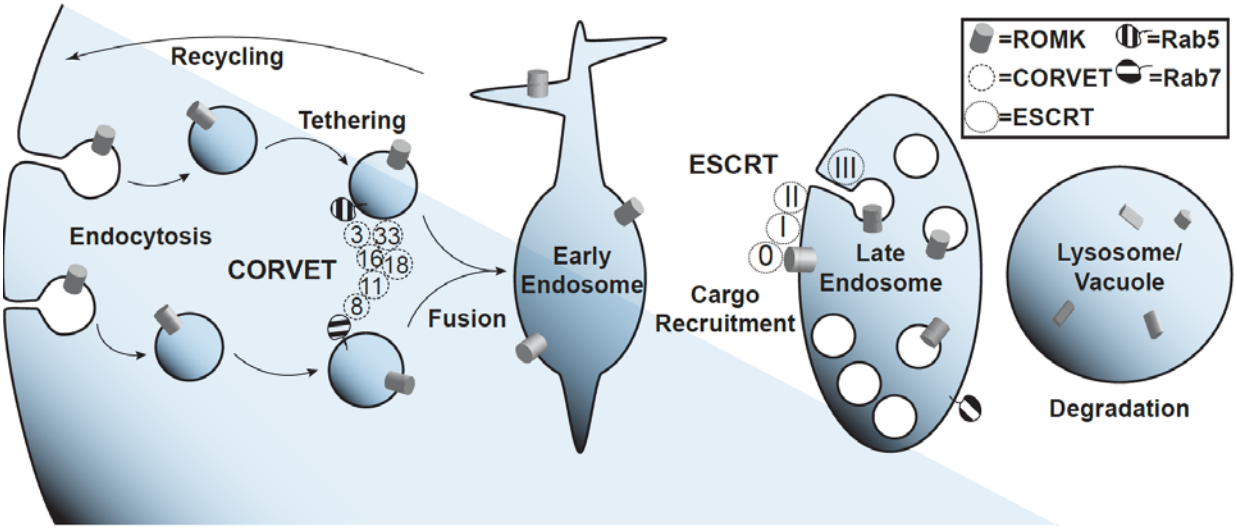

Figure 20: Model of proposed roles for ESCRT and CORVET in ROMK post-endocytic regulation. After endocytosis, ROMK (grey cylinders) accumulates in early endosomes. The hexameric CORVET complex (dotted circles, "Vps" gene numbers indicated) tethers post-endocytic Rab5-positive vesicles to promote their fusion and maturation into early endosomes. ESCRT proteins (dashed circles, complexes 0, I, II, and III) recognize ubiquitinated ROMK and sequester the channel into intra-lumenal vesicles in late endosomes/multi-vesicular bodies. These late endosomes eventually mature and fuse with lysosomes in mammalian cells or vacuoles in yeast, where ROMK is degraded.

The initial screen of the yeast knockout collection uncovered hits in diverse biological pathways, such as endosomal trafficking, mitochondrial function, and translational regulation. I chose to exclude several factors from further analysis as they had been previously identified to act independently of any exogenous potassium channel by altering sensitivity to toxic cations (Barreto *et al.*, 2011). It is possible that the disruption of chromatin remodeling factors such as the RSC complex may phenocopy endosomal trafficking mutants by reducing transcription of

key trafficking components or by affecting cytoskeletal organization (Chai *et al.*, 2002). As endosomal trafficking is an important determinant of a protein's plasma membrane residency, I chose to focus on trafficking factors. Notably, at least one member each of the four ESCRT complexes—ESCRT-0, ESCRT-I, ESCRT-II, and ESCRT-III—was identified as a hit in the initial screen and confirmed by *de novo* strain construction. The first three ESCRTs act sequentially to identify ubiquitinated cargo for recruitment to inwardly-budding membrane invaginations, while ESCRT-III acts as the primary membrane deforming complex that drives intra-lumenal vesicle (ILV) formation (Henne *et al.*, 2013). The ESCRT-0 subunit Vps27 binds ubiquitinated cargo, as does the ESCRT-I subunit Vps23 (Babst, 2005). The ubiquitin-binding subunit of ESCRT-II, Vps36, was also identified in my screen, but as a weaker hit. Since these ubiquitin binding subunits are themselves ubiquitinated, ESCRT is able to recognize both mono- and polyubiquitinated cargoes (Stringer and Piper, 2011). Most ESCRT substrates in yeast are ubiquitinated by the Nedd4 homologue Rsp5 (Erpapazoglou *et al.*, 2012) (Guiney *et al.*, 2016), which I also found contributes to ROMK1$_{S44D+K80M}$ degradation (Figure 16Figure 16B) in accordance with the well-characterized role of Nedd4 in regulating ROMK in the kidney in response to fluctuations in dietary potassium (Ronzaud *et al.*, 2013; Al-Qusairi *et al.*, 2017). Another E3 ligase that acts in the late secretory pathway in yeast, Pib1, can complement Rsp5 activity for some substrates (Shin *et al.*, 2001; Nikko and Pelham, 2009; Kampmeyer *et al.*, 2017). Further study is needed to determine how these respective ligases affect ROMK1 ubiquitination and degradation in the yeast system.

CORVET is a hexameric Rab5-positive vesicle tethering complex consisting of six distinct subunits. Four of these subunits, Vps11, Vps16, Vps18, and Vps33, are also components of the HOPS complex found on Rab7-positive vesicles (Balderhaar *et al.*, 2013). Recent structural studies have shown that these tethering complexes adopt a disordered and highly flexible conformation that coalesces into a tightly ordered structure upon Rab GTPase binding (Bröcker *et al.*, 2012; Chou *et al.*, 2016; Murray *et al.*, 2016). Both of the Rab5-binding subunits that are unique to CORVET, Vps8 and Vps3, were identified in this study as negative regulators of ROMK plasma membrane residence in yeast. Consistent with these data, Vps8 knockdown in mammalian cells increased cell surface expression of ROMK (Figure 12). Strikingly, neither the CORVET/HOPS shared subunits nor the HOPS Rab7-binding subunits were identified as hits in my screen. One model for these data is that CORVET acts upstream of a critical and as yet

uncharacterized sorting step for ROMK (Figure 20). It is also possible that blocking HOPS-mediated tethering arrests ROMK trafficking after it has been packaged into intra-lumenal vesicles by ESCRT and Vps4, at which point its degradative fate is sealed. Trivially, HOPS function may simply be more tolerant of the loss of individual subunits than CORVET. In addition to binding Rab5, Vps8 also contains a RING E3 ubiquitin ligase domain, which is necessary for tethering (Horazdovsky *et al.*, 1996). However, no specific clients for Vps8-ubiquitination have been found. Therefore, Vps8 ubiquitination may be redundant with other E3 ligases acting at endosomes, notably Rsp5 and Pib1 (see above), yet the CORVET-interacting early endosomal SNARE, Pep12, was also identified as a negative regulator of ROMK. These results lead me to hypothesize that CORVET negatively regulates ROMK by promoting endosome maturation and fusion with lysosomes. To my knowledge, my work represents the first study to genetically link CORVET to the regulation of a specific, clinically relevant cargo, as most mechanistic studies of CORVET have utilized synthetic substrates (Galmes *et al.*, 2015).

Other trafficking related genes identified as negative regulators of ROMK include the Golgi-localized SNARE *GOS1*, and the Retromer encoding factors *VPS5* and *VPS35*. The genes were also identified as negative regulators of $K_{ir}2.1$ (Kolb *et al.*, 2014). Retromer is a membrane remodeling complex that facilitates cargo retrieval from endosomes either to the plasma membrane or the *trans*-Golgi network and is generally conceived of as being a “pro-recycling” component, thereby acting in opposition to ESCRT-mediated MVB sorting (Burd and Cullen, 2014). Based on this activity, it is difficult to envision how Retromer functions as a negative regulator of ROMK. However, it is possible that Retromer promotes futile cycling between endosomes and the Golgi, and that a sub population of ROMK is freed and recycled to the plasma membrane through alternative pathways in Retromer mutants. In fact, select cargo have been found in multiple model systems to be enriched at the plasma membrane upon Retromer inhibition (Dang *et al.*, 2011; Xia *et al.*, 2013; Choy *et al.*, 2014).

ROMK may follow a similar trafficking itinerary to that described for the Jen1 lactate permease (Becuwe and Léon, 2014). In this study, the authors demonstrated that endocytosed Jen1 traffics from endosomes back to the Golgi in a Retromer-dependent fashion before transiting back to the endosome and entering the MVB pathway. In this way, Retromer ultimately stimulates protein degradation by promoting the MVB-vacuolar trafficking of cargo proteins. If ROMK follows a similar route, then internalized ROMK would migrate from

endosomes back to the Golgi in a Retromer dependent fashion, but only as a prequel to ROMK trafficking to the MVB-vacuole for degradation.

The results from this study expand upon previous work from the lab with another inward-rectifying potassium channel, $K_{ir}2.1$ (Kolb *et al.*, 2014). Surface expression of both channels was suppressed by many of the same components, identifying the late secretory pathway as a key inhibitory trafficking step for inward rectifying potassium channels. Notably, both channels were primarily ER-localized, with only very small sub-populations detectible at the plasma membrane via sucrose gradient analysis (Kolb *et al.*, 2014) (Figure 15A,B). ROMK and $K_{ir}2.1$ share 42% sequence identity, though neither protein has predicted homology with any endogenous yeast protein (data not shown). Therefore, the yeast trafficking and post-ER degradation machineries may be largely unable to distinguish between the two channels. Nevertheless, I observed some subtle differences. In particular, I found that $K_{ir}2.1$ increased growth rescue better than ROMK1 in all examined cases. I speculate that this is most likely due to stronger inward rectification of $K_{ir}2.1$ (Choe *et al.*, 1999; Hibino *et al.*, 2010), allowing more potassium influx for growth. In contrast, the fact that select genes identified in this study were absent in the prior screen with $K_{ir}2.1$ may have resulted from a higher signal to noise ratio due to differences in conductance properties between ROMK and $K_{ir}2.1$.

The genetic screen described in this report required the use of a non-physiological variant of ROMK1, $ROMK1_{S44D+K80M}$, which contains the phosphomimetic S44D mutation to override an ER-localization signal (Yoo *et al.*, 2005) as well as the K80M mutation to allow ROMK to access its open conformation in the acidic yeast cytosol (Rapedius *et al.*, 2007a; Paynter *et al.*, 2010). My work indicates that the K80M mutation is more important than the S44D mutation in promoting ROMK-mediated rescue on low potassium medium when expressed in the *trk1Δ trk2Δ* strain (Figure 6A). Although I was initially unable to detect a plasma membrane population of $ROMK1_{S44D+K80M}$ by either sucrose density gradient fractionation (Figure 7C) or epifluorescence microscopy (data not shown), a minor fraction of plasma membrane $ROMK1_{S44D+K80M}$ was found in *end3Δ* yeast in which endocytosis is impaired (Figure 14B). Furthermore, rescue of growth on low potassium media correlates directly with increased intracellular potassium (Figure 7B). This result indicates that $ROMK1_{S44D+K80M}$–mediated growth rescue is due to increased potassium influx. Together, it is likely that yeast require only small amounts of $ROMK1_{S44D+K80M}$ at the plasma membrane to achieve sufficient potassium

influx to both increase intracellular potassium and allow growth on low potassium media. These data are consistent with the reported high P_o for ROMK (Choe *et al.*, 1999).

An unforeseen but advantageous consequence of the K80M mutation was that the channel was more ERAD resistant than wild-type ROMK1 in yeast (Figures 6B, 11B,D,F). The Lys-80 side chain is predicted by homology modeling to face the intrasubunit interface of the two transmembrane α-helices and acts as a pH-sensitive gate by hydrogen-bonding with the backbone carbonyl of A177 (Rapedius *et al.*, 2007a).. K80M causes a pronounced acidic shift in ROMK gating, while the reciprocal mutation in K_{ir}2.1 (M84K) introduces an alkaline shift in pH gating (Fakler *et al.*, 1996). While K80 is necessary for acid-sensitivity, occurring at a paralogous position in the other acid-sensitive channels K_{ir}4.x and K_{ir}5.1 but not in the other human K_{ir} channels, it is not sufficient as $ROMK_{K80M}$ still exhibits some low pH gating (Rapedius *et al.*, 2006). A current model to explain pH sensitivity in K_{ir} channels holds that pH-titratable residues are critical for stabilization of the open channel conformation and that pH sensitivity cannot be wholly divorced from channel opening. Accordingly, single mutations that cause an acidic shift in ROMK gating are rare, while those that cause an alkaline shift are quite common (Rapedius *et al.*, 2006). In addition, K_{ir}4.1 homotetramers and K_{ir}4.1/5.1 heterotetramers exhibit different degrees of acid sensitivity, indicating that the "pH sensor" is likely composed of multiple residues (Rapedius *et al.*, 2007b).

It is possible that wild-type ROMK1 residing in the low pH cytosol in yeast is in a closed state that is prone to misfolding, which targets the protein for ERAD. In contrast, the $ROMK1_{S44D+K80M}$ derivative may be more stable in this environment as the K80M mutation destabilizes the closed state of the channel (Rapedius *et al.*, 2007a). Indeed, Dr. Brighid O'Donnell and I recently reported that $ROMK1_{S44D+K80M}$ is less susceptible to *in vitro* proteolysis than wild-type ROMK1 (Figure 6C), and that trafficking-incompetent mutations in ROMK associated with Type II Bartter syndrome destabilize the channel and restore ERAD targeting of $ROMK1_{S44D+K80M}$ (O'Donnell *et al.*, 2017b). It is also noteworthy that neither wild-type ROMK1 nor $ROMK1_{S44D+K80M}$ could rescue growth of potassium-sensitive yeast lacking the ER-resident E3 ubiquitin ligase Doa10 (Figure 21), indicating that inhibiting ERAD is insufficient to promote the forward trafficking of ROMK in yeast. Future studies may wish to examine if the other two mutations known to cause an acidic shift in ROMK gating—I63R and S172T—also decrease ERAD of ROMK in yeast (Schulze *et al.*, 2003; Paynter *et al.*, 2010).

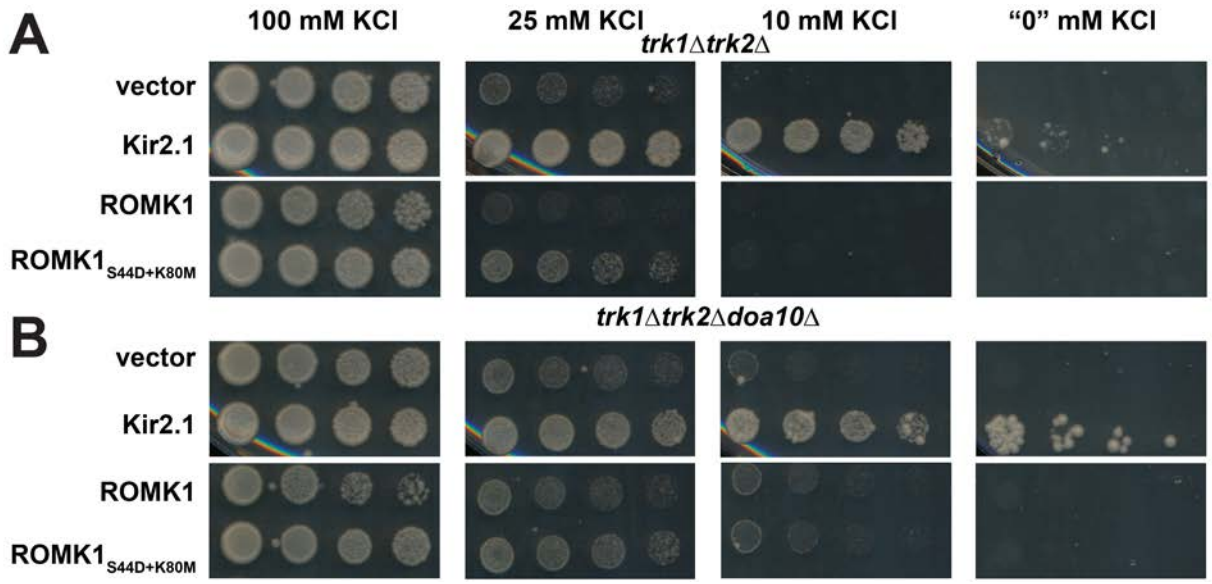

Figure 21: Deletion of ERAD E3 ubiquitin ligase Doa10 does not enhance growth of potassium sensitive yeast expressing ROMK1$_{S44D+K80M}$. Yeast strains with the indicated genotypes transformed with an empty expression vector control or vectors engineered to express Kir2.1, wild-type ROMK1, or ROMK1$_{S44D+K80M}$ were serially diluted onto medium supplemented with the indicated amounts of KCl. Images were captured after two days of growth at 30°C. All experiments were performed in duplicate, and representative assays are shown.

The properties of ROMK1$_{S44D+K80M}$ in yeast are analogous to those of wild-type ROMK1 in mammalian cells, as both are primarily substrates for vacuolar/lysosomal degradation (compare Figure 10B to Figure 19B). Future studies of ROMK in budding yeast should at minimum include the K80M mutation to ensure that the results will be translatable into mammalian systems.

In mammalian cells engineered to inducibly express ROMK1, only a small quantity of the channel resides at the plasma membrane. This necessitated the use of cell surface biotinylation to reproducibly detect it (Figure 19A) as indirect immunofluorescence could only detect an intracellular—primarily ER—ROMK signal (data not shown). The increased cell surface population observed upon silencing of ESCRT and CORVET components might be

further clarified by more efficient knockdown using an siRNA SmartPool or by construction of dedicated gene knockout cell lines via CRISPR. Furthermore, visualization of the plasma membrane ROMK population might be accomplished by immunofluorescence conducted without plasma membrane permeabilization or by total internal reflection fluorescence (TIRF) microscopy. Neither method was pursued in this study as the former would require an extracellular epitope that the R79 anti-ROMK antibody would not recognize (Wade *et al.*, 2011) while the latter requires a fluorescent protein-tagged variant of ROMK.

In conclusion, I have identified key machinery involved in post-endocytic quality control of ROMK. My findings build upon related work on the inwardly-rectifying potassium channel $K_{ir}2.1$ (Kolb *et al.*, 2014), the calcium-gated potassium channel $K_{Ca}3.1$ (Balut *et al.*, 2012), and the voltage-gated potassium channel hERG (Guo *et al.*, 2009; Apaja *et al.*, 2013), adding ROMK to a growing list of channels and transporters regulated by post-endocytic transport (Apaja and Lukacs, 2014). Previous studies of ROMK in yeast focused instead on the identification of ROMK-interaction partners from human cDNA libraries via the yeast two-hybrid method (Bundis *et al.*, 2006; Renigunta *et al.*, 2011a). My report instead represents the first attempt to use a genome-wide screen for negative regulators of ROMK by directly assessing ROMK function in *trk1Δ trk2Δ* yeast.

3.0 CONCLUSIONS AND FUTURE DIRECTIONS

In this section, I will describe how my work advances scientific understanding of ROMK regulation as well as how it fits into the fields of protein trafficking and quality control. I will also propose experiments stemming from my work that might guide future research in the Brodsky lab.

3.1 SIGNIFICANCE OF THIS STUDY

Prior work on the role of protein trafficking in regulating ROMK has focused on ER export and endocytosis. My work is the first to establish post-endocytic trafficking as a mechanism for ROMK degradation.

3.1.1 Known roles of trafficking in ROMK regulation

ROMK is a classic example of an ion channel that must be activated or deactivated through protein trafficking, as gating mechanisms for ROMK are only applicable under conditions of cellular stress. As noted throughout chapter 2, ROMK is steeply gated by low intracellular pH, which may be an adaptation to preserve potassium upon metabolic acidosis. pH gating appears to be tied to its PKA phosphorylation state, and may simply be a mechanism for keeping the dephosphorylated channel closed (Leipziger *et al.*, 2000). Conversely, ROMK channels in the TAL are gated by high intracellular ATP, though this appears to be due to their association with CFTR (an ABC transporter) as ROMK expressed in the absence of CFTR is not ATP-gated (Yoo *et al.*, 2004). This may reflect an adaptation to open the channel under conditions of Na^+/K^+

ATPase stimulation, as occurs following a high potassium meal because the activity of the sodium-potassium pump is a major determinant of intracellular ATP concentration (Welling and Ho, 2009). It is unknown to what extent these gating mechanisms regulate ROMK *in vivo*. In contrast, protein trafficking is widely accepted as the primary means to regulate ROMK (Figure 22).

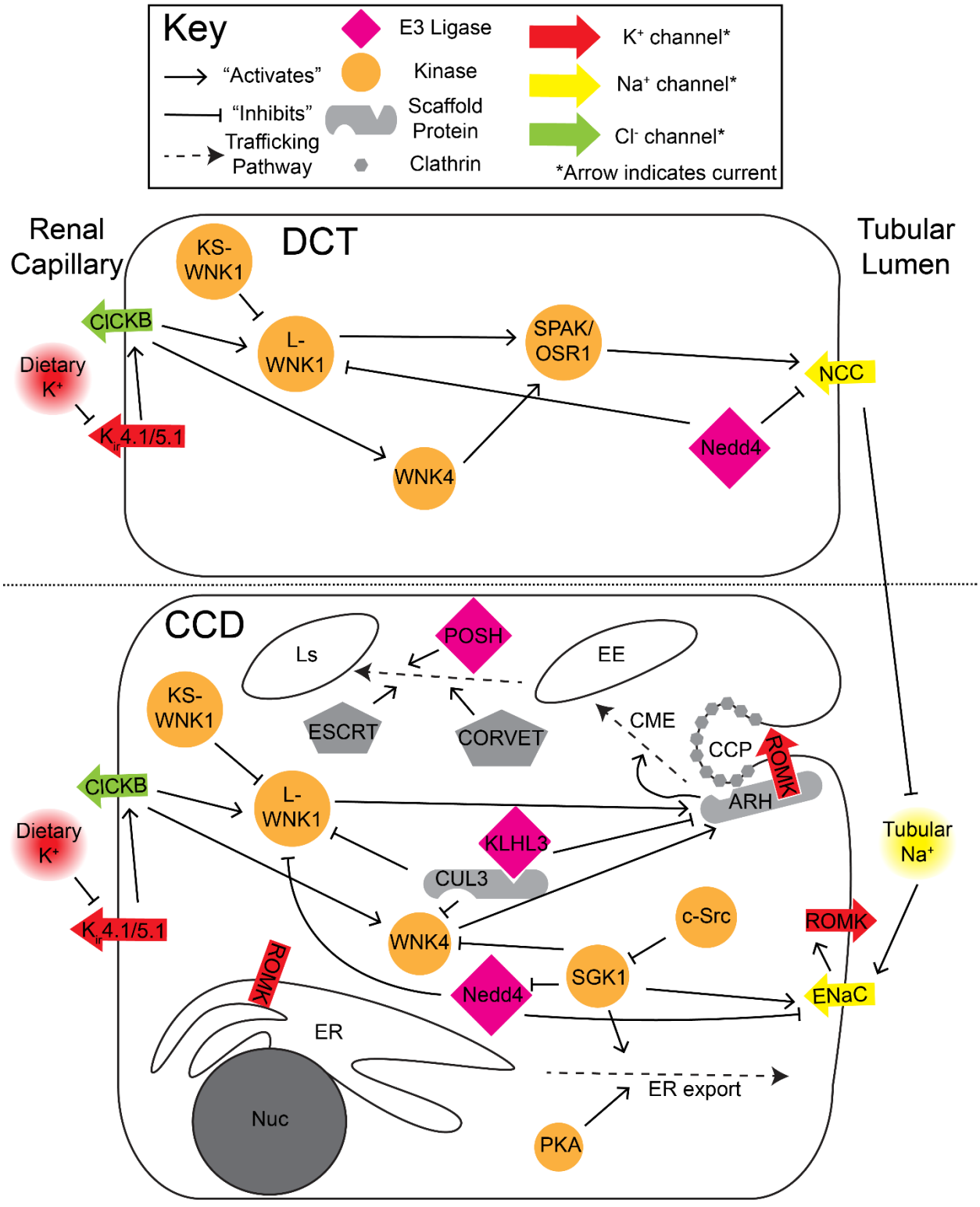
Key
"Activates"
"Inhibits"
Trafficking Pathway
E3 Ligase
Kinase
Scaffold Protein
Clathrin
K+ channel*
Na+ channel*
Cl- channel*
*Arrow indicates current
Renal Capillary
DCT
Tubular Lumen
KS-WNK1
ClCKB
L-WNK1
SPAK/OSR1
NCC
Dietary K+
Kir4.1/5.1
Nedd4
WNK4
CCD
Ls
POSH
EE
ESCRT
CORVET
CME
CCP
ROMK
ARH
KLHL3
CUL3
c-Src
SGK1
ENaC
Tubular Na+
ER
Nuc
ER export
PKA

Figure 22: Visual summary of known regulatory mechanisms for ROMK in the distal nephron. Increases in bloodstream potassium cause depolarization of the basolateral membrane in the distal nephron, setting off a WNK-mediated signaling cascade that activates NCC in the distal convoluted tubule (DCT) and ROMK in the cortical collecting duct (CCD). Other known regulatory mechanisms are shown as applicable. Abbreviations not described in text: Nuc=nucleus, EE=early endosome, Ls=lysosome.

ROMK contains a C-terminal RXR motif and is thus largely retained within the ER. ER export of ROMK is stimulated by channel phosphorylation at one N-terminal and two C-terminal serines. Two kinases are known to be involved in regulating ER retention: protein kinase A (PKA) and serine glucocorticoid kinase-1 (SGK1) (McNicholas *et al.*, 1998; Yoo *et al.*, 2003). SGK1 is transcriptionally upregulated by the mineralocorticoid hormone aldosterone, which is known to stimulate potassium excretion from the distal nephron. For a time, aldosterone signaling was believed to be the primary driver of ROMK apical expression, however recent evidence suggests that ROMK is not directly regulated by aldosterone and that upregulation of ROMK can occur in animals completely insensitive to aldosterone signaling (Todkar *et al.*, 2015). Therefore, the currently favored model is that the distal nephron is capable of directly sensing dietary potassium and stimulating or repressing ROMK endocytosis accordingly (Boyd-Shiwarski and Subramanya, 2017).

Cells in the distal nephron tubule also express potassium channels at their basolateral surface. These channels, K_{ir}4.1/5.l, allow for electroneutral chloride reabsorption into the blood via the chloride channel ClC-KB (Hennings *et al.*, 2017). As these channels are also inward rectifiers, they are exquisitely sensitive to small changes in plasma potassium. A spike in plasma potassium will depolarize the basolateral membrane, thereby inhibiting chloride reabsorption (Cuevas *et al.*, 2017). An increase in intracellular chloride represses the “with-no-lysine” (WNK) kinases, which serve as master regulators of renal sodium/potassium balance (Kahle *et al.*, 2008; Shekarabi *et al.*, 2017).

With-no-lysine is a misnomer, as the lysine in the kinase domain of the WNKs is simply in an unconventional orientation that inactivates the kinase domain upon binding intracellular

chloride (Piala *et al.*, 2014). This unique regulatory mechanism allows WNK activation by changes in membrane voltage, allowing cells to mount a rapid response to changes in electrolyte balance. WNK1 and WNK4 are both expressed in the distal nephron and regulate ROMK function through a two-pronged mechanism. First, in the distal convoluted tubule (DCT), which expresses the sodium-chloride cotransporter (NCC)—but neither ROMK nor the epithelial sodium channel (ENaC)—WNK kinases phosphorylate SPAK, which in turn phosphorylates and activates NCC (Figure 22). Increased sodium reabsorption in the DCT results in less sodium delivery to the downstream CCD, thus hyperpolarizing the CCD apical membrane and stimulating ROMK (Terker *et al.*, 2015). Second, both WNK1 and WNK4 promote ROMK endocytosis in the CCD.

ROMK residence at the plasma membrane is known to be regulated by clathrin-mediated endocytosis (CME) (Zeng *et al.*, 2002). Apical membrane ROMK is recruited to clathrin-coated pits (CCPs) by the scaffold protein ARH, which binds both ROMK and the clathrin adaptor complex AP-2 (Fang *et al.*, 2009). ARH is polyubiquitinated by the E3 ligase complex CUL3/KLHL3, targeting it for proteasomal degradation; however, ARH phosphorylation by WNK1 or WNK4 antagonizes ARH ubiquitination (Paul Welling, personal communication). CUL3/KLHL3 also polyubiquitinate WNKs, promoting their turnover by the proteasome (Shibata *et al.*, 2013). Finding the upstream regulators of this E3 ligase complex is an active area of investigation.

Both WNK1 and WNK4 are downregulated in response to dietary potassium loading. WNK4 is inactivated by SGK1 phosphorylation (Ring *et al.*, 2007), which in turn is inactivated by the known osmoregulatory kinase c-Src (Lin *et al.*, 2015). WNK1 is expressed as two isoforms: the full-length or “long” isoform (L-WNK1) expressed throughout the kidney and in other tissues, and the shorter “kidney-specific” isoform, which is unique to the distal nephron. KS-WNK1 lacks a kinase domain, but inhibits L-WNK1 function by mediating reversible sequestration of WNK1 and related kinases into liquid-liquid phase-separated “WNK bodies” (Boyd-Shiwarski *et al.*, 2018).

Ubiquitination has long been known to negatively regulate ROMK surface abundance (Lin *et al.*, 2005), though the identity of the E3 ligases responsible is not entirely clear. Nedd4-2 (a homologue of yeast Rsp5) is an abundant E3 ligase in the distal nephron with well-established roles in promoting endocytosis and lysosomal degradation of various substrates (Tardiff *et al.*,

2013). While Nedd4-2 promotes degradation of ENaC, NCC, and WNK1 (Rotin and Staub, 2011; Al-Qusairi *et al.*, 2016, 2017), thus affecting renal salt handling, it is uncertain whether Nedd4-2 directly ubiquitinates ROMK. Nedd4-2 recognizes (L/P)PXY motifs, which are present in ENaC, NCC, and WNK1, but not in ROMK. Therefore, if Nedd4-2 ubiquitinates ROMK, it will require an intervening adaptor protein, such as an α-arrestin (Becuwe *et al.*, 2012) (also see Appendix B). However, POSH, a RING-domain E3 ligase, has been shown to directly ubiquitinate and promote the lysosomal degradation of ROMK in the CCD (Lin *et al.*, 2009), yet it is uncertain whether POSH acts at the plasma membrane or in endosomes.

3.1.2 Endosomal sorting as a previously uncharacterized mechanism of ROMK regulation

The vast majority of ROMK studies have examined the channel in its native context of the mammalian nephron or more commonly in heterologous expression systems. Yeast are neither kidneys nor kidney-derived cells and therefore lack much of the signaling machinery described in the previous section, but consequently the yeast model provides an opportunity to answer specific questions about the default pathways that regulate ROMK protein trafficking and quality control. Apart from the experimental pliability mentioned in Chapter I, the yeast system affords us the opportunity to ask which mechanisms *dominate* ROMK regulation in a minimal cellular system. Specifically, my research has implicated the protein trafficking pathway as a major regulator of ROMK. Silencing of ESCRT and CORVET components in mammalian cells also increases ROMK surface expression, suggesting that a key regulatory decision for this channel occurs in endosomes, rather than in the ER or at the plasma membrane.

An endocytosed protein is by no means doomed to degradation, as various mechanisms alter the kinetics of recycling endocytosed material to the plasma membrane or degrading a substrate via the ESCRT/MVB pathway. For example, some plasma membrane proteins contain sorting motifs that target them to specific sorting pathways after endocytosis, but the default pathway for most endocytosed proteins is recycling (van Weering and Cullen, 2014). However, ubiquitination strongly shifts the sorting equilibrium towards degradation as specific components in ESCRT recognize this modification (Shields and Piper, 2011). Post-endocytic sorting is well-established as a regulatory mechanism for many other membrane proteins, including ion

channels such as CFTR (Sharma *et al.*, 2004; Okiyoneda *et al.*, 2018), hERG (Apaja *et al.*, 2013), $K_{Ca}2.3$ (Gao *et al.*, 2010), and $K_v1.1$ (Seebohm *et al.*, 2007). My work represents the first demonstration of ESCRT-mediated regulation of ROMK.

While ubiquitination promotes ROMK lysosomal degradation (Lin *et al.*, 2005), it is unclear whether ubiquitination occurs at the plasma membrane to promote endocytosis or in the endosome to promote sorting into MVBs. I hypothesize that ROMK ubiquitination occurs after endocytosis due to the following lines of evidence: 1) The non-enzymatic scaffolding protein ARH is sufficient to promote CME of ROMK as it binds directly to both clathrin and to an NPXY internalization motif in the C-terminal domain of ROMK (Fang *et al.*, 2009); 2) POSH, the only E3 ligase known to ubiquitinate ROMK in the distal nephron (see above), appears to act downstream of dynamin scission (*i.e.* the final step in CME) (Lin *et al.*, 2009); 3) POSH is localized primarily at early endosomes rather than the plasma membrane (Kim *et al.*, 2006). Similarly, another endosome-localized E3 ligase, RFFL, was recently shown to promote ubiquitination and degradation of endocytosed ΔF508-CFTR (Okiyoneda *et al.*, 2018); 4) The Welling and Staub groups have gathered evidence that an endosome-localized transmembrane Nedd4 adaptor, NDFIP1, promotes lysosomal degradation of ROMK (Paul Welling, personal communication). In accordance with these unpublished data, I found that the yeast NDFIP1 homologue, Bsd2, negatively regulates ROMK function in *trk1Δ trk2Δ* yeast (Figure 13B) and that the Nedd4-2 homologue Rsp5 facilitates $ROMK1_{S44D+K80M}$ degradation (Figure 16B).

3.1.3 Limitations of this study

It is important to highlight several limitations of this work, which are important to consider in light of my discoveries. Such considerations may also direct future efforts in which the yeast system is used to screen for effectors of potassium channel biogenesis.

First, which factors control the balance of ROMK recycling and degradation from endosomes? Is the process stochastic or is it under regulatory selection? This study falls short of answering such questions as the major findings implicate only the machinery of endosomal sorting rather than a high-level regulator such as an E3 ligase. The heterology between yeast and mammals is significant, and many proteins known to regulate ROMK in the kidney—such as ARH or the WNK kinases—lack obvious yeast homologues. Additional research is needed to

determine how cellular signaling pathways might alter the kinetics of ROMK recycling and degradation. As mentioned above, the role of ubiquitin in determining this equilibrium should be pursued.

Second, although the SGA screen conducted in this study ultimately produced verifiable results that were reproducible in mammalian cells (chapter 2), there are several caveats to this technique that bear mention. The raw data from the study were measurements of yeast growth on solid media, which are readily saturable and not necessarily linear. I have shown that increased growth positively correlates with increased cellular potassium through ICP-MS (Figure 6B), but this approach is hardly adaptable to high-throughput analysis. An alternative approach that lends itself better to precise quantitation would be to devise a colorimetric intracellular potassium sensor that would allow precise measurement of ROMK-mediated potassium uptake via a plate reader or FACS sorter. Dr. Jerod Denton's group has devised such a scheme for use with mammalian cells that utilizes a thallium-sensitive dye (Tl^+ is known to readily transit potassium channels) (Raphemot *et al.*, 2013). In addition, a genetically encoded fluorescent protein-based intracellular potassium sensor that is active over a wide range of potassium concentrations and is non-toxic was recently described (Bischof *et al.*, 2017).

Third, the use of *trk1Δ trk2Δ* yeast for the screen precluded any two-tail analysis of hits as this system—at least under the conditions in which I performed my screen—cannot detect mutants which cause decreased growth on low potassium media. Given that ROMK function is linked to hypertension and there is strong interest by academic and industrial research groups to identify ROMK inhibitors (see Section 1.2.1), a yeast screen to identify novel positive regulators of ROMK could yield valuable insight. Such a screen might be feasible using *ena1-4Δ nha1Δ* as a query strain (Bañuelos *et al.*, 1998) (section 1.1.2).

Fourth, although many gene networks in multicellular eukaryotes are generally simpler in yeast (for example, yeast have 11 Rab GTPase genes while humans have over 60 (Stenmark and Olkkonen, 2001)), the yeast genome is rife with paralogues due to an ancestral genome duplication (Kellis *et al.*, 2004). This can make single gene analysis problematic as one paralogue is often able to completely functionally substitute when its counterpart is deleted. Consequently, screens in which single mutants are analyzed will—by definition—miss functionally redundant genes

Fifth, the lore among researchers who have utilized the yeast knockout collection is that about 10-20% of the genes are incorrectly annotated. I certainly found this to be the case in my own endeavors to confirm the genotype of strains of interest (data not shown). In addition, due to the highly compact genome of *S. cerevisiae*, the knockout collection suffers from the "neighboring gene effect" whereby a phenotype ostensibly attributable to an annotated deletion is in fact due to a loss of function of another gene nearby on the chromosome (Ben-Shitrit *et al.*, 2012). It is also worth noting that some gene deletions give rise to profound compensatory effects at the chromosomal level. In a recent example, deletion of a gene that plays a role in ERAD led to a duplication of a functionally similar but non-homologous gene in another region of the genome, resulting in dosage-dependent suppression of the desired mutant phenotype (Neal *et al.*, 2018).

Finally, the decision to recreate hits from the initial SGA screen via mating and tetrad dissection was a response to difficulties in reproducing many initial hits from the screen (data not shown). This vexing phenomenon led to eventual abandonment of several initially exciting hits (see Appendix C). Poor screen reproducibility is a recognized problem in the SGA community (Giaever and Nislow, 2014), but in my case, I believe that the use of *trk1Δ trk2Δ* as a query strain may have exacerbated the problem. This strain exhibits well-characterized growth defects even on high potassium medium (Navarrete *et al.*, 2010) and the long growth times involved in SGA methods may have driven a rate of phenotypic suppression higher than otherwise expected. Ideas to resolve some of these known pitfalls in future genetic screens are described in the next section.

3.2 FUTURE DIRECTIONS

I am currently conducting a random mutagenesis screen to identify and characterize intragenic gain-of-function mutations in ROMK, which is being assessed by increased growth of *trk1Δ trk2Δ* yeast on low potassium medium. This project is described in detail in Appendix A of this document. If I were advising an incoming graduate student on potentially exciting research opportunities related to my work, I would recommend the following lines of inquiry.

3.2.1 Short term future directions

A lingering question from my work is the specific role played by ubiquitination and individual E3 ligases in the regulation of ROMK degradation. Monoubiquitination is established as a mechanism for negative regulation of ROMK in mammalian kidneys (Lin *et al.*, 2005) My work has implicated the ER-localized E3 ligases Hrd1 and Doa10 in degradation of wild-type ROMK1, but not of ROMK1$_{S44D+K80M}$, in yeast (Figure 11C,D). In contrast, ROMK1$_{S44D+K80M}$ degradation is dependent on the post-ER quality control E3 ligase Rsp5, while wild-type ROMK1 is not (Figure 16Figure 16A,B). I also tested the degradation of wild-type ROMK1 and ROMK1$_{S44D+K80M}$ in yeast deleted for the Golgi-localized E3 ligase Tul1 and the endosome-localized E3 Pib1, which have been shown to regulate the residence and degradation of select membrane proteins in yeast (Shin *et al.*, 2001; Reggiori and Pelham, 2002), but found no evidence for altered degradation (data not shown).

It would be fairly simple to test whether or not ROMK variants are ubiquitinated in yeast by immunoprecipitating ROMK from yeast lysate and immunoblotting for ubiquitin (for recent examples from our group, see (Kolb *et al.*, 2014; Ye *et al.*, 2017). However, analysis of these assays can be difficult as yeast have over 60 predicted E3 ligases (as a point of contrast, humans encode ~600), many of which have redundant client sets (Finley *et al.*, 2012). In principle, one might expect to detect an E3 ligase bound to ROMK through co-immunoprecipitation, however such E3-client associations are often transient and low-affinity. Some groups have approached this problem by making ubiquitination-proof substrates that lack all lysines, however this method is laborious and very likely to deleteriously affect protein folding and/or function. An alternate approach is to inactivate the active site in an E3, which may facilitate substrate capture. In contrast, the Piper lab has devised a method for connecting E3 ligases with clients that does not rely on gene deletions or genetic ablation. Fusing a protein of interest to a non-specific deubiquitinating peptidase (DUb) from herpes virus renders that protein effectively nonubiquitinable (Stringer and Piper, 2011). They have also constructed a library of dominant negative DUb-E3 fusion proteins that not only abrogate the ubiqutinating activity of their wild-type counterpart, but also of any other E3 ligases with overlapping client sets (MacDonald *et al.*, 2017). Screening this library for dominant negative E3-ligases that alter ROMK ubiquitination as assayed by immunoprecipitation would likely isolate functionally dominant ligases. The effect of

these ligases on ROMK degradation kinetics could then be assessed by cycloheximide chase. If endosomal sorting is, in fact, the predominant mechanism of ROMK1$_{S44D+K80M}$ regulation in yeast, I would expect that DUb-E3 fusions that abrogate ROMK degradation would also have a phenotype similar to ESCRT mutant strains: increased potassium uptake and defective sorting into the vacuolar lumen (Figures 6,12,18).

If Rsp5 is shown to be a predominant factor in ROMK endosomal sorting and degradation, it will require an adaptor protein as an intermediate. Rsp5 has a very particular client set defined by the (L/P)PXY consensus motif (Belgareh-Touzé *et al.*, 2008), which ROMK lacks. The transmembrane endosomal Rsp5 adapter Bsd2 seems like a promising candidate as deleting it causes increased growth on low potassium (Figure 13) and work from the Staub and Welling labs has shown that a human homologue of Bsd2, NDFIP1, also negatively regulates ROMK. It would be interesting to test whether ROMK ubiquitination is decreased in *bsd2Δ* yeast or in yeast expressing a Bsd2-DUb fusion.

Other Rsp5 adaptors that could conceivably regulate ROMK are the α-arrestins. These cytosolic adaptor proteins regulate a variety of yeast nutrient permeases in response to environmental changes (Lin *et al.*, 2008; O'Donnell, 2012; O'Donnell *et al.*, 2013). There are nine α-arrestins expressed in yeast, many with overlapping client sets, and most with an obvious paralogue resulting from whole genome duplication (Nikko and Pelham, 2009). Despite their highly specialized role in controlling the yeast plasma membrane proteome, Dr. Allyson O'Donnell has shown that overexpression of specific α-arrestins increases K$_{ir}$2.1 function and plasma membrane residence in yeast (Appendix B, O'Donnell *et al.*, *JBC*, in revision). This is a remarkable result given that yeast do not express any inward-rectifying potassium channels. Key experiments from Dr. O'Donnell's study could be easily replicated with ROMK1$_{S44D+K80M}$ given that ROMK and K$_{ir}$2.1 share 42% primary structure identity. In addition, α-arrestins are expressed in mammalian cells and it would be worthwhile to test whether knockdown or overexpression of mammalian α-arrestins affects ROMK surface expression using the ROMK-inducible HEK 293 cell line (Figure 19).

While the *trk1Δ trk2Δ* and *ena1-4Δ nha1Δ* strains have been traditionally used to study potassium channel function, there is in principle no reason why they could not be adapted to study other families of exogenous disease-related ion channels. The *ena1-4Δ nha1Δ* strain seems particularly amenable to this as it exhibits high sensitivity to all alkali metals (Bañuelos *et al.*,

1998). My colleague Dr. Teresa Buck has published several papers on using yeast to identify pro-degradative factors for the epithelial sodium channel (ENaC) (Buck *et al.*, 2013, 2017; Kashlan *et al.*, 2018), however our group has been unable to devise a phenotypic assay for ENaC function. In principle, such an assay would test for decreased growth on high sodium of ENaC-expressing *ena1-4Δ nha1Δ* yeast. This would enable a number of studies using yeast to screen for novel regulators of an ion channel functionally and structurally unrelated to any potassium channel. Current efforts toward this goal are underway in collaboration with Dr. Buck.

3.2.2 Long term future directions

As previously mentioned, there are 15 inward-rectifying potassium channels expressed in humans, and thus far only two, ROMK and K_{ir}2.1, have been analyzed in yeast SGA screens. Other K_{ir} channels that might benefit from such an analysis include K_{ir}3.2 (GIRK2), which has been tied to epilepsy and intellectual disability in Down's syndrome (Rachidi and Lopes, 2007), and K_{ir}4.1, a renal K_{ir} channel expressed on the basolateral surface of distal nephron epithelium that senses changes in blood potassium (Cuevas *et al.*, 2017). K_{ir}4.1 in the kidney forms mixed channels in a 2:2 stoichiometric ratio with K_{ir}5.1 (Paulais *et al.*, 2011), distinguishing it from the homomeric K_{ir} channels described thus far.

Recent advances in yeast genetic technology may allow future SGA screens to avoid issues of low reproducibility when working with a "sick" query strain such as *trk1Δ trk2Δ*. "Traditional" SGA screens on solid medium are now routinely performed by specialized robotic manipulators, which analyze each library strain in quadruplicate. This helps correct for suppressor mutations and experimental artifacts as it is unlikely that such random events would affect all four replicates equally. Data analysis for automated manipulations is also greatly streamlined (Wagih *et al.*, 2013). In addition, advances in DNA sequencing technology enabled SGA screens to be conducted in liquid medium. For example, a version of the yeast knockout collection in which each deletion cassette is marked with a unique DNA barcode is pooled and mated with a query strain to generate a library containing every possible gene deletion. This strain collection is then transferred into permissive and selective liquid growth medium, aliquots are withdrawn periodically, and the relative growth rates of the deletion strains in the pool are

determined by quantitative PCR targeting the deletion barcodes (Pierce *et al.*, 2007). This approach allows for more quantitative ranking of growth rates than analysis of images from solid growth media, which instead relies on image processing that is inexact and easily saturable.

Another approach to deal with growth defects in the *trk1Δ trk2Δ* SGA query strain would be to redesign it to have inducible rather than constitutive knockout of one or both *TRK* genes. In this experimental design, expression of the native potassium transporters would be normal during the process of array construction and then suppressed just before the final transfer onto permissive and selective media. This approach is common in multicellular eukaryotes in which constitutive knockouts are often lethal or induce compensatory effects that confound analysis. There are a number of techniques for controlled repression of a protein in yeast, including repressible promoters such as *GAL4* or the Tet-off system as well as directly targeting mature proteins via the auxin-inducible degron system (Nishimura *et al.*, 2009).

Whether protein multimerization is rate limiting for transport from the ER is an important and generally open question in both the ion channel biology and the ER proteostasis fields. Ion channels are known to vary greatly in their propensity to multimerize. Some channels multimerize co-translationally, as evidenced by fully assembled $K_v1.3$ channels associated with ribosomes (Lu *et al.*, 2001), while others appear to multimerize only after translation and translocation is complete, as evidenced by specialized C-terminal domains that mediate multimerization in retinal rod cells (Zhong *et al.*, 2003). Multimeric ion channels assemble inefficiently upon *in vitro* translation, suggesting that multimerization requires a distinct set of extrinsic factors (Papazian, 1999). Indeed, hERG and its paralogues require specialized transmembrane chaperones that are conserved from nematodes to humans to mediate channel multimerization (Li *et al.*, 2017). Furthermore, post-translational assembly of heterogenous subunits has been proposed as a regulatory mechanism for the functionally heterotrimeric channel ENaC (Butterworth *et al.*, 2008).

Multiprotein complexes must correctly and completely assemble prior to ER exit. ERAD has been shown to degrade “orphaned” subunits of large ER protein complexes such as the oligosaccharyl-transferase (OST) complex (Mueller *et al.*, 2015). When mutations in a functional multimeric protein increase targeting for ERAD, they may do so by affecting either monomer folding or multimer assembly. ROMK tetramerization appears to involves several sites of intersubunit contact involving the N- and C- termini as well as the transmembrane helices

(Koster *et al.*, 1998). A few functionally important residues that mediate intersubunit contact have been identified (Leng *et al.*, 2006), and it is currently unknown if any Bartter syndrome-associated mutations interfere with tetramerization. To test whether or not a residue is involved in tetramerization, a mutant subunit and a wild-type subunit tagged with different epitopes could be co-expressed and co-immunoprecipitated under non-denaturing conditions. In addition, multimerization could be directly observed by immunoprecipitation followed by native PAGE or by resolution of tetramers and monomers on a size exclusion column (see for example (Preston *et al.*, 2018)). In addition to ROMK, the renal K_{ir}4.1/5.1 channel would be a good candidate for studying multimerization as it forms an obligate heterotetramer

The ER chaperones that mediate hERG tetramerization, DNAJB12 and DNAJB14, are transmembrane proteins containing a cytosolic J-domain (Li *et al.*, 2017). It is currently unknown whether these or other J-proteins promote tetramerization of any K_{ir} channels. J-domains are known to act as Hsp70 cochaperones by increasing Hsp70's substrate specificity and kinetics of substrate binding and release. There are 41 J-proteins in the human genome, exhibiting great functional and structural divergence (Kampinga and Craig, 2010). A small scale siRNA screen targeting these J-proteins in ROMK-expressing HEK 293 cells using the colorimetric thallium uptake assay developed by the Denton lab as a functional readout (Raphemot *et al.*, 2013) would determine whether or not any of them had a role in ROMK tetramerization.

Ultimately, renal ion channels and transporters are best understood in the context of the mammalian kidney. The use of the Tet-on Cre-Lox recombinase system expressed only in specific nephron segments has enabled inducible knockout or modification of many components of the ROMK regulatory pathway (*e.g.* (Todkar *et al.*, 2015; Grimm *et al.*, 2017)). Using such a system to knockdown a component of CORVET and ESCRT in the distal nephron of adult mice would likely induce hypokalemia due to ROMK overactivation at the apical membrane. While laborious, such a system would undoubtedly serve as an ultimate proof-of-principle implicating endosomal sorting in ROMK regulation.

The work presented herein focuses almost exclusively on ROMK1, however future studies should validate whether endosomal sorting also regulates ROMK2. Aside from their different tissue expression patterns (section 1.2.1 and Figure 4), the two isoforms display different subcellular localization patterns in their respective cell types. In rodent kidneys,

ROMK2 is invariantly localized to the apical plasma membrane of TAL cells while ROMK1 is confined to the ER of CCD cells unless the animal is challenged with a high potassium diet (Yoo *et al.*, 2005; Renigunta *et al.*, 2011b). This disparity between the two isoforms puzzles researchers as the two isoforms differ by only a 19 amino acid N-terminal extension present in ROMK1 but absent in ROMK2. These 19 amino acids do not contain any obvious linear sorting motifs nor do they alter electrophysiological properties. Two hypotheses spring to mind: either the extra 19 amino acids in ROMK1 promote its ER retention through an as yet uncharacterized mechanism, or the different cellular itineraries of the two isoforms arise from *trans*-acting regulatory factors that may be active in the TAL but not the CCD or *vice versa*. To distinguish between these two possibilities, future studies should attempt to disrupt only the exon of *KCNJ1* encoding the ROMK1 N-terminal extension while leaving the rest of the gene intact, effectively forcing expression of ROMK2 in the CCD. If the 19 additional amino acids of ROMK1 are a *cis*-acting factor that promotes ER retention, I would hypothesize that replacing ROMK1 with ROMK2 in the CCD would cause strong apical surface expression of ROMK leading to potassium wasting and hypokalemia.

APPENDIX A

A SCREEN FOR ROMK GAIN-OF-FUNCTION MUTATIONS

This project was developed in collaboration with undergraduate researcher Jackson Parr and graduate rotation student Nga (Katie) Nguyen, both with my supervision and mentorship. This project is ongoing and this appendix represents its status as of March 2018.

A.1 INTRODUCTION

Hypertension is the greatest single cause of human mortality worldwide (Murray and Lopez, 2013). While many environmental and lifestyle factors have been linked to hypertension, the condition is commonly known to run in families and its heritable contribution is estimated at 30-60% (Kupper *et al.*, 2006). Due to the diversity and complexity of signaling pathways and organ systems that modulate blood pressure, heritable hypertension is presumably highly polygenic. The salt-handling channels and transporters of the distal nephron are prime regulators of extracellular fluid volume and blood pressure. Loss of function mutations known to cause Bartter syndrome and Gitelman syndrome in the genes encoding NKCC2, NCC, and ROMK are associated with a mild decrease in blood pressure in heterozygous individuals (Ji *et al.*, 2008). This is likely due to decreased distal nephron sodium reabsorption via NKCC2 and ENaC in these individuals, leading to a reduction in blood volume and pressure that nevertheless falls within the healthy range.

If a loss-of-function mutation in ROMK lowers blood pressure, it follows that a gain-of-function mutation in ROMK will increase blood pressure. These mutations might be part of a cadre of polymorphisms that synergize to increase the risk of hypertension; however, when the effects of each mutation are considered in isolation they may lie below threshold of detection. Due to this presumed uncertainty, there is no reliable way to predict whether a polymorphism in ROMK identified by genome-wide association studies (GWAS) causes gain-of-function. Conversely, we know which polymorphisms cause loss-of-function because they have been identified in patients with the monogenic trait Type II Bartter Syndrome. Therefore, an experimental approach to identify gain-of-function mutations in ROMK would be a great asset in identifying the genetic factors responsible for heritable hypertension.

Random mutagenesis screens in *trk1Δ trk2Δ* yeast offer a straightforward approach to identifying gain-of-function mutations in ROMK or other K_{ir} channels (see section 1.1.5). In collaboration with two junior researchers, I designed and implemented such a screen for $ROMK1_{K80M}$. I decided to perform the screen in the presence of the K80M mutation as a prior random mutagenesis screen had been frustrated by an overwhelming bias for that particular amino acid substitution (Paynter *et al.*, 2010). This is undoubtedly due to the salubrious effect of deleting the pH gate on ROMK function in yeast (see section 2.3.1, Figure 6, 7).

A.2 MATERIALS AND METHODS

All yeast were propagated at 30^{o}C as previously described (section 2.2.1). $ROMK1_{K80M}$ in the yeast expression vector pRS415 (O'Donnell *et al.*, 2017b; Mackie *et al.*, 2018) under the control of the *TEF1* promoter and the *CYC1* terminator (Mumberg *et al.*, 1995) was amplified by PCR with Go-Taq DNA polymerase (Promega, Madison, WI) for 35 cycles according to the manufacturer's instructions. The oligonucleotides were used to guarantee ~100 bp of homology to the pRS415 backbone upstream and downstream of the ROMK ORF to facilitate yeast gap repair. Taq (*Thermophilus aquaticus*) DNA polymerase has an estimated error rate of 1 in $2.28x10^{-5}$. Therefore, the number of cycles was chosen to favor an average of one error per 1.4 kbp amplicon. After PCR, the amplicons were purified from an agarose gel to remove any

template DNA. In parallel, the pRS415 vector containing the *TEF1* promoter and the *CYC1* terminator, but lacking an ORF, was restriction digested with Fast Digest BamHI and XhoI (Thermo) per the manufacturer's instructions. Linearized vector and mutagenized cassette were transformed into *trk1Δ trk2Δ* yeast using a slightly modified lithium acetate transformation protocol (Ito *et al.*, 1983) in which the yeast were rotated overnight at room temperature after the addition of PEG and the cells were treated with 10% ethanol during the last 5 min of heat shock. Transformed yeast were grown for three days at 30ºC on SC-leu medium supplemented with 100 mM KCl. They were then replica plated onto SC-leu medium supplemented with 100, 25, 10, and 0 mM KCl. After two days of incubation at 30ºC, any colonies observed to be growing robustly on both the 10 and 0 mM plates were restruck for further analysis. Plasmids were isolated from these cell by lysing them with glass beads followed by a Qiagen mini-prep. The plasmids were then transformed into chemically competent *E. coli*, re-isolated, and transformed into naïve *trk1Δ trk2Δ* yeast. These yeast were then arrayed in a serial dilution assay as previously described (section 2.2.1). Clones able to reproducibly rescue *trk1Δ trk2Δ* growth on low potassium medium were analyzed by Sanger sequencing (GENEWIZ, South Plainfield, NJ).

A.3 RESULTS AND DISCUSSION

To generate a library of gain-of-function ROMK mutants, $ROMK1_{K80M}$ was amplified with error-prone PCR and transformed into *trk1Δ trk2Δ* yeast along with a linearized expression vector to facilitate gap repair (Weir and Keeney, 2014). Putative gain-of-function clones were confirmed by purification and retransformation of *trk1Δ trk2Δ* yeast (Figure 23C).

After four independent iterations of the mutagenesis protocol, we identified identical mutations in multiple independent clones, indicating that the screen is nearly saturated. We estimate the incidence of gain-of-function clones at 0.92%, assuming an average error rate of one per amplicon. These data indicate that the acquisition of a gain-of-function mutation is a rare event and likely confined to select amino acids. However, it is possible that the GoTaq PCR error rate is higher than the published value. Further study is needed to determine whether or not we have achieved our targeted error rate.

The mutations identified thus far are summarized in Table 7 and Figure 23A, including several in the HA tag. Although the tag does not appear to interfere with channel conductance in *Xenopus* oocytes (Yoo *et al.*, 2003), it is possible that the tag interferes with channel function in yeast, and that the mutations suppress this activity. In the future, the mutations will be introduced in untagged ROMK1$_{K80M}$ in yeast. It is also possible that the tag inhibits transport to the plasma membrane, and the mutations similarly suppress this activity. These future experiments should be straightforward as I have validated that the ROMK R79 antibody is competent for Western analysis of yeast lysate (Figure 18C).

Table 7: Gain-of-function mutations in ROMK. Nucleotide and amino acid level changes in ROMK1$_{K80M}$ leading to increased growth on low potassium medium. All numberings are given for untagged ROMK1. Mutations in the HA tag are numbered separately starting from the N-terminal diglycine linker. "Linkage" indicates that the mutation was identified in the context of another mutation. * indicates also identified in Paynter *et al.* 2010. † indicates found in human populations via GWAS.

Nucleotide Change	**Amino Acid Change**	**Domain**	**# of Clones**	**Linkage**
T35C	L12P	N-terminal	1	S305G
T302C	V101A	Extracellular Pore	1	
a1g	g1r	HA-tag	1	
a8g	y3c	HA-tag	6	
t13c	y5h	HA-tag	3	
A338G	Y113C*	Extracellular Pore	4	
C352T	R118C	Extracellular Pore	2	
G367A	E123K	Extracellular Pore	1	
T405C	S135P	Extracellular Pore	1	Y113C
G419A	V140M*	Extracellular Pore	1	
T725C	I242T	IgLD	1	D245G
A734G	D245G	IgLD	1	I242T
T831C	F278L	IgLD	1	
A913G	S305G	IgLD	1	T35C
T983C	I328T	C-terminal†	3	
A1027G	N343D	C-terminal	3	

Given that the HA tag is inserted between residues F112 and Y113 in the native sequence, it is likely that the HA y3c and native Y113C mutations have equivalent effects. Along with the nearby R118C alteration, the extracellular gain-of-function mutations may possess novel disulfide bonds which increase channel activity. Analysis of a ROMK homology model indicates that these substituted cysteines are most likely to form an intramolecular disulfide with C121 (Figure 23B). To test this hypothesis, we will substitute C121 to alanine in the context of Y113C and R118C and analyze whether or not the gain-of-function phenotype reverts.

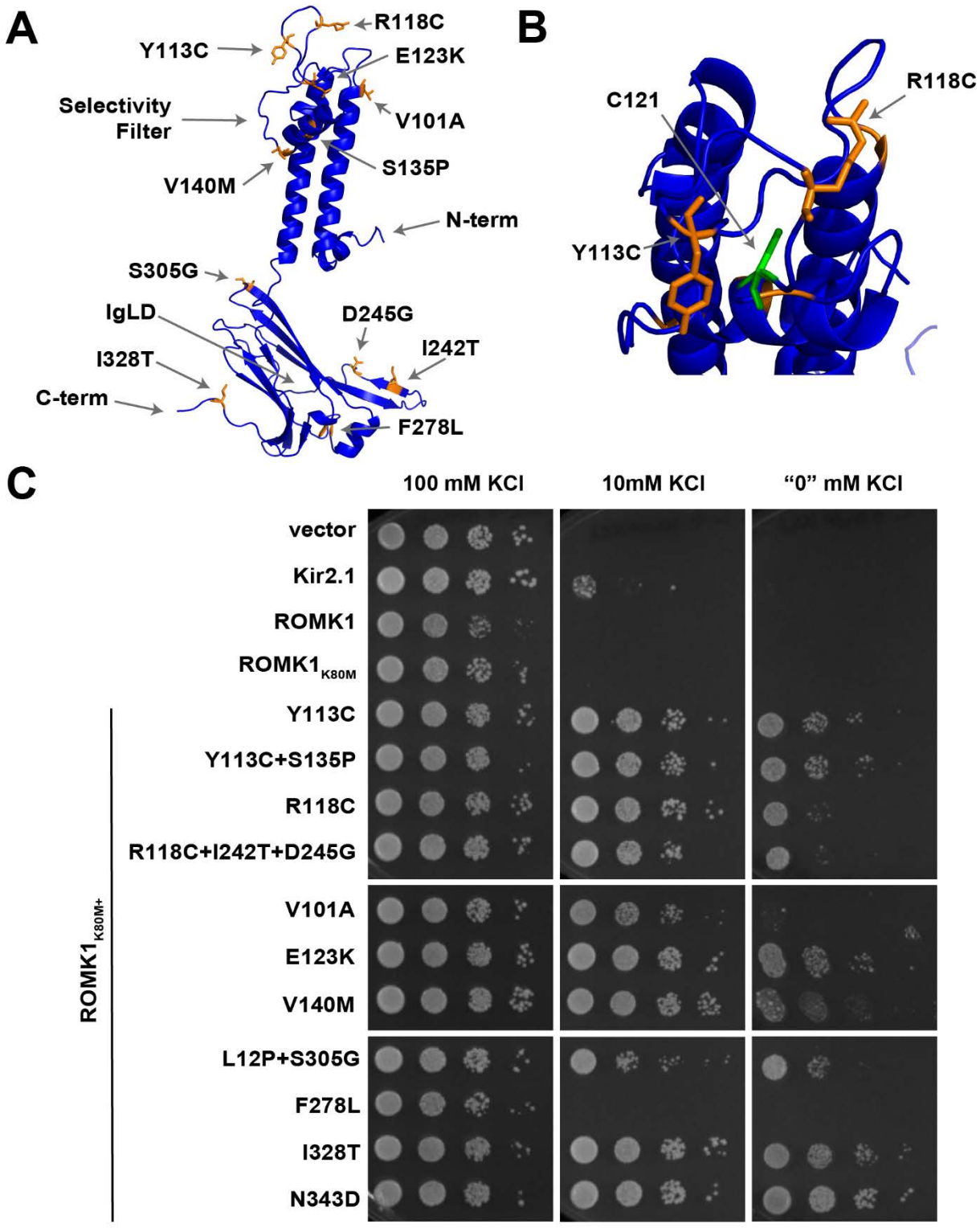

Figure 23: ROMK gain-of-function mutations and relative phenotypes. A. Homology model of ROMK based on KirBac3.1 from *Magnetospirillum magnetotaceticum* showing a single

monomer with residues mutated in gain-of-function alleles rendered in orange. L12P and N343D are not pictured as the template protein lacks homology to the corresponding ROMK sequence. B. Close-up of external pore domain showing a potential novel disulfide bridge between Y113C or R118C and native C121 (green). Renderings created in PyMol (v.1.8.6). C. Yeast strains with the indicated genotypes transformed with an empty expression vector control or vectors engineered to express Kir2.1, wild-type ROMK1, $ROMK1_{K80M,}$ or the indicated gain-of-function mutations in the context of K80M were serially diluted onto medium supplemented with the indicated amounts of KCl. Images were captured after two days of growth at $30^{O}C$.

The N343D mutation in the unstructured C-terminal region of ROMK is in a region known to harbor several trafficking motifs, including the RxR ER-retention motif (residues 379-381) and the NPxΦ endocytosis motif (residues 388-391). It is possible that this mutation increases the plasma membrane expression of the channel by inhibiting ER retention and/or endocytosis from the plasma membrane.

A previous screen for ROMK gain-of-function mutations was only able to identify the well-studied acid desensitizing mutation K80V (Paynter *et al.*, 2010). In this published study, the authors performed a similar screen using a ROMK1-K_{ir}4.1 chimera consisting of the N-terminus and transmembrane-pore domains of $ROMK1_{K80M}$ fused to the C-terminal domains of K_{ir}4.1. Two of the gain-of-function mutations we identified—Y113C and V140M—were also found in this previous screen, however the authors of this study did not perform any subsequent experiments other than testing their effect on pH gating. Only one of their isolated mutants—the conservative S172T—was found to measurably decrease pH gating. It is also likely that these authors were unable to screen full-length ROMK as their growth medium was buffered to a near neutral pH of 6.5, whereas the medium used in our study is considerably more acidic (pH~4.5). Acidic media increase the sensitivity of *trk1Δ trk2Δ* yeast to low potassium, providing the necessary signal-to-noise ratio to perform genetic screens. Paynter and colleagues observed near complete growth rescue of *trk1Δ trk2Δ* growth with $ROMK1_{K80(M/V)}$ and K_{ir}2.1 on limiting potassium (Paynter *et al.*, 2010), which we do not observe on our acidic medium (Figure 6). These seemingly trivial technical differences have provided us with an advantage over this

previous work. This has allowed us to identify novel mutations, including several in the C-terminal domain that were excluded from the previous study.

Analysis of the Trans-Omics for Precision Medicine (TOPMed) database—a repository of known human genetic variation collated from numerous GWAS—indicates that the I328T mutation has been identified in at least one individual. The absence of the other mutations could be due to purifying selection if they are extremely deleterious, or more trivially due to the limited subset of the human population that has been captured by whole exome sequencing.

A.4 FUTURE DIRECTIONS

In principle, a gain-of-function mutation may affect one of three broad channel attributes: open probability, conductance, and plasma membrane residence. To test gain-of-function mutation effects on protein stability, the mutations will be recreated in wild-type ROMK1 by site-directed mutagenesis and stability will be assessed by cycloheximide chase analysis. Addition of MG132 will determine if gain-of-function ROMK is degraded by the proteasome. To test the effect of gain-of-function mutations on plasma membrane residency, yeast expressing these mutants will be analyzed by indirect immunofluorescence microscopy.

As several of the mutations cluster near the selectivity filter, it is possible that they alter the permeability of ROMK to monovalent cations other than potassium. Indeed, mutations in the sequence flanking the selectivity filter of KAT1 have been shown to alter conductance of sodium and cesium (section 1.1.5) (Nakamura *et al.*, 1997). To test this effect in budding yeast, relevant gain-of-function mutants will be expressed in *ena1-4Δ nha1Δ* yeast and growth will be assessed on medium supplemented with several concentrations of lithium, sodium, potassium, and cesium.

Taq-polymerase has a strong bias for transition over transversion mutations, and indeed all of the mutations identified in this study are transitions. PCR kits optimized for unbiased mutagenesis are available and repeating this screen with such a kit may reveal previously undiscovered gain-of-function mutations. Transversion polymorphisms are less common in the

human genome, particularly in protein-coding regions, but are often more consequential due to the degeneracy of the genetic code.

To determine the effects of these mutations on channel conductance, selectivity, and rectification, we have partnered with Drs. Thomas Kleyman and Shaohu Sheng of the University of Pittsburgh School of Medicine to perform two-electrode voltage clamp (TEVC) on *Xenopus* oocytes expressing these mutants. Briefly, *in vitro* transcribed ROMK mRNA will be injected into oocytes. ROMK activity is determined by measuring barium-sensitive whole-cell transmembrane conductance.

If a gain-of-function mutation is found to consistently increase ROMK function in multiple heterologous expression systems, it would seem prudent to make a knock-in mouse expressing gain-of-function ROMK in their distal nephron. I hypothesize that these mice would be at minimum hypertensive and hypokalemic and they may also exhibit hypernatremia that responds to amiloride treatment due to ENaC overactivity.

APPENDIX B

DETECTING INWARD RECTIFYING POTASSIUM CHANNELS AT THE PLASMA MEMBRANE

This project was spearheaded by Dr. Allyson O'Donnell of Duquesne University: an expert in yeast α-arrestins. As of this writing, a report on the major findings is in revision at the *Journal of Biological Chemistry*.

B.1 INTRODUCTION

The proteins of the plasma membrane are the primary means by which a living cell interfaces with its environment. Cells endocytose plasma membrane proteins in response to signaling, misfolding, environmental changes, or changes in cellular needs. α-arrestins are trafficking adaptors conserved throughout eukaryotes. They are the base of a clade that includes β-arrestins, which are best known for their roles in GPCR trafficking (Kang *et al.*, 2013). In contrast, yeast α-arrestins couple substrates destined for endocytosis with the E3 ubiquitin ligase Rsp5 (Lin *et al.*, 2008; Nikko and Pelham, 2009; O'Donnell, 2012; Becuwe and Léon, 2014).

α-arrestins client selection is both promiscuous and redundant. As K_{ir} channel plasma membrane residency has a clear phenotypic profile (*i.e.* increased growth of *trk1Δ trk2Δ* yeast on low potassium medium), we sought to determine if yeast α-arrestins can recognize and regulate

mammalian K_{ir} channels. Initially, this project encompassed both $ROMK1_{S44D+K80M}$ and $K_{ir}2.1$, but came to focus exclusively on $K_{ir}2.1$.

In most of the α-arrestin literature, fluorescent protein-tagged amino acid permeases have been used as model substrates. These proteins have a clear plasma membrane distribution when α-arrestin activity is suppressed and a clear vacuolar distribution when α-arrestins are actively mediating their endocytosis (*e.g.* (Guiney *et al.*, 2016)). Mammalian K_{ir} channels, however, are primarily observed to colocalize with ER markers when expressed in yeast (Figure 18A) (Kolb *et al.*, 2014; O'Donnell *et al.*, 2017b; Mackie *et al.*, 2018). The yeast cortical ER is tethered to the plasma membrane, making quantitative assessment of the relative ER and PM populations of a protein by fluorescent microscopy a dubious prospect (Manford *et al.*, 2012). Fortunately, the research groups of Drs. Christopher Szent-Gyorgyi, Marcel Bruchez, and Alan Waggoner at Carnegie Mellon University have designed a fluorescence protein tagging technology that is rapidly inducible, non-toxic, and can discriminate surface-exposed and intracellular populations of membrane proteins. Briefly, the tag was developed by fusing a single-chain antibody (SCA) cDNA library to the yeast plasma membrane protein Aga2 and expressing this library in yeast (Feldhaus *et al.*, 2003). Clones were selected by FACS for their affinity for the fluorescent dyes malachite green (MG) and thiazole orange (TO). Next, the dye molecules were chemically modified to render them cell permeant or impermeant. The final product was a fluorogen-activated peptide (FAP) that may be appended to a protein of interest. Cells expressing FAP-tagged proteins are then treated with permeant or impermeant variants of the dyes, which increase in fluorescent intensity several thousand-fold upon FAP binding (Szent-Gyorgyi *et al.*, 2008).

As both termini of K_{ir} channel proteins are cytosolic, an additional transmembrane domain derived from platelet-derived growth factor receptor (PGFR) was added to the N-terminus of $K_{ir}2.1$ to ensure that the FAP would face the extracellular surface. To ensure that FAP-$K_{ir}2.1$ would be also inserted into the membrane in the correct orientation, an N-terminal signal sequence derived from the yeast ER-lumenal chaperone Kar2 was also added. My primary contribution to the project was to validate that the activity and stability of FAP-$K_{ir}2.1$ was comparable to the untagged channel. To this end, I measured the ability of FAP-$K_{ir}2.1$ to support the growth of *trk1Δ trk2Δ* yeast grown on low potassium medium. I also determined the stability and aggregation propensity of FAP-$K_{ir}2.1$ relative to its untagged counterpart. These studies

have validated FAP technology as a novel method for detecting very small cell surface populations of a protein of interest.

B.2 MATERIALS AND METHODS

All serial dilution assays, cycloheximide chases, and Western blots were performed as previously described (section 2.2.1).

ER-enriched microsomes were prepared from yeast expressing either Kir2.1 or SCA-Kir2.1 using the previously described "small scale" protocol (Nakatsukasa and Brodsky, 2010). A total of 1.5 μL of microsomes at an OD_{600} of approximately 0.2 was added to 30 μL of PBS containing 250 mM sorbitol along with the indicated concentrations of *n*-dodecyl-β-D-maltoside (DDM; EMD Millipore, Billerica, MA) or SDS. Samples were agitated on a Vortex mixer for 5 seconds, incubated on ice for 30 min, and centrifuged at 18,000 g for 10 min at 4°C. The soluble fraction was transferred to a new tube and the supernatant and pellet (insoluble) samples were incubated with SDS-PAGE sample buffer prior at room temperature for one hour prior to SDS-PAGE and Western Blot analysis.

B.3 RESULTS AND DISCUSSION

Dr. O'Donnell found that the subcellular distribution of FAP-K_{ir}2.1 matches what has been previously reported for the wild-type protein (Kolb *et al.,* 2014). To test if FAP-K_{ir}2.1 could form a functional potassium channel after expression in yeast. I introduced the expression vector into *trk1Δ trk2Δ vps35Δ* yeast as Vps35 had been previously identified as a negative regulator of K_{ir}2.1 (Kolb *et al.,* 2014). Compared to wild-type K_{ir}2.1, FAP-K_{ir}2.1 mediates poorer growth rescue on low potassium medium, though it is still well above the vector control (*i.e.*, the background) (Figure 24A). I hypothesized that the addition of the exogenous SCA and TMD might destabilize the protein and cause increased targeted for protein quality control. Indeed, FAP-K_{ir}2.1 was aggressively degraded in a proteasome-dependent manner, while its wild-type

counterpart was minimally degraded over the course of a 90 min cycloheximide chase (Figure 24B,C). Furthermore, I showed that this decreased stability correlates with an increased propensity of FAP-K_{ir}2.1 to aggregate into detergent (DDM)-resistant inclusions relative to wild-type K_{ir}2.1 (Figure 24D,E). Taken together, these data indicate that the FAP tag combined with the exogenous TMD from PGFR are not benign and destabilize the protein when expressed in yeast. Nonetheless, enough protein is able to escape ER protein quality control to function at the plasma membrane as a potassium channel in yeast. Dr. O'Donnell further confirmed this conclusion by demonstrating via ICP-MS that FAP-K_{ir}2.1 facilitates and increase in intracellular potassium in *trk1Δ trk2Δ vps35Δ* yeast (O'Donnell *et al*, 2018, In Revision). Together, these results show that FAP-tagging represents a promising tool for resolving the dilemma of imaging small populations of a protein at the plasma membrane in yeast.

I have also constructed a FAP-tagged version of $ROMK1_{S44D+K80M}$ that is analogous to FAP-K_{ir}2.1. The function of FAP-K_{ir}2.1 was validated with the same experiments described above. Like FAP-K_{ir}2.1, FAP-$ROMK1_{S44D+K80M}$ is less stable than its untagged counterpart (Figure 25), but still forms a functional channel in potassium uptake-deficient yeast (data not shown). Future studies of ROMK in budding yeast may benefit from this sensitive and precise molecular tool.

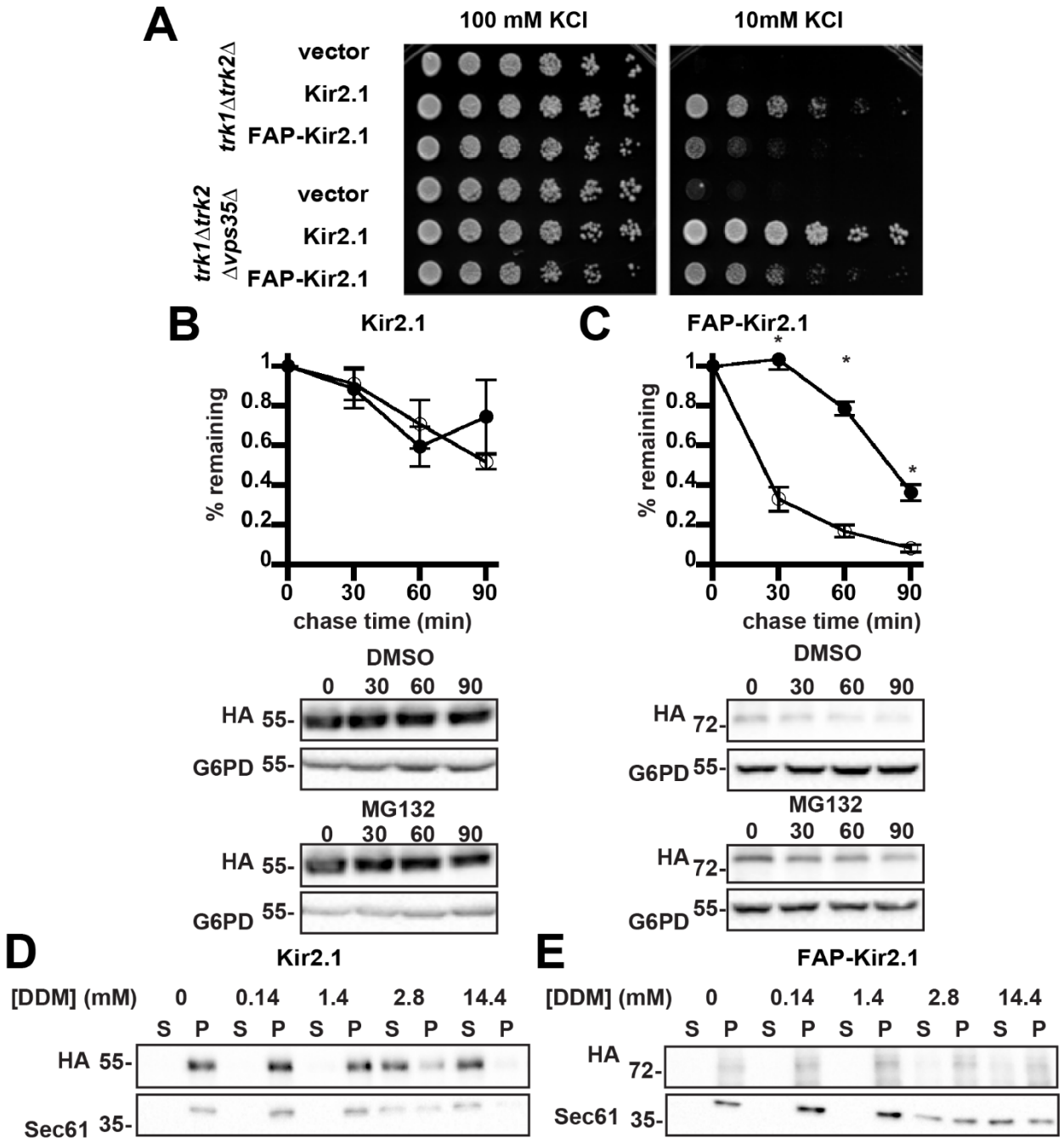

Figure 24: FAP-tagging Kir2.1 reduces channel function and protein stability. A. Yeast strains with the indicated genotypes transformed with an empty expression vector control or vectors engineered to express Kir2.1 or FAP-Kir2.1were serially diluted onto medium supplemented with the indicated amounts of KCl. Images were captured after two days of growth at 30^{O}C. B,C. Yeast cultures expressing HA-tagged versions of either (B) Kir2.1 or (C) FAP-Kir2.1 grown to mid-logarithmic phase were treated with MG132 (closed circles) or DMSO

(open circles) for 30 min, dosed with cycloheximide, and aliquots were withdrawn at 0, 30, 60, and 90 minutes. Kir2.1 expression was assessed by Western Blot and normalized to the initial timepoint. Representative blots are shown and all blots were stripped and reprobed for glucose-6-phosphate dehydrogenase (G6PD) as a loading control. Data represent the means of three independent experiments. Error bars show standard errors of the mean and *indicates a significant ($p<0.05$) difference as assessed by Student's t-test. D,E. ER-enriched microsomes from yeast engineered to express Kir2.1 (D) or FAP-Kir2.1 (E) were treated with the indicated concentrations of DDM and then centrifuged to separate the soluble supernatant (S) from the insoluble pellet (P). The native yeast integral membrane protein Sec61 was used as a loading control.

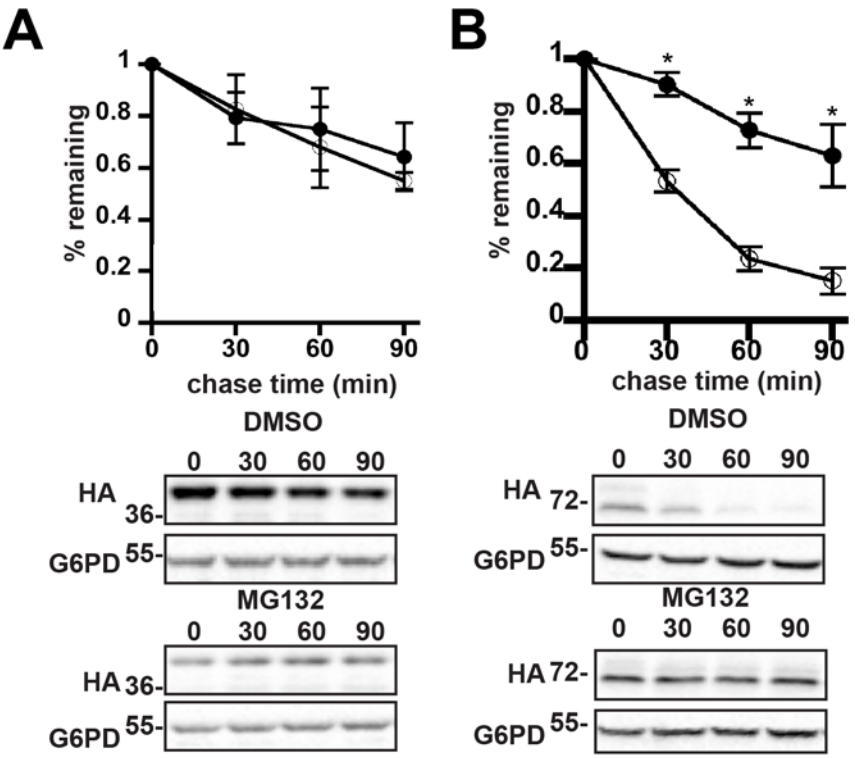

Figure 25: Appending the FAP tag to ROMK1$_{S44D+K80M}$ increases ERAD of the protein. Yeast cultures expressing HA-tagged versions of either (A) ROMK1$_{S44D+K80M}$ or (B) FAP-ROMK1$_{S44D+K80M}$ grown to mid-logarithmic phase were treated with MG132 (closed circles) or DMSO (open circles) for 30 min, dosed with cycloheximide, and aliquots were withdrawn at 0, 30, 60, and 90 minutes. ROMK expression was assessed by Western Blot and normalized to the initial timepoint. Representative blots are shown and all blots were stripped and reprobed for glucose-6-phosphate dehydrogenase (G6PD) as a loading control. Data represent the means of three independent experiments. Error bars show standard errors of the mean and *indicates a significant ($p<0.05$) difference as assessed by Student's t-test. Part A is identical to Figure 6B.

APPENDIX C

HSP90 IS A POTENTIAL NEGATIVE REGULATOR OF ROMK

The following work is neither published nor being considered for publication as of this writing. It is, however, potentially of interest to the research community, so I have briefly summarized it here.

C.1 INTRODUCTION

Hsp90s are a major molecular chaperone in eukaryotic cells that serves to buffer the disordered components of the eukaryotic proteome (Karras *et al.*, 2017). The action of his conserved and abundant chaperone is coordinated with Hsp70s and Hsp90s are generally believed to function as "late-acting" chaperones, targeting proteins that have misfolded into states refractory to Hsp70 activity (Taipale *et al.*, 2010). In addition to their role in protein quality control, Hsp90s are also key regulators of protein kinases and steroid hormone receptors, and facilitate the assembly of large multi-protein complexes (McClellan *et al.*, 2007; Makhnevych and Houry, 2012).

I became interested in Hsp90s upon identifying the Hsp90 co-chaperone Sse1 as a strong hit in the SGA screen (see Appendix D). However, upon *de novo* recreation of the *trk1Δ trk2Δ sse1Δ* strain, there was no increased growth mediated by exogenous potassium channels in this strain background when propagated on low potassium medium (data not shown). Furthermore, ROMK degradation was unaffected in multiple verified *sse1Δ* strains when examined by cycloheximide chase analysis (data not shown). However, upon investigating ROMK

degradation kinetics in a yeast strain expressing a temperature-sensitive variant of Hsp90, I found that ROMK was modestly stabilized at the non-permissive temperature. This encouraged me to investigate whether Hsp90 played a role in regulating ROMK stability in mammalian cells. I found that inhibiting Hsp90 in HEK 293H cells transfected with a ROMK1 expression vector greatly increased steady-state protein levels.

C.2 MATERIALS AND METHODS

All cycloheximide chases and Western blots were performed as previously described (section 2.2.3).

HEK293H cells cultured as previously described (2.2.6) were transformed with HA-tagged ROMK1 in pcDNA3.1 (O'Donnell *et al.*, 2017b) with Lipofectamine 2000 (Invitrogen) per the manufacturer's instructions. The cells were then treated with the indicated quantities of Tanespimycin (17-allylamino-17-demethoxygeldanamycin) for 24 hours. The cells were washed twice with DPBS and then detached with PBS. They were lysed for 30 minutes with PBS containing 1% Triton X-100 and a protease inhibitor cocktail (Roche). Lysate protein concentrations were determined with a BCA colorimetric assay per the manufacturer's instructions prior to SDS-PAGE and Western analysis.

C.3 RESULTS AND DISCUSSION

Yeast express two nearly identical isoforms of Hsp90: Hsp82 and Hsc82. To ascertain if Hsp90 is a pro-degradative factor for ROMK in yeast, I performed cycloheximide chases in *hsp82Δ hsc82Δ* yeast expressing either wild-type Hsp82 or the temperature-sensitive G313N allele (Nathan and Lindquist, 1995). I observed a modest, but reproducible reduction in ROMK degradation in the Hsp90 mutant strain (Figure 26A).

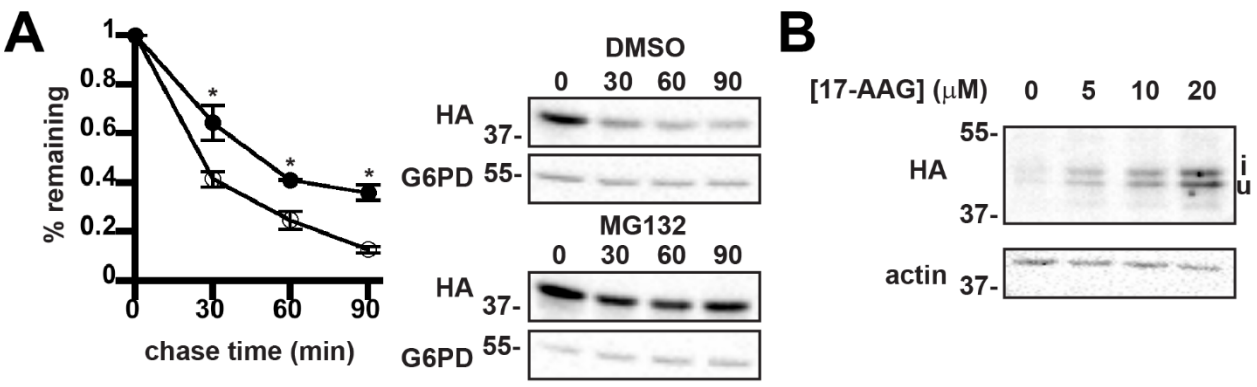

Figure 26: Hsp90 inhibition increases ROMK expression in yeast and mammalian cells. A. Yeast strains containing either a temperature sensitive mutation in the gene encoding Hsp82 (*hsp82-G313N*, filled circles) or lacking the mutant allele (*HSP82*) expressing wild-type ROMK1 were shifted from room temperature to 37^{O}C for 30 min before addition of cycloheximide. For all experiments, ROMK expression was assessed by Western Blot and normalized to the initial timepoint. Representative images are shown and all blots were stripped and reprobed for glucose-6-phosphate dehydrogenase (G6PD) as a loading control. Data represent the means of three independent experiments. Error bars show standard errors of the mean and *indicates a significant ($p<0.05$) difference as assessed by Student's t-test. B. HEK293H cells transfected with HA-tagged ROMK1 expression vector were treated with 17-AAG at the indicated concentrations for 24 hours. Cells lysates were analyzed by Western blot. u=unglycosylated. i=immaturely glycosylated. A representative image is shown and the blots were stripped and reprobed for actin as a loading control.

As Hsp90 is a prominent survival factor for many cancers (Whitesell and Lindquist, 2005), Hsp90 inhibitors have been broadly investigated as chemotherapeutics. The synthetic Hsp90 inhibitor Tanespimycin (17-AAG) is currently undergoing phase-III clinical trials for its efficacy in multiple myeloma. Hsp90s are known to promote folding and maturation of several potassium channels, such as the cardiac channel hERG (Ficker *et al.*, 2003; Peterson *et al.*, 2012), the cochlear channel KCNQ4 (Gao *et al.*, 2013), and the pancreatic β-cell channel K_{ir}6.1/SUR (Yan *et al.*, 2010). However, different Hsp90 isoforms in mammalian cells can

promote degradation or maturation of the same client protein (Gao *et al.*, 2013). To test if Hsp90 promotes the folding or maturation of ROMK, I treated HEK 293H cells expressing ROMK with 17-AAG and observed a dosage dependent increase in ROMK steady-state protein levels (Figure 26B). Note that transiently transfected cells only express the unglycosylated (u) and immaturely glycosylated (i) forms of ROMK in contrast to the Tet-On cells which also express the maturely glycosylated form (Figure 19). This result was intriguing as our group in collaboration with the Subramanya lab at the University of Pittsburgh School of Medicine has shown that Hsp90 inhibition is deleterious for the folding and expression of NCC (Donnelly *et al.*, 2013), which reabsorbs sodium and chloride in the distal nephron and is regulated in tandem with ROMK in response to fluctuating extracellular potassium levels (Figure 23). Therefore, Hsp90 may constitute an as yet uncharacterized node in the distal nephron potassium response network. Further study is needed to determine if the effects of Hsp90 on ROMK expression are due to direct chaperone-client interaction or modulation of a cellular signaling pathway.

APPENDIX D

FULL LIST OF HITS FROM SGA SCREEN

Table 8: Full list of hits from SGA screen. All hits from SGA screen described in section 2.3.3 arranged by z-score cutoff. For more information on genes not discussed in the text, refer to the *Saccharomyces* genome database (SGD).

z-score	Systemic Name	Standard Name	z-score	Systemic Name	Standard Name	z-score	Systemic Name	Standard Name
3	YAL002W	VPS8	2	YER185W	PUG1	1	YLR069C	MEF1
3	YAL011W	SWC3	2	YFL006W		1	YLR074C	BUD20
3	YAL051W	OAF1	2	YFL007W	BLM10	1	YLR083C	EMP70
3	YAL053W	FLC2	2	YFL019C		1	YLR099C	ICT1
3	YAL068C	PAU8	1	YFL020C	PAU5	1	YLR108C	
3	YAR002C-A	ERP1	1	YFL028C	CAF16	1	YLR109W	AHP1
3	YBL006C	LDB7	1	YFL031W	HAC1	1	YLR110C	CCW12
3	YBL011W	SCT1	1	YFL032W		1	YLR111W	
3	YBL049W	MOH1	1	YFL034C-A	RPL22B	1	YLR118C	
3	YBL057C	PTH2	1	YFL042C	LAM5	1	YLR139C	SLS1
3	YBL064C	PRX1	1	YFL055W	AGP3	1	YLR184W	
3	YBL065W		1	YFR010W	UBP6	1	YLR187W	SKG3

3	YBL078C	ATG8	1	YFR024C-A	LSB3	1	YLR201C	COQ9
3	YBL091C	MAP2	1	YFR026C	ULI1	1	YLR205C	HMX1
3	YBL094C		1	YFR032C	RRT5	1	YLR214W	FRE1
3	YBR018C	GAL7	1	YFR043C	IRC6	1	YLR217W	
3	YBR019C	GAL10	1	YFR046C	CNN1	1	YLR226W	BUR2
3	YBR020W	GAL1	1	YGL013C	PDR1	1	YLR234W	TOP3
3	YBR022W	POA1	1	YGL014W	PUF4	1	YLR236C	
3	YBR024W	SCO2	1	YGL025C	PGD1	1	YLR239C	LIP2
3	YBR025C	OLA1	1	YGL027C	CWH41	1	YLR254C	NDL1
3	YBR026C	ETR1	1	YGL028C	SCW11	1	YLR261C	VPS63
3	YBR033W	EDS1	1	YGL033W	HOP2	1	YLR352W	
3	YBR041W	FAT1	1	YGL064C	MRH4	1	YLR356W	ATG33
3	YBR051W		1	YGL066W	SGF73	1	YLR357W	RSC2
3	YBR059C	AKL1	1	YGL071W	AFT1	1	YLR360W	VPS38
3	YBR106W	PHO88	1	YGL072C		1	YLR364W	GRX8
3	YBR127C	VMA2	1	YGL080W	MPC1	1	YLR369W	SSQ1
3	YBR128C	ATG14	1	YGL084C	GUP1	1	YLR370C	ARC18
3	YBR130C	SHE3	1	YGL087C	MMS2	1	YLR371W	ROM2
3	YBR132C	AGP2	1	YGL105W	ARC1	1	YLR377C	FBP1
3	YBR134W		1	YGL114W		1	YLR381W	CTF3
3	YBR137W		1	YGL117W		1	YLR382C	NAM2
3	YBR150C	TBS1	1	YGL118C		1	YLR387C	REH1
3	YBR151W	APD1	1	YGL121C	GPG1	1	YLR395C	COX8
3	YBR158W	AMN1	1	YGL125W	MET13	1	YLR399C	BDF1
3	YBR161W	CSH1	1	YGL126W	SCS3	1	YLR404W	SEI1
3	YBR169C	SSE2	1	YGL167C	PMR1	1	YLR412W	BER1
3	YBR175W	SWD3	1	YGL170C	SPO74	1	YLR413W	INA1
3	YBR176W	ECM31	1	YGL173C	XRN1	1	YLR417W	VPS36
2	YBR187W	GDT1	1	YGL195W	GCN1	1	YLR436C	ECM30

2	YBR189W	RPS9B	1	YGL244W	RTF1	1	YLR438W	CAR2
2	YBR191W	RPL21A	1	YGL249W	ZIP2	1	YLR447C	VMA6
2	YBR197C		1	YGL261C	PAU11	1	YLR454W	FMP27
2	YBR200W	BEM1	1	YGR010W	NMA2	1	YLR460C	
2	YBR206W		1	YGR011W		1	YLR461W	PAU4
2	YBR207W	FTH1	1	YGR012W	MCY1	1	YML001W	YPT7
2	YBR208C	DUR1,2	1	YGR015C		1	YML002W	
2	YBR220C		1	YGR026W		1	YML009C	MRPL39
2	YBR221C	PDB1	1	YGR027C	RPS25A	1	YML012C-A	
2	YBR224W		1	YGR036C	CAX4	1	YML014W	TRM9
2	YBR225W		1	YGR041W	BUD9	1	YML041C	VPS71
2	YBR231C	SWC5	1	YGR056W	RSC1	1	YML061C	PIF1
2	YBR248C	HIS7	1	YGR057C	LST7	1	YML075C	HMG1
2	YBR249C	ARO4	1	YGR064W		1	YML080W	DUS1
2	YBR262C	MIC12	1	YGR071C	ENV11	1	YML081W	TDA9
2	YBR264C	YPT10	1	YGR084C	MRP13	1	YML082W	
2	YBR266C	SLM6	1	YGR096W	TPC1	1	YML086C	ALO1
2	YBR267W	REI1	1	YGR097W	ASK10	1	YML087C	AIM33
2	YBR269C	SDH8	1	YGR100W	MDR1	1	YML089C	
2	YBR272C	HSM3	1	YGR104C	SRB5	1	YMR016C	SOK2
2	YBR276C	PPS1	1	YGR118W	RPS23A	1	YMR031W-A	
2	YBR286W	APE3	1	YGR121C	MEP1	1	YMR032W	HOF1
2	YBR287W		1	YGR122W		1	YMR052C-A	
2	YBR291C	CTP1	1	YGR131W	FHN1	1	YMR062C	ARG7
2	YCL001W-A		1	YGR136W	LSB1	1	YMR072W	ABF2
2	YCL005W	LDB16	1	YGR142W	BTN2	1	YMR073C	IRC21

2	YCL008C	STP22	1	YGR149W	GPC1	1	YMR077C	VPS20
2	YCL026C		1	YGR153W		1	YMR082C	
2	YCL030C	HIS4	1	YGR160W		1	YMR086C-A	
2	YCL040W	GLK1	1	YGR164W		1	YMR091C	NPL6
2	YCL061C	MRC1	1	YGR169C	PUS6	1	YMR142C	RPL13B
2	YCR002C	CDC10	1	YGR174C	CBP4	1	YMR155W	
2	YCR007C		1	YGR188C	BUB1	1	YMR169C	ALD3
2	YCR020W-B	HTL1	1	YGR189C	CRH1	1	YMR179W	SPT21
2	YCR026C	NPP1	1	YGR192C	TDH3	1	YMR184W	ADD37
2	YCR032W	BPH1	1	YGR199W	PMT6	1	YMR230W	RPS10B
2	YCR036W	RBK1	1	YGR207C	CIR1	1	YMR232W	FUS2
2	YCR043C		1	YGR208W	SER2	1	YMR243C	ZRC1
2	YCR045C	RRT12	1	YGR215W	RSM27	1	YMR244C-A	COA6
2	YCR053W	THR4	1	YGR224W	AZR1	1	YMR252C	
2	YCR069W	CPR4	1	YGR240C	PFK1	1	YMR253C	
2	YCR084C	TUP1	1	YGR255C	COQ6	1	YMR254C	
2	YCR087W		1	YHL003C	LAG1	1	YMR257C	PET111
2	YCR089W	FIG2	1	YHL014C	YLF2	1	YMR264W	CUE1
2	YDL010W	GRX6	1	YHL016C	DUR3	1	YMR271C	URA10
2	YDL013W	SLX5	1	YHL028W	WSC4	1	YMR282C	AEP2
2	YDL021W	GPM2	1	YHL029C	OCA5	1	YMR286W	MRPL33
2	YDL048C	STP4	1	YHL030W	ECM29	1	YNL052W	COX5A
2	YDL069C	CBS1	1	YHL031C	GOS1	1	YNL057W	
2	YDL070W	BDF2	1	YHL033C	RPL8A	1	YNL066W	SUN4
2	YDL101C	DUN1	1	YHL042W		1	YNL080C	EOS1
2	YDL121C		1	YHL043W	ECM34	1	YNL085W	MKT1
2	YDL130W-A	STF1	1	YHL044W		1	YNL086W	SNN1
2	YDL131W	LYS21	1	YHL045W		1	YNL096C	RPS7B

2	YDL133C-A	RPL41B	1	YHR010W	RPL27A	1	YNL097C	PHO23
2	YDL151C	BUD30	1	YHR013C	ARD1	1	YNL117W	MLS1
2	YDL157C		1	YHR015W	MIP6	1	YNL133C	FYV6
2	YDL161W	ENT1	1	YHR017W	YSC83	1	YNL144C	
2	YDL182W	LYS20	1	YHR018C	ARG4	1	YNL145W	MFA2
2	YDL233W	MFG1	1	YHR033W		1	YNL160W	YGP1
2	YDR004W	RAD57	1	YHR037W	PUT2	1	YNL176C	TDA7
2	YDR006C	SOK1	1	YHR038W	RRF1	1	YNL179C	
2	YDR028C	REG1	1	YHR044C	DOG1	1	YNL187W	SWT21
2	YDR029W		1	YHR047C	AAP1	1	YNL197C	WHI3
2	YDR030C	RAD28	1	YHR051W	COX6	1	YNL224C	SQS1
2	YDR046C	BAP3	1	YHR060W	VMA22	1	YNL227C	JJJ1
2	YDR059C	UBC5	1	YHR073W	OSH3	1	YNL234W	
2	YDR061W		1	YHR081W	LRP1	1	YNL238W	KEX2
2	YDR063W	AIM7	1	YHR082C	KSP1	1	YNL239W	LAP3
2	YDR067C	OCA6	1	YHR092C	HXT4	1	YNL246W	VPS75
2	YDR069C	DOA4	1	YHR104W	GRE3	1	YNL248C	RPA49
2	YDR071C	PAA1	1	YHR111W	UBA4	1	YNL253W	TEX1
2	YDR084C	TVP23	1	YHR124W	NDT80	1	YNL266W	
2	YDR100W	TVP15	1	YHR125W		1	YNL268W	LYP1
2	YDR101C	ARX1	1	YHR134W	WSS1	1	YNL270C	ALP1
2	YDR112W	IRC2	1	YHR147C	MRPL6	1	YNL273W	TOF1
2	YDR114C		1	YHR151C	MTC6	1	YNL275W	BOR1
2	YDR117C	TMA64	1	YHR154W	RTT107	1	YNL280C	ERG24
2	YDR120C	TRM1	1	YHR162W	MPC2	1	YNL293W	MSB3
2	YDR123C	INO2	1	YHR167W	THP2	1	YNL298W	CLA4

2	YDR129C	SAC6	1	YHR181W	SVP26	1	YNR032C-A	HUB1
2	YDR130C	FIN1	1	YHR183W	GND1	1	YNR070W	PDR18
2	YDR136C	VPS61	1	YHR198C	AIM18	1	YOL001W	PHO80
2	YDR138W	HPR1	1	YIL012W		1	YOL003C	PFA4
2	YDR140W	MTQ2	1	YIL014W	MNT3	1	YOL008W	COQ10
2	YDR143C	SAN1	1	YIL020C	HIS6	1	YOL014W	
2	YDR195W	REF2	1	YIL035C	CKA1	1	YOL015W	IRC10
2	YDR199W		1	YIL043C	CBR1	1	YOL018C	TLG2
2	YDR200C	VPS64	1	YIL059C		1	YOL036W	
2	YDR204W	COQ4	1	YIL067C		1	YOL037C	
2	YDR207C	UME6	1	YIL090W	ICE2	1	YOL049W	GSH2
2	YDR218C	SPR28	1	YIL107C	PFK26	1	YOL050C	
2	YDR220C		1	YIL116W	HIS5	1	YOL053W	AIM39
2	YDR226W	ADK1	1	YIL136W	OM45	1	YOL054W	PSH1
2	YDR231C	COX20	1	YIL145C	PAN6	1	YOL058W	ARG1
2	YDR233C	RTN1	1	YIL153W	RRD1	1	YOL067C	RTG1
2	YDR237W	MRPL7	1	YIL154C	IMP2'	1	YOL075C	
2	YDR252W	BTT1	1	YIL157C	COA1	1	YOL096C	COQ3
2	YDR261C	EXG2	1	YIL160C	POT1	1	YOL111C	MDY2
2	YDR270W	CCC2	1	YIL161W		1	YOL112W	MSB4
2	YDR286C		1	YIL170W	HXT12	1	YOL115W	PAP2
2	YDR290W		1	YIR032C	DAL3	1	YOL151W	GRE2
2	YDR297W	SUR2	1	YJL038C	LOH1	1	YOR002W	ALG6
2	YDR305C	HNT2	1	YJL088W	ARG3	1	YOR011W	AUS1
2	YDR307W	PMT7	1	YJL094C	KHA1	1	YOR026W	BUB3
2	YDR315C	IPK1	1	YJL101C	GSH1	1	YOR065W	CYT1
2	YDR323C	PEP7	1	YJL127C	SPT10	1	YOR068C	VAM10
2	YDR326C	YSP2	1	YJL128C	PBS2	1	YOR069W	VPS5
2	YDR334W	SWR1	1	YJL129C	TRK1	1	YOR079C	ATX2
2	YDR347W	MRP1	1	YJL130C	URA2	1	YOR089C	VPS21
2	YDR348C	PAL1	1	YJL131C	AIM23	1	YOR096W	RPS7A
2	YDR349C	YPS7	1	YJL132W		1	YOR130C	ORT1
2	YDR352W	YPQ2	1	YJL135W		1	YOR141C	ARP8
2	YDR358W	GGA1	1	YJL136C	RPS21B	1	YOR172W	YRM1
2	YDR363W	ESC2	1	YJL140W	RPB4	1	YOR187W	TUF1
2	YDR363W-A	SEM1	1	YJL142C	IRC9	1	YOR198C	BFR1
2	YDR374C	PHO92	1	YJL146W	IDS2	1	YOR199W	
2	YDR383C	NKP1	1	YJL147C	MRX5	1	YOR200W	
2	YDR384C	ATO3	1	YJL159W	HSP150	1	YOR215C	AIM41

2	YDR385W	EFT2	1	YJL161W	FMP33	1	YOR216C	RUD3
2	YDR392W	SPT3	1	YJL163C		1	YOR219C	STE13
2	YDR399W	HPT1	1	YJL166W	QCR8	1	YOR221C	MCT1
2	YDR400W	URH1	1	YJL168C	SET2	1	YOR227W	HER1
2	YDR417C		1	YJL172W	CPS1	1	YOR228C	MCP1
2	YDR419W	RAD30	1	YJL176C	SWI3	1	YOR233W	KIN4
2	YDR421W	ARO80	1	YJL178C	ATG27	1	YOR239W	ABP140
2	YDR422C	SIP1	1	YJL179W	PFD1	1	YOR241W	MET7
2	YDR431W		1	YJL182C		1	YOR245C	DGA1
2	YDR432W	NPL3	1	YJL184W	GON7	1	YOR258W	HNT3
2	YDR435C	PPM1	1	YJL189W	RPL39	1	YOR268C	
2	YDR465C	RMT2	1	YJL191W	RPS14B	1	YOR274W	MOD5
2	YDR475C	JIP4	1	YJL218W		1	YOR288C	MPD1
2	YDR482C	CWC21	1	YJR018W		1	YOR355W	GDS1
2	YDR490C	PKH1	1	YJR030C	RBH2	1	YOR365C	
2	YDR516C	EMI2	1	YJR031C	GEA1	1	YPL002C	SNF8
2	YDR518W	EUG1	1	YJR033C	RAV1	1	YPL022W	RAD1
2	YDR533C	HSP31	1	YJR049C	UTR1	1	YPL027W	SMA1
2	YDR535C		1	YJR054W	KCH1	1	YPL034W	
2	YDR540C	IRC4	1	YJR055W	HIT1	1	YPL036W	PMA2
2	YEL001C	IRC22	1	YJR061W		1	YPL059W	GRX5
2	YEL009C	GCN4	1	YJR066W	TOR1	1	YPL069C	BTS1
2	YEL017C-A	PMP2	1	YJR088C	EMC2	1	YPL074W	YTA6
2	YEL017W	GTT3	1	YJR122W	IBA57	1	YPL079W	RPL21B
2	YEL024W	RIP1	1	YKL003C	MRP17	1	YPL084W	BRO1
2	YEL027W	VMA3	1	YKL009W	MRT4	1	YPL091W	GLR1
2	YEL040W	UTR2	1	YKL011C	CCE1	1	YPL097W	MSY1
2	YEL045C		1	YKL026C	GPX1	1	YPL104W	MSD1
2	YEL046C	GLY1	1	YKL027W	TCD2	1	YPL105C	SYH1
2	YEL051W	VMA8	1	YKL038W	RGT1	1	YPL106C	SSE1
2	YEL054C	RPL12A	1	YKL044W	MMO1	1	YPL144W	POC4
2	YEL063C	CAN1	1	YKL054C	DEF1	1	YPL152W	RRD2
2	YEL067C		1	YKL070W		1	YPL157W	TGS1
2	YER019C-A	SBH2	1	YKL080W	VMA5	1	YPL158C	AIM44
2	YER038W-A	FMP49	1	YKL081W	TEF4	1	YPL163C	SVS1

2	YER040W	GLN3	1	YKL103C	APE1	1	YPL167C	REV3
2	YER049W	TPA1	1	YKL109W	HAP4	1	YPL168W	MRX4
2	YER051W	JHD1	1	YKL117W	SBA1	1	YPL173W	MRPL40
2	YER052C	HOM3	1	YKL118W		1	YPL174C	NIP100
2	YER056C-A	RPL34A	1	YKL120W	OAC1	1	YPL180W	TCO89
2	YER061C	CEM1	1	YKL123W		1	YPL182C	
2	YER065C	ICL1	1	YKL124W	SSH4	1	YPL188W	POS5
2	YER068C-A		1	YKL127W	PGM1	1	YPL195W	APL5
2	YER068W	MOT2	1	YKL130C	SHE2	1	YPL196W	OXR1
2	YER069W	ARG5,6	1	YKL138C	MRPL31	1	YPL207W	TYW1
2	YER071C	TDA2	1	YKL139W	CTK1	1	YPL208W	RKM1
2	YER072W	VTC1	1	YKL142W	MRP8	1	YPL212C	PUS1
2	YER073W	ALD5	1	YKL143W	LTV1	1	YPL213W	LEA1
2	YER097W		1	YKL146W	AVT3	1	YPL215W	CBP3
2	YER106W	MAM1	1	YKL147C		1	YPL216W	
2	YER109C	FLO8	1	YKL151C	NNR2	1	YPL219W	PCL8
2	YER135C		1	YKL156W	RPS27A	1	YPL227C	ALG5
2	YER150W	SPI1	1	YKL157W	APE2	1	YPL230W	USV1
2	YER151C	UBP3	1	YKL162C-A		1	YPL232W	SSO1
2	YER155C	BEM2	1	YKL170W	MRPL38	1	YPL234C	VMA11
2	YER164W	CHD1	1	YKL184W	SPE1	1	YPL249C	GYP5
2	YER166W	DNF1	1	YKL185W	ASH1	1	YPL264C	
2	YER169W	RPH1	1	YKL187C	FAT3	1	YPR002W	PDH1
2	YER170W	ADK2	1	YKL194C	MST1	1	YPR011C	
2	YER173W	RAD24	1	YKL200C		1	YPR043W	RPL43A
2	YER174C	GRX4	1	YKL201C	MNN4	1	YPR044C	OPI11

2	YER176W	ECM32	1	YKL205W	LOS1	1	YPR045C	THP3
2	YER182W	FMP10	1	YKL216W	URA1	1	YPR101W	SNT309
2	YER183C	FAU1	1	YKL218C	SRY1	1	YPR120C	CLB5
1	YLL013C	PUF3	1	YKR031C	SPO14	1	YPR121W	THI22
1	YLL021W	SPA2	1	YKR041W		1	YPR140W	TAZ1
1	YLL043W	FPS1	1	YKR043C	SHB17	1	YPR141C	KAR3
1	YLL044W		1	YKR044W	UIP5	1	YPR159W	KRE6
1	YLR024C	UBR2	1	YKR045C		1	YPR160W	GPH1
1	YLR027C	AAT2	1	YKR050W	TRK2	1	YPR163C	TIF3
1	YLR048W	RPS0B	1	YKR054C	DYN1	1	YPR166C	MRP2
1	YLR064W	PER33	1	YKR057W	RPS21A	1	YPR173C	VPS4
1	YLR068W	FYV7	1	YKR059W	TIF1	1	YPR196W	
1	YLL005C	SPO75	1	YPR200C	ARR2			

BIBLIOGRAPHY

Adams, A., and Kaiser, C. A. (1998). Methods in Yeast Genetics: A Cold Spring Harbor Laboratory Course Manual, Plainview, NY: Cold Spring Harbor Laboratory Press.

Al-Qusairi, L. *et al.* (2016). Renal tubular SGK1 deficiency causes impaired K^+ excretion via loss of regulation of NEDD4-2/WNK1 and ENaC. Am. J. Physiol. Physiol. *311*, F330–F342.

Al-Qusairi, L., Basquin, D., Roy, A., Rajaram, R. D., Maillard, M. P., Subramanya, A. R., and Staub, O. (2017). Renal Tubular Ubiquitin-Protein Ligase NEDD4-2 Is Required for Renal Adaptation during Long-Term Potassium Depletion. J. Am. Soc. Nephrol. *28*, 2431–2442.

Alemán, F., Caballero, F., Ródenas, R., Rivero, R. M., Martínez, V., and Rubio, F. (2014). The F130S point mutation in the Arabidopsis high-affinity K(+) transporter AtHAK5 increases K(+) over Na(+) and Cs(+) selectivity and confers Na(+) and Cs(+) tolerance to yeast under heterologous expression. Front. Plant Sci. *5*, 430.

Anderson, C. L., Delisle, B. P., Anson, B. D., Kilby, J. A., Will, M. L., Tester, D. J., Gong, Q., Zhou, Z., Ackerman, M. J., and January, C. T. (2006). Most LQT2 Mutations Reduce Kv11.1 (hERG) Current by a Class 2 (Trafficking-Deficient) Mechanism. Circulation *113*, 365–373.

Anderson, J. A., Huprikar, S. S., Kochian, L. V, Lucas, W. J., and Gaber, R. F. (1992). Functional expression of a probable Arabidopsis thaliana potassium channel in Saccharomyces cerevisiae. Proc. Natl. Acad. Sci. U. S. A. *89*, 3736–3740.

André, B., Chérif-Zahar, B., Marini, A.-M., Matassi, G., Raynal, V., and Cartron, J.-P. (2000). The human Rhesus-associated RhAG protein and a kidney homologue promote ammonium transport in yeast. Nat. Genet. *26*, 341–344.

De Angelis, E., Watkins, A., Schäfer, M., Brümmendorf, T., and Kenwrick, S. (2002). Disease-associated mutations in L1 CAM interfere with ligand interactions and cell-surface expression. Hum. Mol. Genet. *11*, 1–12.

Apaja, P. M., Foo, B., Okiyoneda, T., Valinsky, W. C., Barriere, H., Atanasiu, R., Ficker, E., Lukacs, G. L., and Shrier, A. (2013). Ubiquitination-dependent quality control of hERG K+ channel with acquired and inherited conformational defect at the plasma membrane. Mol. Biol. Cell *24*, 3787–3804.

Apaja, P. M., and Lukacs, G. L. (2014). Protein homeostasis at the plasma membrane. Physiology (Bethesda). *29*, 265–277.

Ariño, J., Ramos, J., and Sychrová, H. (2010). Alkali metal cation transport and homeostasis in yeasts. Microbiol. Mol. Biol. Rev. *74*, 95–120.

Arrigoni, C., Schroeder, I., Romani, G., Van Etten, J. L., Thiel, G., and Moroni, A. (2013). The voltage-sensing domain of a phosphatase gates the pore of a potassium channel. J. Gen. Physiol. *141*, 389–395.

Arvan, P., Zhao, X., Ramos-Castaneda, J., and Chang, A. (2002). Secretory Pathway Quality Control Operating in Golgi, Plasmalemmal, and Endosomal Systems. Traffic *3*, 771–780.

Ast, T., Michaelis, S., and Schuldiner, M. (2015). The Protease Ste24 Clears Clogged Translocons. Cell *164*, 103–114.

Babst, M. (2005). A protein's final ESCRT. Traffic *6*, 2–9.

Bagriantsev, S. N., Ang, K.-H., Gallardo-Godoy, A., Clark, K. A., Arkin, M. R., Renslo, A. R., and Minor, D. L. (2013). A High-Throughput Functional Screen Identifies Small Molecule Regulators of Temperature- and Mechano-Sensitive K_{2P} Channels. ACS Chem. Biol. *8*, 1841–1851.

Bagriantsev, S. N., Chatelain, F. C., Clark, K. A., Alagem, N., Reuveny, E., and Minor, D. L. (2014). Tethered Protein Display Identifies a Novel Kir3.2 (GIRK2) Regulator from Protein Scaffold Libraries. ACS Chem. Neurosci. *5*, 812–822.

Balchin, D., Hayer-Hartl, M., and Hartl, F. U. (2016). In vivo aspects of protein folding and quality control. Science *353*, aac4354.

Balderhaar, H. J. kleine, Lachmann, J., Yavavli, E., Bröcker, C., Lürick, A., and Ungermann, C. (2013). The CORVET complex promotes tethering and fusion of Rab5/Vps21-positive membranes. Proc. Natl. Acad. Sci. U. S. A. *110*, 3823–3828.

Balss, J. *et al.* (2008). Transmembrane domain length of viral K+ channels is a signal for mitochondria targeting. Proc. Natl. Acad. Sci. U. S. A. *105*, 12313–12318.

Balut, C. M., Hamilton, K. L., and Devor, D. C. (2012). Trafficking of intermediate (KCa3.1) and small (KCa2.x) conductance, Ca(2+)-activated K(+) channels: a novel target for medicinal chemistry efforts? ChemMedChem *7*, 1741–1755.

Bañuelos, M. A., Sychrova, H., Bleykasten-Grosshans, C., Souciet, J.-L., and Potier, S. (1998). The Nhal antiporter of Saccharomyces cerevisiae mediates sodium and potassium efflux. Microbiology *144*, 2749–2758.

Barreto, L. *et al.* (2011). A genomewide screen for tolerance to cationic drugs reveals genes important for potassium homeostasis in Saccharomyces cerevisiae. Eukaryot. Cell *10*, 1241–1250.

Becker, J., Walter, W., Yan, W., and Craig, E. A. (1996). Functional interaction of cytosolic hsp70 and a DnaJ-related protein, Ydj1p, in protein translocation in vivo. Mol. Cell. Biol. *16*, 4378–4386.

Becuwe, M., Herrador, A., Haguenauer-Tsapis, R., Vincent, O., and Léon, S. (2012). Ubiquitin-Mediated Regulation of Endocytosis by Proteins of the Arrestin Family. Biochem. Res. Int. *2012*, 1–12.

Becuwe, M., and Léon, S. (2014). Integrated control of transporter endocytosis and recycling by the arrestin-related protein Rod1 and the ubiquitin ligase Rsp5. Elife *3*.

Beerten, J., Jonckheere, W., Rudyak, S., Xu, J., Wilkinson, H., De Smet, F., Schymkowitz, J., and Rousseau, F. (2012). Aggregation gatekeepers modulate protein homeostasis of aggregating sequences and affect bacterial fitness. Protein Eng. Des. Sel. *25*, 357–366.

Belgareh-Touzé, N., Léon, S., Erpapazoglou, Z., Stawiecka-Mirota, M., Urban-Grimal, D., and Haguenauer-Tsapis, R. (2008). Versatile role of the yeast ubiquitin ligase Rsp5p in intracellular trafficking: Figure 1. Biochem. Soc. Trans. *36*, 791–796.

Ben-Shitrit, T., Yosef, N., Shemesh, K., Sharan, R., Ruppin, E., and Kupiec, M. (2012). Systematic identification of gene annotation errors in the widely used yeast mutation collections.

Nat. Methods *9*, 373–378.

Bengtson, M. H., and Joazeiro, C. A. P. (2010). Role of a ribosome-associated E3 ubiquitin ligase in protein quality control. Nature *467*, 470–473.

Bernstein, J. D., Okamoto, Y., Kim, M., and Shikano, S. (2013). Potential use of potassium efflux-deficient yeast for studying trafficking signals and potassium channel functions. FEBS Open Bio *3*, 196–203.

Bertl, A., Ramos, J., Ludwig, J., Lichtenberg-Fraté, H., Reid, J., Bihler, H., Calero, F., Martínez, P., and Ljungdahl, P. O. (2003). Characterization of potassium transport in wild-type and isogenic yeast strains carrying all combinations of trk1, trk2 and tok1 null mutations. Mol. Microbiol. *47*, 767–780.

Bhamidipati, A., Denic, V., Quan, E. M., and Weissman, J. S. (2005). Exploration of the Topological Requirements of ERAD Identifies Yos9p as a Lectin Sensor of Misfolded Glycoproteins in the ER Lumen. Mol. Cell *19*, 741–751.

Bhat, Y. R., Vinayaka, G., and Sreelakshmi, K. (2012). Antenatal bartter syndrome: a review. Int. J. Pediatr. *2012*, 857136.

Bhave, G. *et al.* (2011). Development of a selective small-molecule inhibitor of Kir1.1, the renal outer medullary potassium channel. Mol. Pharmacol. *79*, 42–50.

Bihler, H., Slayman, C. L., and Bertl, A. (1998). NSC1: a novel high-current inward rectifier for cations in the plasma membrane of Saccharomyces cerevisiae. FEBS Lett. *432*, 59–64.

Bischof, H. *et al.* (2017). Novel genetically encoded fluorescent probes enable real-time detection of potassium in vitro and in vivo. Nat. Commun. *8*, 1422.

Bodnar, N. O., and Rapoport, T. A. (2017). Molecular Mechanism of Substrate Processing by the Cdc48 ATPase Complex. Cell *169*, 722–735.e9.

Bonifacino, J. S., and Weissman, A. M. (1998). UBIQUITIN AND THE CONTROL OF PROTEIN FATE IN THE SECRETORY AND ENDOCYTIC PATHWAYS. Annu. Rev. Cell Dev. Biol. *14*, 19–57.

Bowen, A. B., Bourke, A. M., Hiester, B. G., Hanus, C., and Kennedy, M. J. (2017). Golgi-independent secretory trafficking through recycling endosomes in neuronal dendrites and spines. Elife *6*.

Boyd-Shiwarski, C. R. *et al.* (2018). Potassium-regulated distal tubule WNK bodies are kidney-specific WNK1 dependent. Mol. Biol. Cell *29*, 499–509.

Boyd-Shiwarski, C. R., and Subramanya, A. R. (2017). The renal response to potassium stress. Curr. Opin. Nephrol. Hypertens. *26*, 411–418.

Brandman, O. *et al.* (2012). A Ribosome-Bound Quality Control Complex Triggers Degradation of Nascent Peptides and Signals Translation Stress. Cell *151*, 1042–1054.

Briant, K., Johnson, N., and Swanton, E. (2017). Transmembrane domain quality control systems operate at the endoplasmic reticulum and Golgi apparatus. PLoS One *12*, e0173924.

Bröcker, C., Kuhlee, A., Gatsogiannis, C., Balderhaar, H. J. kleine, Hönscher, C., Engelbrecht-Vandré, S., Ungermann, C., and Raunser, S. (2012). Molecular architecture of the multisubunit homotypic fusion and vacuole protein sorting (HOPS) tethering complex. Proc. Natl. Acad. Sci. U. S. A. *109*, 1991–1996.

Buck, T. M., Jordahl, A. S., Yates, M. E., Preston, G. M., Cook, E., Kleyman, T. R., and Brodsky, J. L. (2017). Interactions between intersubunit transmembrane domains regulate the chaperone-dependent degradation of an oligomeric membrane protein. Biochem. J. *474*, 357–376.

Buck, T. M., Plavchak, L., Roy, A., Donnelly, B. F., Kashlan, O. B., Kleyman, T. R., Subramanya, A. R., and Brodsky, J. L. (2013). The Lhs1/GRP170 chaperones facilitate the endoplasmic reticulum-associated degradation of the epithelial sodium channel. J. Biol. Chem. *288*, 18366–18380.

Bundis, F., Neagoe, I., Schwappach, B., and Steinmeye, K. (2006). Involvement of Golgin-160 in Cell Surface Transport of Renal ROMK Channel: Co-expression of Golgin-160 Increases ROMK Currents. Cell. Physiol. Biochem. *17*, 1–12.

Burd, C., and Cullen, P. J. (2014). Retromer: a master conductor of endosome sorting. Cold Spring Harb. Perspect. Biol. *6*, 1–13.

Butterworth, M. B., Weisz, O. A., and Johnson, J. P. (2008). Some assembly required: putting the epithelial sodium channel together. J. Biol. Chem. *283*, 35305–35309.

Cagnac, O., Leterrier, M., Yeager, M., and Blumwald, E. (2007). Identification and characterization of Vnx1p, a novel type of vacuolar monovalent cation/H+ antiporter of Saccharomyces cerevisiae. J. Biol. Chem. *282*, 24284–24293.

Cahalan, M. D., Wulff, H., and Chandy, K. G. (2001). Molecular Properties and Physiological Roles of Ion Channels in the Immune System. J. Clin. Immunol. *21*, 235–252.

Cao, Y., Ward, J. M., Kelly, W. B., Ichida, A. M., Gaber, R. F., Anderson, J. A., Uozumi, N., Schroeder, J. I., and Crawford, N. M. (1995). Multiple genes, tissue specificity, and expression-dependent modulationcontribute to the functional diversity of potassium channels in Arabidopsis thaliana. Plant Physiol. *109*, 1093–1106.

Chai, B., Hsu, J., Du, J., and Laurent, B. C. (2002). Yeast RSC function is required for organization of the cellular cytoskeleton via an alternative PKC1 pathway. Genetics *161*, 575–584.

Chatelain, F. C., Gazzarrini, S., Fujiwara, Y., Arrigoni, C., Domigan, C., Ferrara, G., Pantoja, C., Thiel, G., Moroni, A., and Minor, D. L. (2009). Selection of Inhibitor-Resistant Viral Potassium Channels Identifies a Selectivity Filter Site that Affects Barium and Amantadine Block. PLoS One *4*, e7496.

Cho, H. C., Tsushima, R. G., Nguyen, T. T., Guy, H. R., and Backx, P. H. (2000). Two critical cysteine residues implicated in disulfide bond formation and proper folding of Kir2.1. Biochemistry *39*, 4649–4657.

Choe, H., Palmer, L. G., and Sackin, H. (1999). Structural determinants of gating in inward-rectifier K+ channels. Biophys. J. *76*, 1988–2003.

Chou, H.-T., Dukovski, D., Chambers, M. G., Reinisch, K. M., and Walz, T. (2016). CATCHR, HOPS and CORVET tethering complexes share a similar architecture. Nat. Struct. Mol. Biol. *23*, 761–763.

Choy, R. W.-Y., Park, M., Temkin, P., Herring, B. E., Marley, A., Nicoll, R. A., and von Zastrow, M. (2014). Retromer mediates a discrete route of local membrane delivery to dendrites. Neuron *82*, 55–62.

Clarke, O. B., Caputo, A. T., Hill, A. P., Vandenberg, J. I., Smith, B. J., and Gulbis, J. M. (2010). Domain Reorientation and Rotation of an Intracellular Assembly Regulate Conduction in Kir Potassium Channels. Cell *141*, 1018–1029.

Cosentino, C. *et al.* (2015). Engineering of a light-gated potassium channel. Science (80-.). *348*, 707–710.

Cuevas, C. A., Su, X.-T., Wang, M.-X., Terker, A. S., Lin, D.-H., McCormick, J. A., Yang, C.-L., Ellison, D. H., and Wang, W.-H. (2017). Potassium Sensing by Renal Distal Tubules Requires Kir4.1. J. Am. Soc. Nephrol., ASN.2016090935.

D'Avanzo, N., Cheng, W. W. L., Xia, X., Dong, L., Savitsky, P., Nichols, C. G., and Doyle, D. A. (2010). Expression and purification of recombinant human inward rectifier K+ (KCNJ) channels in Saccharomyces cerevisiae. Protein Expr. Purif. *71*, 115–121.

Dang, H., Klokk, T. I., Schaheen, B., McLaughlin, B. M., Thomas, A. J., Durns, T. A., Bitler, B. G., Sandvig, K., and Fares, H. (2011). Derlin-dependent retrograde transport from endosomes to the Golgi apparatus. Traffic *12*, 1417–1431.

Deshaies, R. J., and Schekman, R. (1987). A yeast mutant defective at an early stage in import of secretory protein precursors into the endoplasmic reticulum. J. Cell Biol. *105*, 633–645.

Dobzinski, N., Chuartzman, S. G., Kama, R., Schuldiner, M., Gerst Correspondence, J. E., and Gerst, J. E. (2015). Starvation-Dependent Regulation of Golgi Quality Control Links the TOR Signaling and Vacuolar Protein Sorting Pathways. Cell Rep. *12*, 1876–1886.

Donnelly, B. F., Needham, P. G., Snyder, A. C., Roy, A., Khadem, S., Brodsky, J. L., and Subramanya, A. R. (2013). Hsp70 and Hsp90 multichaperone complexes sequentially regulate thiazide-sensitive cotransporter endoplasmic reticulum-associated degradation and biogenesis. J. Biol. Chem. *288*, 13124–13135.

Doyle, D. A., Morais Cabral, J., Pfuetzner, R. A., Kuo, A., Gulbis, J. M., Cohen, S. L., Chait, B. T., MacKinnon, R., Moroni, A., and Thiel, G. (1998). The structure of the potassium channel: molecular basis of K+ conduction and selectivity. Science *280*, 69–77.

Dreyer, I., and Uozumi, N. (2011). Potassium channels in plant cells. FEBS J. *278*, 4293–4303.

Dunn, R., and Hicke, L. (2001). Domains of the Rsp5 Ubiquitin-Protein Ligase Required for Receptor-mediated and Fluid-Phase Endocytosis. Mol. Biol. Cell *12*, 421–435.

Einhorn, L. M., Zhan, M., Hsu, V. D., Walker, L. D., Moen, M. F., Seliger, S. L., Weir, M. R., and Fink, J. C. (2009). The frequency of hyperkalemia and its significance in chronic kidney disease. Arch. Intern. Med. *169*, 1156–1162.

Ellgaard, L., McCaul, N., Chatsisvili, A., and Braakman, I. (2016). Co- and Post-Translational Protein Folding in the ER. Traffic *17*, 615–638.

Ellgaard, L., Molinari, M., and Helenius, A. (1999). Setting the standards: quality control in the secretory pathway. Science *286*, 1882–1888.

Enyedi, P., and Czirják, G. (2010). Molecular Background of Leak K^+ Currents: Two-Pore Domain Potassium Channels. Physiol. Rev. *90*, 559–605.

Epshtein, Y., Chopra, A. P., Rosenhouse-Dantsker, A., Kowalsky, G. B., Logothetis, D. E., and Levitan, I. (2009). Identification of a C-terminus domain critical for the sensitivity of Kir2.1 to cholesterol. Proc. Natl. Acad. Sci. U. S. A. *106*, 8055–8060.

Erpapazoglou, Z., Dhaoui, M., Pantazopoulou, M., Giordano, F., Mari, M., Léon, S., Raposo, G., Reggiori, F., and Haguenauer-Tsapis, R. (2012). A dual role for K63-linked ubiquitin chains in multivesicular body biogenesis and cargo sorting. Mol. Biol. Cell *23*, 2170–2183.

Evangelinos, M., Martzoukou, O., Chorozian, K., Amillis, S., and Diallinas, G. (2016). BsdA ^{Bsd2} -dependent vacuolar turnover of a misfolded version of the UapA transporter along the secretory pathway: Prominent role of selective autophagy. Mol. Microbiol. *0*, n/a-n/a.

Fakler, B., Schultz, J. H., Yang, J., Schulte, U., Brandle, U., Zenner, H. P., Jan, L. Y., and Ruppersberg, J. P. (1996). Identification of a titratable lysine residue that determines sensitivity of kidney potassium channels (ROMK) to intracellular pH. EMBO J. *15*, 4093–4099.

Fallen, K., Banerjee, S., Sheehan, J., Addison, D., Lewis, L. M., Meiler, J., and Denton, J.

S. (2009). The Kir channel immunoglobulin domain is essential for Kir1.1 (ROMK) thermodynamic stability, trafficking and gating. Channels (Austin). *3*, 57–68.

Fang, L., Garuti, R., Kim, B.-Y., Wade, J. B., and Welling, P. A. (2009). The ARH adaptor protein regulates endocytosis of the ROMK potassium secretory channel in mouse kidney. J. Clin. Invest. *119*, 3278–3289.

Fang, L., Li, D., and Welling, P. A. (2010). Hypertension resistance polymorphisms in ROMK (Kir1.1) alter channel function by different mechanisms. Am. J. Physiol. Renal Physiol. *299*, F1359-64.

Feldhaus, M. J. *et al.* (2003). Flow-cytometric isolation of human antibodies from a nonimmune Saccharomyces cerevisiae surface display library. Nat. Biotechnol. *21*, 163–170.

Ficker, E., Dennis, A. T., Wang, L., and Brown, A. M. (2003). Role of the cytosolic chaperones Hsp70 and Hsp90 in maturation of the cardiac potassium channel HERG. Circ. Res. *92*, e87–e100.

Finley, D., Ulrich, H. D., Sommer, T., and Kaiser, P. (2012). The ubiquitin-proteasome system of Saccharomyces cerevisiae. Genetics *192*, 319–360.

Fisher, E. A., Khanna, N. A., and McLeod, R. S. (2011). Ubiquitination regulates the assembly of VLDL in HepG2 cells and is the committing step of the apoB-100 ERAD pathway. J. Lipid Res. *52*, 1170–1180.

Frausto da Silva, J. J. R., and Williams, R. J. P. (2001). The Biological Chemistry of the Elements: The Inorganic Chemistry of Life - J. J. R. Frausto da Silva, R. J. P. Williams - Google Books, Oxford: Oxford University Press.

Fremont, O. T., and Chan, J. C. M. (2012). Understanding Bartter syndrome and Gitelman syndrome. World J. Pediatr. *8*, 25–30.

Frindt, G., Shah, A., Edvinsson, J., and Palmer, L. G. (2009). Dietary K regulates ROMK channels in connecting tubule and cortical collecting duct of rat kidney. Am. J. Physiol. Renal Physiol. *296*, F347-54.

Gaber, R. F., Styles, C. A., and Fink, G. R. (1988). TRK1 encodes a plasma membrane protein required for high-affinity potassium transport in Saccharomyces cerevisiae. Mol. Cell. Biol. *8*, 2848–2859.

Gajewski, C., Dagcan, A., Roux, B., and Deutsch, C. (2011). Biogenesis of the pore architecture of a voltage-gated potassium channel. Proc. Natl. Acad. Sci. U. S. A. *108*, 3240–3245.

Galmes, R., Ten Brink, C., Oorschot, V., Veenendaal, T., Jonker, C., van der Sluijs, P., and Klumperman, J. (2015). Vps33B is required for delivery of endocytosed cargo to lysosomes. Traffic *16*, 1288–1305.

Gao, Y., Balut, C. M., Bailey, M. A., Patino-Lopez, G., Shaw, S., and Devor, D. C. (2010). Recycling of the Ca2+-activated K+ channel, KCa2.3, is dependent upon RME-1, Rab35/EPI64C, and an N-terminal domain. J. Biol. Chem. *285*, 17938–17953.

Gao, Y., Bertuccio, C. A., Balut, C. M., Watkins, S. C., and Devor, D. C. (2012). Dynamin- and Rab5-dependent endocytosis of a Ca2+ -activated K+ channel, KCa2.3. PLoS One *7*, e44150.

Gao, Y., Yechikov, S., Vazquez, A. E., Chen, D., and Nie, L. (2013). Distinct roles of molecular chaperones HSP90α and HSP90β in the biogenesis of KCNQ4 channels. PLoS One *8*, e57282.

Gazzarrini, S., Severino, M., Lombardi, M., Morandi, M., DiFrancesco, D., Van Etten, J. L., Thiel, G., and Moroni, A. (2003). The viral potassium channel Kcv: structural and functional

features. FEBS Lett. *552*, 12–16.

Geva, Y., and Schuldiner, M. (2014). The Back and Forth of Cargo Exit from the Endoplasmic Reticulum. Curr. Biol. *24*, R130–R136.

Ghatta, S., Nimmagadda, D., Xu, X., and O'Rourke, S. T. (2006). Large-conductance, calcium-activated potassium channels: Structural and functional implications. Pharmacol. Ther. *110*, 103–116.

Giaever, G. *et al.* (2002). Functional profiling of the Saccharomyces cerevisiae genome. Nature *418*, 387–391.

Giaever, G., and Nislow, C. (2014). The Yeast Deletion Collection: A Decade of Functional Genomics. Genetics *197*, 451–465.

Gianulis, E. C., and Trudeau, M. C. (2011). Rescue of aberrant gating by a genetically encoded PAS (Per-Arnt-Sim) domain in several long QT syndrome mutant human ether-á-go-go-related gene potassium channels. J. Biol. Chem. *286*, 22160–22169.

Glick, B. S., and Luini, A. (2011). Models for Golgi traffic: a critical assessment. Cold Spring Harb. Perspect. Biol. *3*, a005215.

Goldstein, S. A., Price, L. A., Rosenthal, D. N., and Pausch, M. H. (1996). ORK1, a potassium-selective leak channel with two pore domains cloned from Drosophila melanogaster by expression in Saccharomyces cerevisiae. Proc. Natl. Acad. Sci. U. S. A. *93*, 13256–13261.

Gong, Q., Keeney, D. R., Molinari, M., and Zhou, Z. (2005). Degradation of trafficking-defective long QT syndrome type II mutant channels by the ubiquitin-proteasome pathway. J. Biol. Chem. *280*, 19419–19425.

Van Goor, F. *et al.* (2011). Correction of the F508del-CFTR protein processing defect in vitro by the investigational drug VX-809. Proc. Natl. Acad. Sci. U. S. A. *108*, 18843–18848.

Gottschling, D. E., and Nyström, T. (2017). The Upsides and Downsides of Organelle Interconnectivity. Cell *169*, 24–34.

Grant, B. D., and Donaldson, J. G. (2009). Pathways and mechanisms of endocytic recycling. Nat. Rev. Mol. Cell Biol. *10*, 597–608.

Graves, F. M., and Tinker, A. (2000). Functional Expression of the Pore Forming Subunit of the ATP-Sensitive Potassium Channel in Saccharomyces cerevisiae. Biochem. Biophys. Res. Commun. *272*, 403–409.

Greiner, T., Ramos, J., Alvarez, M. C., Gurnon, J. R., Kang, M., Van Etten, J. L., Moroni, A., and Thiel, G. (2011). Functional HAK/KUP/KT-like potassium transporter encoded by chlorella viruses. Plant J. *68*, 977–986.

Griffith, L. C. (2001). Potassium channels: The importance of transport signals. Curr. Biol. *11*, R226–R228.

Grimm, P. R., Coleman, R., Delpire, E., and Welling, P. A. (2017). Constitutively Active SPAK Causes Hyperkalemia by Activating NCC and Remodeling Distal Tubules. 1–10.

Grishin, A., Li, H., Levitan, E. S., and Zaks-Makhina, E. (2006). Identification of gamma-aminobutyric acid receptor-interacting factor 1 (TRAK2) as a trafficking factor for the K+ channel Kir2.1. J. Biol. Chem. *281*, 30104–30111.

Guerriero, C. J., and Brodsky, J. L. (2012). The Delicate Balance Between Secreted Protein Folding And Endoplasmic Reticulum-Associated Degradation In Human Physiology. Physiol Rev *92*, 537–576.

Guiney, E. L., Klecker, T., and Emr, S. D. (2016). Identification of the endocytic sorting signal recognized by the Art1-Rsp5 ubiquitin ligase complex. Mol. Biol. Cell *27*, 4043–4054.

Guo, J., Massaeli, H., Xu, J., Jia, Z., Wigle, J. T., Mesaeli, N., and Zhang, S. (2009).

Extracellular K+ concentration controls cell surface density of IKr in rabbit hearts and of the HERG channel in human cell lines. J. Clin. Invest. *119*, 2745–2757.

Haass, F. A., Jonikas, M., Walter, P., Weissman, J. S., Jan, Y.-N., Jan, L. Y., and Schuldiner, M. (2007). Identification of yeast proteins necessary for cell-surface function of a potassium channel. Proc. Natl. Acad. Sci. U. S. A. *104*, 18079–18084.

Hampton, R. Y., and Rine, J. (1994). Regulated degradation of HMG-CoA reductase, an integral membrane protein of the endoplasmic reticulum, in yeast. J. Cell Biol. *125*, 299–312.

Hasenbrink, G., Schwarzer, S., Kolacna, L., Ludwig, J., Sychrova, H., and Lichtenberg-Fraté, H. (2005). Analysis of the mKir2.1 channel activity in potassium influx defective Saccharomyces cerevisiae strains determined as changes in growth characteristics. FEBS Lett. *579*, 1723–1731.

Henne, W. M., Stenmark, H., and Emr, S. D. (2013). Molecular Mechanisms of the Membrane Sculpting ESCRT Pathway. Cold Spring Harb. Perspect. Biol. *5*, 1–12.

Hennings, J. C. *et al.* (2017). The ClC-K2 Chloride Channel Is Critical for Salt Handling in the Distal Nephron. J. Am. Soc. Nephrol. *28*, 209–217.

Herrero, L., Monroy, N., and González, M. E. (2013). HIV-1 Vpu Protein Mediates the Transport of Potassium in *Saccharomyces cerevisiae*. Biochemistry *52*, 171–177.

Hibino, H., Inanobe, A., Furutani, K., Murakami, S., Findlay, I., and Kurachi, Y. (2010). Inwardly rectifying potassium channels: their structure, function, and physiological roles. Physiol Rev *90*, 291–366.

Hicke, L., and Dunn, R. (2003). Regulation of Membrane Protein Transport by Ubiquitin and Ubiquitin-Binding Proteins. Annu. Rev. Cell Dev. Biol. *19*, 141–172.

Hirota, Y. *et al.* (2008). Functional stabilization of Kv1.5 protein by Hsp70 in mammalian cell lines. Biochem. Biophys. Res. Commun. *372*, 469–474.

Hirsch, R. E., Lewis, B. D., Spalding, E. P., and Sussman, M. R. (1998). A role for the AKT1 potassium channel in plant nutrition. Science *280*, 918–921.

Ho, K., Nichols, C. G., Lederer, W. J., Lytton, J., Vassilev, P. M., Kanazirska, M. V., and Hebert, S. C. (1993). Cloning and expression of an inwardly rectifying ATP-regulated potassium channel. Nature *362*, 31–38.

Horazdovsky, B. F., Cowles, C. R., Mustol, P., Holmes, M., and Emr, S. D. (1996). A novel RING finger protein, Vps8p, functionally interacts with the small GTPase, Vps21p, to facilitate soluble vacuolar protein localization. J. Biol. Chem. *271*, 33607–33615.

Huang, X., and Jan, L. Y. (2014). Targeting potassium channels in cancer. J. Cell Biol. *206*, 151–162.

Huh, W.-K. K., Falvo, J. V, Gerke, L. C., Carroll, A. S., Howson, R. W., Weissman, J. S., and O'Shea, E. K. (2003). Global analysis of protein localization in budding yeast. Nature *425*, 686–691.

Ihara, Y., Tomonoh, Y., Deshimaru, M., Zhang, B., Uchida, T., Ishii, A., and Hirose, S. (2016). Retigabine, a Kv7.2/Kv7.3-Channel Opener, Attenuates Drug-Induced Seizures in Knock-In Mice Harboring Kcnq2 Mutations. PLoS One *11*, e0150095.

Isacoff, E. Y., Jan, L. Y., and Minor, D. L. (2013). Conduits of life's spark: A perspective on ion channel research since the birth of neuron. Neuron *80*, 658–674.

Ito, H., Fukuda, Y., Murata, K., and Kimura, A. (1983). Transformation of intact yeast cells treated with alkali cations. J. Bacteriol. *153*, 163–168.

Iwai, C. *et al.* (2013). Hsp90 prevents interaction between CHIP and HERG proteins to facilitate maturation of wild-type and mutant HERG proteins. Cardiovasc. Res. *100*, 520–528.

Jarosch, E., Taxis, C., Volkwein, C., Bordallo, J., Finley, D., Wolf, D. H., and Sommer, T. (2002). Protein dislocation from the ER requires polyubiquitination and the AAA-ATPase Cdc48. Nat. Cell Biol. *4*, 134–139.

Jensen, C. S., Watanabe, S., Rasmussen, H. B., Schmitt, N., Olesen, S.-P., Frost, N. a, Blanpied, T. a, and Misonou, H. (2014). Specific Sorting and Post-Golgi trafficking of Dendritic Potassium Channels in Living Neurons. J. Biol. Chem., 10566–10581.

Ji, W., Foo, J. N., O'Roak, B. J., Zhao, H., Larson, M. G., Simon, D. B., Newton-Cheh, C., State, M. W., Levy, D., and Lifton, R. P. (2008). Rare independent mutations in renal salt handling genes contribute to blood pressure variation. Nat. Genet. *40*, 592–599.

Jimenez, V., and Docampo, R. (2012). Molecular and Electrophysiological Characterization of a Novel Cation Channel of Trypanosoma cruzi. PLoS Pathog. *8*, e1002750.

Kaczorowski, G. J., McManus, O. B., Priest, B. T., and Garcia, M. L. (2008). Ion channels as drug targets: the next GPCRs. J. Gen. Physiol. *131*, 399–405.

Kahle, K. T., Ring, A. M., and Lifton, R. P. (2008). Molecular physiology of the WNK kinases. Annu. Rev. Physiol. *70*, 329–355.

Kaiser, C. A., and Schekman, R. (1990). Distinct sets of SEC genes govern transport vesicle formation and fusion early in the secretory pathway. Cell *61*, 723–733.

Kampinga, H. H., and Craig, E. A. (2010). The HSP70 chaperone machinery: J proteins as drivers of functional specificity. Nat. Rev. Mol. Cell Biol. *11*, 579–592.

Kampmeyer, C., Karakostova, A., Schenstrøm, S. M., Abildgaard, A. B., Lauridsen, A.-M., Jourdain, I., and Hartmann-Petersen, R. (2017). The exocyst subunit Sec3 is regulated by a protein quality control pathway. J. Biol. Chem. *292*, 15240–15253.

Kang, D. S., Tian, X., and Benovic, J. L. (2013). β-Arrestins and G protein-coupled receptor trafficking. Methods Enzymol. *521*, 91–108.

Karras, G. I., Yi, S., Sahni, N., Fischer, M., Xie, J., Vidal, M., D'Andrea, A. D., Whitesell, L., and Lindquist, S. (2017). HSP90 Shapes the Consequences of Human Genetic Variation. Cell *0*, 856–866.

Kashlan, O. B., Kinlough, C. L., Myerburg, M. M., Shi, S., Chen, J., Blobner, B. M., Buck, T. M., Brodsky, J. L., Hughey, R. P., and Kleyman, T. R. (2018). *N* -linked glycans are required on epithelial Na^+ channel subunits for maturation and surface expression. Am. J. Physiol. Physiol. *314*, F483–F492.

Kawada, H., Inanobe, A., and Kurachi, Y. (2016). Isolation of proflavine as a blocker of G protein-gated inward rectifier potassium channels by a cell growth-based screening system. Neuropharmacology *109*, 18–28.

Kellis, M., Birren, B. W., and Lander, E. S. (2004). Proof and evolutionary analysis of ancient genome duplication in the yeast Saccharomyces cerevisiae. Nature *428*, 617–624.

Kharade, S. V, Sheehan, J. H., Figueroa, E. E., Meiler, J., and Denton, J. S. (2017). Pore Polarity and Charge Determine Differential Block of Kir1.1 and Kir7.1 Potassium Channels by Small-Molecule Inhibitor VU590. Mol. Pharmacol. *92*, 338–346.

Kienzle, C., and von Blume, J. (2014). Secretory cargo sorting at the trans-Golgi network. Trends Cell Biol. *24*, 584–593.

Kim, G.-H., Park, E., Kong, Y.-Y., and Han, J.-K. (2006). Novel function of POSH, a JNK scaffold, as an E3 ubiquitin ligase for the Hrs stability on early endosomes. Cell. Signal. *18*, 553–563.

Kim, J.-B. (2014). Channelopathies. Korean J. Pediatr. *57*, 1–18.

Kinclová, O., Ramos, J., Potier, S., and Sychrová, H. (2001). Functional study of the

Saccharomyces cerevisiae Nha1p C-terminus. Mol. Microbiol. *40*, 656–668.

Kingsbury, J. M., Sen, N. D., Maeda, T., Heitman, J., and Cardenas, M. E. (2014). Endolysosomal Membrane Trafficking Complexes Drive Nutrient-Dependent TORC1 Signaling to Control Cell Growth in Saccharomyces cerevisiae. Genetics *196*, 1077–1089.

Klionsky, D. J., Herman, P. K., and Emr, S. D. (1990). The fungal vacuole: composition, function, and biogenesis. Microbiol. Rev. *54*, 266–292.

Ko, C. H., and Gaber, R. F. (1991). TRK1 and TRK2 encode structurally related K+ transporters in Saccharomyces cerevisiae. Mol. Cell. Biol. *11*, 4266–4273.

Ko, C. H., Liang, H., and Gaber, R. F. (1993). Roles of multiple glucose transporters in Saccharomyces cerevisiae. Mol. Cell. Biol. *13*, 638–648.

Kojima, A., Toshima, J. Y., Kanno, C., Kawata, C., and Toshima, J. (2012). Localization and functional requirement of yeast Na +/H + exchanger, Nhx1p, in the endocytic and protein recycling pathway. Biochim. Biophys. Acta - Mol. Cell Res. *1823*, 534–543.

Kolb, A. R., Needham, P. G., Rothenberg, C., Guerriero, C. J., Welling, P. A., and Brodsky, J. L. (2014). ESCRT regulates surface expression of the Kir2.1 potassium channel. Mol. Biol. Cell *25*, 276–289.

Koster, J. C., Bentle, K. A., Nichols, C. G., and Ho, K. (1998). Assembly of ROMK1 (Kir 1.1a) Inward Rectifier K+ Channel Subunits Involves Multiple Interaction Sites. Biophys. J. *74*, 1821–1829.

Koushik, S. V, Chen, H., Thaler, C., Puhl, H. L., Vogel, S. S., and Vogel, S. S. (2006). Cerulean, Venus, and VenusY67C FRET reference standards. Biophys. J. *91*, L99–L101.

Kraft, C., Peter, M., and Hofmann, K. (2010). Selective autophagy: ubiquitin-mediated recognition and beyond. Nat. Cell Biol. *12*, 836–841.

Kukol, A., and Arkin, I. T. (1999). vpu Transmembrane Peptide Structure Obtained by Site-Specific Fourier Transform Infrared Dichroism and Global Molecular Dynamics Searching. Biophys. J. *77*, 1594–1601.

Kumar, R. (2017). An account of fungal 14-3-3 proteins. Eur. J. Cell Biol. *96*, 206–217.

Kupper, N., Ge, D., Treiber, F. A., and Snieder, H. (2006). Emergence of novel genetic effects on blood pressure and hemodynamics in adolescence: the Georgia Cardiovascular Twin Study. Hypertens. (Dallas, Tex. 1979) *47*, 948–954.

Lachmann, J., Glaubke, E., Moore, P. S., and Ungermann, C. (2014). The Vps39-like TRAP1 is an effector of Rab5 and likely the missing Vps3 subunit of human CORVET. Cell. Logist. *4*, e970840.

Lai, H. C., Grabe, M., Jan, Y. N., and Jan, L. Y. (2005). The S4 Voltage Sensor Packs Against the Pore Domain in the KAT1 Voltage-Gated Potassium Channel. Neuron *47*, 395–406.

Leipziger, J., MacGregor, G. G., Cooper, G. J., Xu, J., Hebert, S. C., and Giebisch, G. (2000). PKA site mutations of ROMK2 channels shift the pH dependence to more alkaline values. Am. J. Physiol. Physiol. *279*, F919–F926.

Leng, Q., MacGregor, G. G., Dong, K., Giebisch, G., and Hebert, S. C. (2006). Subunit-subunit interactions are critical for proton sensitivity of ROMK: evidence in support of an intermolecular gating mechanism. Proc. Natl. Acad. Sci. U. S. A. *103*, 1982–1987.

Leung, Y.-M. (2000). Phosphatidylinositol 4,5-Bisphosphate and Intracellular pH Regulate the ROMK1 Potassium Channel via Separate but Interrelated Mechanisms. J. Biol. Chem. *275*, 10182–10189.

Li, K., Jiang, Q., Bai, X., Yang, Y.-F., Ruan, M.-Y., and Cai, S.-Q. (2017). Tetrameric Assembly of K+ Channels Requires ER-Located Chaperone Proteins. Mol. Cell *65*, 52–65.

Li, X., Ortega, B., Kim, B., and Welling, P. A. (2016). A Common Signal Patch Drives AP-1 Protein-dependent Golgi Export of Inwardly Rectifying Potassium Channels. J. Biol. Chem. *291*, 14963–14972.

Liang, H., Ko, C. H., Herman, T., and Gaber, R. F. (1998). Trinucleotide insertions, deletions, and point mutations in glucose transporters confer K+ uptake in Saccharomyces cerevisiae. Mol. Cell. Biol. *18*, 926–935.

Lin, C. H., MacGurn, J. A., Chu, T., Stefan, C. J., and Emr, S. D. (2008). Arrestin-related ubiquitin-ligase adaptors regulate endocytosis and protein turnover at the cell surface. Cell *135*, 714–725.

Lin, D.-H., Sterling, H., Wang, Z., Babilonia, E., Yang, B., Dong, K., Hebert, S. C., Giebisch, G., and Wang, W.-H. (2005). ROMK1 channel activity is regulated by monoubiquitination. Proc. Natl. Acad. Sci. U. S. A. *102*, 4306–4311.

Lin, D.-H., Yue, P., Pan, C.-Y., Sun, P., Zhang, X., Han, Z., Roos, M., Caplan, M., Giebisch, G., and Wang, W.-H. (2009). POSH stimulates the ubiquitination and the clathrin-independent endocytosis of ROMK1 channels. J. Biol. Chem. *284*, 29614–29624.

Lin, D.-H., Yue, P., Yarborough, O., Scholl, U. I., Giebisch, G., Lifton, R. P., Rinehart, J., and Wang, W.-H. (2015). Src-family protein tyrosine kinase phosphorylates WNK4 and modulates its inhibitory effect on KCNJ1 (ROMK). Proc. Natl. Acad. Sci. U. S. A. *112*, 4495–4500.

Long, S. B., Campbell, E. B., and Mackinnon, R. (2005). Crystal structure of a mammalian voltage-dependent Shaker family K+ channel. Science *309*, 897–903.

Loukin, S. H., Kuo, M. M.-C., Zhou, X.-L., Haynes, W. J., Kung, C., and Saimi, Y. (2005). Microbial K+ channels. J. Gen. Physiol. *125*, 521–527.

Loukin, S., Su, Z., Zhou, X., and Kung, C. (2010). Forward genetic analysis reveals multiple gating mechanisms of TRPV4. J. Biol. Chem. *285*, 19884–19890.

Lu, J., Robinson, J. M., Edwards, D., and Deutsch, C. (2001). T1−T1 Interactions Occur in ER Membranes while Nascent Kv Peptides Are Still Attached to Ribosomes. Biochemistry *40*, 10934–10946.

Lu, M., Wang, T., Yan, Q., Yang, X., Dong, K., Knepper, M. A., Wang, W., Giebisch, G., Shull, G. E., and Hebert, S. C. (2002). Absence of small conductance K+ channel (SK) activity in apical membranes of thick ascending limb and cortical collecting duct in ROMK (Bartter's) knockout mice. J. Biol. Chem. *277*, 37881–37887.

Lu, Z., and MacKinnon, R. (1994). Electrostatic tuning of Mg2+ affinity in an inward-rectifier K+ channel. Nature *371*, 243–246.

Luciani, A. *et al.* (2010). Defective CFTR induces aggresome formation and lung inflammation in cystic fibrosis through ROS-mediated autophagy inhibition. Nat. Cell Biol. *12*, 863–875.

Lukacs, G. L., Mohamed, A., Kartner, N., Chang, X. B., Riordan, J. R., and Grinstein, S. (1994). Conformational maturation of CFTR but not its mutant counterpart (delta F508) occurs in the endoplasmic reticulum and requires ATP. EMBO J. *13*, 6076–6086.

Lukacs, G. L., and Verkman, A. S. (2012). CFTR: folding, misfolding and correcting the ΔF508 conformational defect. Trends Mol. Med. *18*, 81–91.

Luo, W. J., and Chang, A. (2000). An endosome-to-plasma membrane pathway involved in trafficking of a mutant plasma membrane ATPase in yeast. Mol. Biol. Cell *11*, 579–592.

Ma, D., Taneja, T. K., Hagen, B. M., Kim, B.-Y., Ortega, B., Lederer, W. J., and Welling, P. A. (2011). Golgi export of the Kir2.1 channel is driven by a trafficking signal located

within its tertiary structure. Cell *145*, 1102–1115.

MacDonald, C., and Piper, R. C. (2016). Cell surface recycling in yeast: mechanisms and machineries. Biochem. Soc. Trans. *44*, 474–478.

MacDonald, C., Winistorfer, S., Pope, R. M., Wright, M. E., and Piper, R. C. (2017). Enzyme reversal to explore the function of yeast E3 ubiquitin-ligases. Traffic *18*, 465–484.

MacGurn, J. A. (2014). Garbage on, garbage off: new insights into plasma membrane protein quality control. Curr. Opin. Cell Biol. *29*, 92–98.

MacGurn, J. A., Hsu, P.-C., and Emr, S. D. (2012). Ubiquitin and Membrane Protein Turnover: From Cradle to Grave. Annu. Rev. Biochem. *81*, 231–259.

Mackie, T. D., Kim, B.-Y., Subramanya, A. R., Bain, D. J., O'Donnell, A. F., Welling, P. A., and Brodsky, J. L. (2018). The endosomal trafficking factors CORVET and ESCRT suppress plasma membrane residence of the renal outer medullary potassium channel (ROMK). J. Biol. Chem., jbc.M117.819086.

MacKinnon, R. (1991). Determination of the subunit stoichiometry of a voltage-activated potassium channel. Nature *350*, 232–235.

MacKinnon, R. (2003). Potassium channels and the atomic basis of selective ion conduction.

Madrid, R., Gómez, M. J., Ramos, J., and Rodríguez-Navarro, A. (1998). Ectopic potassium uptake in trk1 trk2 mutants of Saccharomyces cerevisiae correlates with a highly hyperpolarized membrane potential. J. Biol. Chem. *273*, 14838–14844.

Makhnevych, T., and Houry, W. A. (2012). The role of Hsp90 in protein complex assembly. Biochim. Biophys. Acta - Mol. Cell Res. *1823*, 674–682.

von der Malsburg, K., Shao, S., and Hegde, R. S. (2015). The ribosome quality control pathway can access nascent polypeptides stalled at the Sec61 translocon. Mol. Biol. Cell *26*, 2168–2180.

Manford, A. G., Stefan, C. J., Yuan, H. L., MacGurn, J. A., and Emr, S. D. (2012). ER-to-Plasma Membrane Tethering Proteins Regulate Cell Signaling and ER Morphology. Dev. Cell *23*, 1129–1140.

Mangano, S., Silberstein, S., and Santa-María, G. E. (2008). Point mutations in the barley HvHAK1 potassium transporter lead to improved K + -nutrition and enhanced resistance to salt stress. FEBS Lett. *582*, 3922–3928.

Märquez, J., and Serrano, R. (1996). Multiple transduction pathways regulate the sodium-extrusion gene PMR2/ENA1 during salt stress in yeast. FEBS Lett. *382*, 89–92.

Mathie, A., and Veale, E. L. (2009). Neuronal Potassium Channels. In: Encyclopedia of Neuroscience, Berlin, Heidelberg: Springer Berlin Heidelberg, 2792–2797.

Matsuura-Tokita, K., Takeuchi, M., Ichihara, A., Mikuriya, K., and Nakano, A. (2006). Live imaging of yeast Golgi cisternal maturation. Nature *441*, 1007–1010.

McClellan, A. J., Xia, Y., Deutschbauer, A. M., Davis, R. W., Gerstein, M., and Frydman, J. (2007). Diverse Cellular Functions of the Hsp90 Molecular Chaperone Uncovered Using Systems Approaches. Cell *131*, 121–135.

McCracken, A. A., Karpichev, I. V, Ernaga, J. E., Werner, E. D., Dillin, A. G., and Courchesne, W. E. (1996). Yeast mutants deficient in ER-associated degradation of the Z variant of alpha-1-protease inhibitor. Genetics *144*, 1355–1362.

McMahon, H. T., and Boucrot, E. (2011). Molecular mechanism and physiological functions of clathrin-mediated endocytosis. Nat. Rev. Mol. Cell Biol. *12*, 517–533.

McNally, K. E. *et al.* (2017). Retriever is a multiprotein complex for retromer-

independent endosomal cargo recycling. Nat. Cell Biol. *19*.

McNicholas, C. M., MacGregor, G. G., Islas, L. D., Yang, Y., Hebert, S. C., and Giebisch, G. (1998). pH-dependent modulation of the cloned renal K+ channel, ROMK. Am J Physiol *275*, F972-81.

Mendoza, J. L., Schmidt, A., Li, Q., Nuvaga, E., Barrett, T., Bridges, R. J., Feranchak, A. P., Brautigam, C. A., and Thomas, P. J. (2012). Requirements for Efficient Correction of ΔF508 CFTR Revealed by Analyses of Evolved Sequences. Cell *148*, 164–174.

Mente, A. *et al.* (2014). Association of Urinary Sodium and Potassium Excretion with Blood Pressure. N. Engl. J. Med. *371*, 601–611.

Metzger, M. B., and Michaelis, S. (2009). Analysis of quality control substrates in distinct cellular compartments reveals a unique role for Rpn4p in tolerating misfolded membrane proteins. Mol. Biol. Cell *20*, 1006–1019.

Miller, C. (2000). An overview of the potassium channel family. Genome Biol. *1*, reviews0004.1.

Minor, D. L., Masseling, S. J., Jan, Y. N., and Jan, L. Y. (1999). Transmembrane structure of an inwardly rectifying potassium channel. Cell *96*, 879–891.

Moir, D., Stewart, S. E., Osmond, B. C., and Botstein, D. (1982). COLD-SENSITIVE CELL-DIVISION-CYCLE MUTANTS OF YEAST: ISOLATION, PROPERTIES, AND PSEUDOREVERSION STUDIES. Genetics *100*.

Morsomme, P., Slayman, C. W., and Goffeau, A. (2000). Mutagenic study of the structure, function and biogenesis of the yeast plasma membrane H+-ATPase. Biochim. Biophys. Acta - Rev. Biomembr. *1469*, 133–157.

Mueller, S., Wahlander, A., Selevsek, N., Otto, C., Ngwa, E. M., Poljak, K., Frey, A. D., Aebi, M., and Gauss, R. (2015). Protein degradation corrects for imbalanced subunit stoichiometry in OST complex assembly. Mol. Biol. Cell *26*, 2596–2608.

Mumberg, D., Müller, R., and Funk, M. (1995). Yeast vectors for the controlled expression of heterologous proteins in different genetic backgrounds. Gene *156*, 119–122.

Mund, T., and Pelham, H. R. B. (2009). Control of the activity of WW-HECT domain E3 ubiquitin ligases by NDFIP proteins. EMBO Rep. *10*, 501–507.

Murray, C. J. L., and Lopez, A. D. (2013). Measuring the Global Burden of Disease. N. Engl. J. Med. *369*, 448–457.

Murray, D. H. *et al.* (2016). An endosomal tether undergoes an entropic collapse to bring vesicles together. Nature *537*, 107–111.

Muslin, A. J., Tanner, J. W., Allen, P. M., and Shaw, A. S. (1996). Interaction of 14-3-3 with Signaling Proteins Is Mediated by the Recognition of Phosphoserine. Cell *84*, 889–897.

Nakamura, R. L., Anderson, J. A., and Gaber, R. F. (1997). Determination of key structural requirements of a K+ channel pore. J. Biol. Chem. *272*, 1011–1018.

Nakamura, R. L., and Gaber, R. F. (1998). Studying Ion Channels Using Yeast Genetics. In: Methods in Enzymology, Elsevier, 89–104.

Nakamura, R. L., and Gaber, R. F. (2009). Ion selectivity of the Kat1 K^+ channel pore. Mol. Membr. Biol. *26*, 293–308.

Nakatsukasa, K., and Brodsky, J. L. (2010). in vitro reconstitution of the selection, ubiquitination, and membrane extraction of a polytopic ERAD substrate. Methods Mol. Biol. *619*, 365–376.

Nathan, D. F., and Lindquist, S. (1995). Mutational analysis of Hsp90 function: interactions with a steroid receptor and a protein kinase. Mol. Cell. Biol. *15*, 3917–3925.

Navarrete, C., Petrezsélyová, S., Barreto, L., Martínez, J. L., Zahrádka, J., Ariño, J., Sychrová, H., and Ramos, J. (2010). Lack of main K+ uptake systems in Saccharomyces cerevisiae cells affects yeast performance in both potassium-sufficient and potassium-limiting conditions. FEMS Yeast Res. *10*.

Neal, S. *et al.* (2018). The Dfm1 Derlin Is Required for ERAD Retrotranslocation of Integral Membrane Proteins Article The Dfm1 Derlin Is Required for ERAD Retrotranslocation of Integral Membrane Proteins. Mol. Cell *69*, 306–320.e4.

Nieva, J. L., Madan, V., and Carrasco, L. (2012). Viroporins: structure and biological functions. Nat. Rev. Microbiol. *10*, 563–574.

Nikko, E., and Pelham, H. R. B. (2009). Arrestin-mediated endocytosis of yeast plasma membrane transporters. Traffic *10*, 1856–1867.

Nishimura, K., Fukagawa, T., Takisawa, H., Kakimoto, T., and Kanemaki, M. (2009). An auxin-based degron system for the rapid depletion of proteins in nonplant cells. Nat. Methods *6*, 917–922.

Novick, P., Field, C., and Schekman, R. (1980). Identification of 23 complementation groups required for post-translational events in the yeast secretory pathway. Cell *21*, 205–215.

O'Donnell, A. F. (2012). The running of the Buls: control of permease trafficking by α-arrestins Bul1 and Bul2. Mol. Cell. Biol. *32*, 4506–4509.

O'Donnell, A. F., Huang, L., Thorner, J., and Cyert, M. S. (2013). A calcineurin-dependent switch controls the trafficking function of α-arrestin Aly1/Art6. J. Biol. Chem. *288*, 24063–24080.

O'Donnell, B. M., Mackie, T. D., and Brodsky, J. L. (2017a). Linking chanelopathies with endoplasmic reticulum associated degradation. Channels *0*, 1–3.

O'Donnell, B. M., Mackie, T. D., Subramanya, A. R., and Brodsky, J. L. (2017b). Endoplasmic Reticulum-Associated Degradation of the Renal Potassium Channel, ROMK, Leads to Type II Bartter Syndrome. J. Biol. Chem. *292*, 12813–12827.

Okamoto, Y., and Shikano, S. (2011). Phosphorylation-dependent C-terminal binding of 14-3-3 proteins promotes cell surface expression of HIV co-receptor GPR15. J. Biol. Chem. *286*, 7171–7181.

Okiyoneda, T. *et al.* (2018). Chaperone-Independent Peripheral Quality Control of CFTR by RFFL E3 Ligase. Dev. Cell *44*, 1–15.

Okiyoneda, T., Barrière, H., Bagdány, M., Rabeh, W. M., Du, K., Höhfeld, J., Young, J. C., and Lukacs, G. L. (2010). Peripheral protein quality control removes unfolded CFTR from the plasma membrane. Science *329*, 805–810.

Ortega, B., Millar, I. D., Beesley, A. H., Robson, L., and White, S. J. (2000). Stable, polarised, functional expression of Kir1.1b channel protein in Madin-Darby canine kidney cell line. J. Physiol. *528 Pt 1*, 5–13.

Pagant, S., Kung, L., Dorrington, M., Lee, M. C. S., and Miller, E. A. (2007). Inhibiting Endoplasmic Reticulum (ER)-associated Degradation of Misfolded Yor1p Does Not Permit ER Export Despite the Presence of a Diacidic Sorting Signal. Mol. Biol. Cell *18*, 3398–3413.

Papazian, D. M. (1999). Potassium channels: some assembly required. Neuron *23*, 7–10.

Paulais, M. *et al.* (2011). Renal phenotype in mice lacking the Kir5.1 (Kcnj16) K+ channel subunit contrasts with that observed in SeSAME/EAST syndrome. Proc. Natl. Acad. Sci. U. S. A. *108*, 10361–10366.

Paynter, J. J., Sarkies, P., Andres-Enguix, I., and Tucker, S. J. (2008). Genetic selection of activatory mutations in KcsA. Channels *2*, 413–418.

Paynter, J. J., Shang, L., Bollepalli, M. K., Baukrowitz, T., and Tucker, S. J. (2010). Random mutagenesis screening indicates the absence of a separate H + -sensor in the pH-sensitive Kir channels. Channels *4*, 390–396.

Pearse, B. (2000). Clathrin coat construction in endocytosis. Curr. Opin. Struct. Biol. *10*, 220–228.

Perier, F., Coulter, K. L., Liang, H., Radeke, C. M., Gaber, R. F., and Vandenberg, C. A. (1994). Identification of a novel mammalian member of the NSF/CDC48p/Paslp/TBP-1 family through heterologous expression in yeast. FEBS Lett. *351*, 290–14492.

Perini, E. D., Schaefer, R., Stöter, M., Kalaidzidis, Y., and Zerial, M. (2014). Mammalian CORVET Is Required for Fusion and Conversion of Distinct Early Endosome Subpopulations. Traffic *15*, 1366–1389.

Persson, B. L., Berhe, A., Fristedt, U., Martinez, P., Pattison, J., Petersson, J., and Weinander, R. (1998). Phosphate permeases of Saccharomyces cerevisiae. Biochim. Biophys. Acta - Bioenerg. *1365*, 23–30.

Peters, M., Ermert, S., Jeck, N., Derst, C., Pechmann, U., Weber, S., Schlingmann, K. P., Seyberth, H. W., Waldegger, S., and Konrad, M. (2003). Classification and rescue of ROMK mutations underlying hyperprostaglandin E syndrome/antenatal Bartter syndrome. Kidney Int. *64*, 923–932.

Peterson, L. B., Eskew, J. D., Vielhauer, G. A., and Blagg, B. S. J. (2012). The hERG channel is dependent upon the Hsp90α isoform for maturation and trafficking. Mol. Pharm. *9*, 1841–1846.

Petrezselyova, S., Zahradka, J., and Sychrova, H. (2010). Saccharomyces cerevisiae BY4741 and W303-1A laboratory strains differ in salt tolerance. Fungal Biol. *114*, 144–150.

Piala, A. T., Moon, T. M., Akella, R., He, H., Cobb, M. H., and Goldsmith, E. J. (2014). Chloride sensing by WNK1 involves inhibition of autophosphorylation. Sci. Signal. *7*, ra41.

Pierce, S. E., Davis, R. W., Nislow, C., and Giaever, G. (2007). Genome-wide analysis of barcoded Saccharomyces cerevisiae gene-deletion mutants in pooled cultures. Nat. Protoc. *2*, 2958–2974.

Plemel, R. L., Lobingier, B. T., Brett, C. L., Angers, C. G., Nickerson, D. P., Paulsel, A., Sprague, D., and Merz, A. J. (2011). Subunit organization and Rab interactions of Vps-C protein complexes that control endolysosomal membrane traffic. Mol. Biol. Cell *22*, 1353–1363.

Plemenitaš, A., Konte, T., Gostinčar, C., and Cimerman, N. G. (2016). Transport Systems in Halophilic Fungi. Springer, Cham, 307–325.

Plugge, B., Gazzarrini, S., Nelson, M., Cerana, R., Van Etten, J. L., Derst, C., DiFrancesco, D., Moroni, A., and Thiel, G. (2000). A potassium channel protein encoded by chlorella virus PBCV-1. Science *287*, 1641–1644.

Pols, M. S., ten Brink, C., Gosavi, P., Oorschot, V., and Klumperman, J. (2013). The HOPS Proteins hVps41 and hVps39 Are Required for Homotypic and Heterotypic Late Endosome Fusion. Traffic *14*, 219–232.

Preston, G. M., and Brodsky, J. L. (2017). The evolving role of ubiquitin modification in endoplasmic reticulum-associated degradation. Biochem. J. *474*, 445–469.

Preston, G. M., Guerriero, C. J., Metzger, M. B., Michaelis, S., and Brodsky, J. L. (2018). Substrate insolubility dictates Hsp104-dependent endoplasmic-reticulum-associate degradation. Mol. Cell.

Priest, B. T., Bell, I. M., and Garcia, M. L. (2008). Role of hERG potassium channel assays in drug development. Channels (Austin). *2*, 87–93.

Puricelli, E., Bettinelli, A., Borsa, N., Sironi, F., Mattiello, C., Tammaro, F., Tedeschi, S., Bianchetti, M. G., and Italian Collaborative Group for Bartter Syndrome (2010). Long-term follow-up of patients with Bartter syndrome type I and II. Nephrol. Dial. Transplant. *25*, 2976–2981.

Rabeh, W. M. *et al.* (2012). Correction of both NBD1 energetics and domain interface is required to restore ΔF508 CFTR folding and function. Cell *148*, 150–163.

Rabinovich, E., Kerem, A., Fröhlich, K.-U., Diamant, N., and Bar-Nun, S. (2002). AAA-ATPase p97/Cdc48p, a cytosolic chaperone required for endoplasmic reticulum-associated protein degradation. Mol. Cell. Biol. *22*, 626–634.

Rachidi, M., and Lopes, C. (2007). Mental retardation in Down syndrome: From gene dosage imbalance to molecular and cellular mechanisms. Neurosci. Res. *59*, 349–369.

Randles, L. G., Lappalainen, I., Fowler, S. B., Moore, B., Hamill, S. J., and Clarke, J. (2006). Using model proteins to quantify the effects of pathogenic mutations in Ig-like proteins. J. Biol. Chem. *281*, 24216–24226.

Rapedius, M., Fowler, P. W., Shang, L., Sansom, M. S. P., Tucker, S. J., and Baukrowitz, T. (2007a). H bonding at the helix-bundle crossing controls gating in Kir potassium channels. Neuron *55*, 602–614.

Rapedius, M., Haider, S., Browne, K. F., Shang, L., Sansom, M. S. P., Baukrowitz, T., and Tucker, S. J. (2006). Structural and functional analysis of the putative pH sensor in the Kir1.1 (ROMK) potassium channel. EMBO Rep. *7*, 611–616.

Rapedius, M., Paynter, J. J., Fowler, P., Shang, L., Sansom, M., Tucker, S. J., and Baukrowitz, T. (2007b). Control of pH and PIP $_2$ Gating in Heteromeric Kir4.1/Kir5.1 Channels by H-Bonding at the Helix-Bundle Crossing. Channels *1*, 327–330.

Raphemot, R., Weaver, C. D., and Denton, J. S. (2013). High-throughput screening for small-molecule modulators of inward rectifier potassium channels. J. Vis. Exp., 1–8.

Reggiori, F., and Pelham, H. R. B. (2002). A transmembrane ubiquitin ligase required to sort membrane proteins into multivesicular bodies. Nat. Cell Biol. *4*, 117–123.

Renigunta, A., Mutig, K., Rottermann, K., Schlichthörl, G., Preisig-Müller, R., Daut, J., Waldegger, S., and Renigunta, V. (2011a). The Glycolytic Enzymes Glyceraldehyde 3-Phosphate Dehydrogenase and Enolase Interact with the Renal Epithelial K+ Channel ROMK2 and Regulate its Function. Cell. Physiol. Biochem. *28*, 663–672.

Renigunta, A., Renigunta, V., Saritas, T., Decher, N., Mutig, K., and Waldegger, S. (2011b). Tamm-Horsfall glycoprotein interacts with renal outer medullary potassium channel ROMK2 and regulates its function. J. Biol. Chem. *286*, 2224–2235.

Rieg, T., Vallon, V., Sausbier, M., Sausbier, U., Kaissling, B., Ruth, P., and Osswald, H. (2007). The role of the BK channel in potassium homeostasis and flow-induced renal potassium excretion. Kidney Int. *72*, 566–573.

Ring, A. M., Leng, Q., Rinehart, J., Wilson, F. H., Kahle, K. T., Hebert, S. C., and Lifton, R. P. (2007). An SGK1 site in WNK4 regulates Na+ channel and K+ channel activity and has implications for aldosterone signaling and K+ homeostasis. Proc. Natl. Acad. Sci. U. S. A. *104*, 4025–4029.

Roberg, K. J., Rowley, N., and Kaiser, C. A. (1997). Physiological regulation of membrane protein sorting late in the secretory pathway of Saccharomyces cerevisiae. J. Cell Biol. *137*, 1469–1482.

Robinson, J. S., Klionsky, D. J., Banta, L. M., and Emr, S. D. (1988). Protein sorting in Saccharomyces cerevisiae: isolation of mutants defective in the delivery and processing of

multiple vacuolar hydrolases. Mol. Cell. Biol. *8*, 4936.

Rodan, A. R. (2016). Potassium: friend or foe? Pediatr. Nephrol., 1–13.

Rodríguez-Navarro, A., and Rubio, F. (2006). High-affinity potassium and sodium transport systems in plants. J. Exp. Bot. *57*, 1149–1160.

Ronzaud, C. *et al.* (2013). Renal tubular NEDD4-2 deficiency causes NCC-mediated salt-dependent hypertension. J. Clin. Invest. *123*, 657–665.

Ros, R., Lemaillet, G., Fonrouge, A. G., Daram, P., Enjuto, M., Salmon, J. M., Thibaud, J. B., and Sentenac, H. (1999). Molecular determinants of the Arabidopsis AKT1 K+ channel ionic selectivity investigated by expression in yeast of randomly mutated channels. Physiol. Plant. *105*, 459–468.

Rossier, B. C., Baker, M. E., and Studer, R. A. (2015). Epithelial Sodium Transport and Its Control by Aldosterone: The Story of Our Internal Environment Revisited. Physiol. Rev. *95*, 297–340.

Rotin, D., and Staub, O. (2011). Role of the ubiquitin system in regulating ion transport. Pflugers Arch. *461*, 1–21.

Roux, B., and MacKinnon, R. (1999). The Cavity and Pore Helices in the KcsA K+ Channel: Electrostatic Stabilization of Monovalent Cations. Science (80-.). *285*.

Sanguinetti, M. C., and Tristani-Firouzi, M. (2006). hERG potassium channels and cardiac arrhythmia. Nature *440*, 463–469.

Schachtman, D. P., and Schroeder, J. I. (1994). Structure and transport mechanism of a high-affinity potassium uptake transporter from higher plants. Nature *370*, 655–658.

Schachtman, D. P., Schroeder, J. I., Lucas, W. J., Anderson, J. A., and Gaber, R. F. (1992). Expression of an inward-rectifying potassium channel by the Arabidopsis KAT1 cDNA. Science (80-.). *258*, 1654–1659.

Schekman, R. (2010). Charting the secretory pathway in a simple eukaryote. Mol. Biol. Cell *21*, 3781–3784.

Schmidt, M., and Finley, D. (2014). Regulation of proteasome activity in health and disease. Biochim. Biophys. Acta *1843*, 13–25.

Schulze, D., Krauter, T., Fritzenschaft, H., Soom, M., and Baukrowitz, T. (2003). Phosphatidylinositol 4,5-bisphosphate (PIP2) modulation of ATP and pH sensitivity in Kir channels. A tale of an active and a silent PIP2 site in the N terminus. J. Biol. Chem. *278*, 10500–10505.

Schwalbe, R. A., Bianchi, L., Accili, E. A., and Brown, A. M. (1998). Functional consequences of ROMK mutants linked to antenatal Bartter's syndrome and implications for treatment. Hum. Mol. Genet. *7*, 975–980.

Schwarzer, S., Kolacna, L., Lichtenberg-Fraté, H., Sychrova, H., and Ludwig, J. (2008). Functional expression of the voltage-gated neuronal mammalian potassium channel rat ether à go-go1 in yeast. FEMS Yeast Res. *8*, 405–413.

Scott, P. M., Bilodeau, P. S., Zhdankina, O., Winistorfer, S. C., Hauglund, M. J., Allaman, M. M., Kearney, W. R., Robertson, A. D., Boman, A. L., and Piper, R. C. (2004). GGA proteins bind ubiquitin to facilitate sorting at the trans-Golgi network. Nat. Cell Biol. *6*, 252–259.

Seaayfan, E., Defontaine, N., Demaretz, S., Zaarour, N., and Laghmani, K. (2016). OS9 interacts with NKCC2 and targets its immature form for the endoplasmic-reticulum-associated degradation pathway. J. Biol. Chem. *291*, 4487–4502.

Seebohm, G. *et al.* (2007). Regulation of endocytic recycling of KCNQ1/KCNE1

potassium channels. Circ. Res. *100*, 686–692.

Sentenac, H., Bonneaud, N., Minet, M., Lacroute, F., Salmon, J. M., Gaymard, F., and Grignon, C. (1992). Cloning and expression in yeast of a plant potassium ion transport system. Science *256*, 663–665.

Shaer, A. J. (2001). Inherited primary renal tubular hypokalemic alkalosis: a review of Gitelman and Bartter syndromes. Am. J. Med. Sci. *322*, 316–332.

Sharma, M. *et al.* (2004). Misfolding diverts CFTR from recycling to degradation. J. Cell Biol. *164*, 923–933.

Shekarabi, M., Zhang, J., Khanna, A. R., Ellison, D. H., Delpire, E., and Kahle, K. T. (2017). WNK Kinase Signaling in Ion Homeostasis and Human Disease. Cell Metab. *25*, 285–299.

Shibata, S., Zhang, J., Puthumana, J., Stone, K. L., and Lifton, R. P. (2013). Kelch-like 3 and Cullin 3 regulate electrolyte homeostasis via ubiquitination and degradation of WNK4. Proc. Natl. Acad. Sci. U. S. A. *110*, 7838–7843.

Shields, S. B., and Piper, R. C. (2011). How Ubiquitin Functions with ESCRTs. Traffic *12*, 1306–1317.

Shikano, S., Coblitz, B., Sun, H., and Li, M. (2005). Genetic isolation of transport signals directing cell surface expression. Nat. Cell Biol. *7*, 985–992.

Shin, M. E., Ogburn, K. D., Varban, O. A., Gilbert, P. M., and Burd, C. G. (2001). FYVE Domain Targets Pib1p Ubiquitin Ligase to Endosome and Vacuolar Membranes. J. Biol. Chem. *276*, 41388–41393.

Simon, D. B., Karet, F. E., Rodriguez-Soriano, J., Hamdan, J. H., DiPietro, A., Trachtman, H., Sanjad, S. A., and Lifton, R. P. (1996a). Genetic heterogeneity of Barter's syndrome revealed by mutations in the K+ channel, ROMK. Nat. Genet. *14*, 152–156.

Simon, D. B., Karet, F. E., Rodriguez-Soriano, J., Hamdan, J. H., DiPietro, A., Trachtman, H., Sanjad, S. A., and Lifton, R. P. (1996b). Genetic heterogeneity of Bartter's syndrome revealed by mutations in the K+ channel, ROMK. Nat. Genet. *14*, 152–156.

Smith, C. J., Grigorieff, N., and Pearse, B. M. (1998). Clathrin coats at 21 A resolution: a cellular assembly designed to recycle multiple membrane receptors. EMBO J. *17*, 4943–4953.

Spear, E. D., and Ng, D. T. W. (2003). Stress tolerance of misfolded carboxypeptidase Y requires maintenance of protein trafficking and degradative pathways. Mol. Biol. Cell *14*, 2756–2767.

Stenmark, H., and Olkkonen, V. M. (2001). The Rab GTPase family. Genome Biol. *2*, REVIEWS3007.

Stirling, C. J., Rothblatt, J., Hosobuchi, M., Deshaies, R., and Schekman, R. (1992). Protein translocation mutants defective in the insertion of integral membrane proteins into the endoplasmic reticulum. Mol. Biol. Cell *3*, 129–142.

Stringer, D. K., and Piper, R. C. (2011). A single ubiquitin is sufficient for cargo protein entry into MVBs in the absence of ESCRT ubiquitination. J. Cell Biol. *192*, 229–242.

Szathmary, R., Bielmann, R., Nita-Lazar, M., Burda, P., and Jakob, C. A. (2005). Yos9 Protein Is Essential for Degradation of Misfolded Glycoproteins and May Function as Lectin in ERAD. Mol. Cell *19*, 765–775.

Szent-Gyorgyi, C. *et al.* (2008). Fluorogen-activating single-chain antibodies for imaging cell surface proteins. Nat. Biotechnol. *26*, 235–240.

Taipale, M., Jarosz, D. F., and Lindquist, S. (2010). HSP90 at the hub of protein homeostasis: emerging mechanistic insights. Nat. Rev. Mol. Cell Biol. *11*, 515–528.

Tang, H. *et al.* (2016). Discovery of MK-7145, an Oral Small Molecule ROMK Inhibitor for the Treatment of Hypertension and Heart Failure. ACS Med. Chem. Lett. *7*, 697–701.

Tang, W., Ruknudin, A., Yang, W. P., Shaw, S. Y., Knickerbocker, A., and Kurtz, S. (1995). Functional expression of a vertebrate inwardly rectifying K+ channel in yeast. Mol. Biol. Cell *6*, 1231–1240.

Tardiff, D. F. *et al.* (2013). Yeast reveal a "druggable" Rsp5/Nedd4 network that ameliorates α-synuclein toxicity in neurons. Science *342*, 979–983.

Tempel, B. L., Papazian, D. M., Schwarz, T. L., Jan, Y. N., and Jan, L. Y. (1987). Sequence of a probable potassium channel component encoded at Shaker locus of Drosophila. Science *237*, 770–775.

Terker, A. S. *et al.* (2015). Potassium modulates electrolyte balance and blood pressure through effects on distal cell voltage and chloride. Cell Metab. *21*, 39–50.

Todkar, A., Picard, N., Loffing-Cueni, D., Sorensen, M. V, Mihailova, M., Nesterov, V., Makhanova, N., Korbmacher, C., Wagner, C. A., and Loffing, J. (2015). Mechanisms of renal control of potassium homeostasis in complete aldosterone deficiency. J. Am. Soc. Nephrol. *26*, 425–438.

Tong, A. H. Y., and Boone, C. (2006). Synthetic genetic array analysis in Saccharomyces cerevisiae. Methods Mol. Biol. *313*, 171–192.

Tsukada, M., and Ohsumi, Y. (1993). Isolation and characterization of autophagy-defective mutants of *Saccharomyces cerevisiae*. FEBS Lett. *333*, 169–174.

Ungar, D., and Hughson, F. M. (2003). SNARE protein structure and function. Annu. Rev. Cell Dev. Biol. *19*, 493–517.

Ungewickell, E., and Branton, D. (1981). Assembly units of clathrin coats. Nature *289*, 420–422.

Vacata, V., Kotyk, A., and Sigler, K. (1981). Membrane potentials in yeast cells measured by direct and indirect methods. Biochim. Biophys. Acta *643*, 265–268.

Vembar, S. S., and Brodsky, J. L. (2008). One step at a time: endoplasmic reticulum-associated degradation. Nat. Rev. Mol. Cell Biol. *9*, 944–957.

Vergara, C., Latorre, R., Marrion, N. V, and Adelman, J. P. (1998). Calcium-activated potassium channels. Curr. Opin. Neurobiol. *8*, 321–329.

Vida, T. A., and Emr, S. D. (1995). A new vital stain for visualizing vacuolar membrane dynamics and endocytosis in yeast. J. Cell Biol. *128*, 779–792.

Volkov, V. (2015). Quantitative description of ion transport via plasma membrane of yeast and small cells. Front. Plant Sci. *6*, 5–22.

Wade, J. B., Fang, L., Coleman, R. A., Liu, J., Grimm, P. R., Wang, T., and Welling, P. A. (2011). Differential regulation of ROMK (Kir1.1) in distal nephron segments by dietary potassium. Am. J. Physiol. Renal Physiol. *300*, F1385-93.

Wagih, O., Usaj, M., Baryshnikova, A., VanderSluis, B., Kuzmin, E., Costanzo, M., Myers, C. L., Andrews, B. J., Boone, C. M., and Parts, L. (2013). SGAtools: one-stop analysis and visualization of array-based genetic interaction screens. Nucleic Acids Res. *41*, W591-6.

Wang, K. *et al.* (2012a). PEDV ORF3 encodes an ion channel protein and regulates virus production. FEBS Lett. *586*, 384–391.

Wang, W.-H., Yue, P., Sun, P., and Lin, D.-H. (2010). Regulation and function of potassium channels in aldosterone-sensitive distal nephron. Curr. Opin. Nephrol. Hypertens. *19*, 463–470.

Wang, W. H., Schwab, A., and Giebisch, G. (1990). Regulation of small-conductance K+

channel in apical membrane of rat cortical collecting tubule. Am. J. Physiol. *259*, F494-502.

Wang, Y., Huang, X., Zhou, J., Yang, X., Li, D., Mao, H., Sun, H. H., Liu, N., and Lian, J. (2012b). Trafficking-deficient G572R-hERG and E637K-hERG activate stress and clearance pathways in endoplasmic reticulum. PLoS One *7*, e29885.

Wangemann, P. (2006). Supporting sensory transduction: cochlear fluid homeostasis and the endocochlear potential. J. Physiol. *576*, 11–21.

Ward, C. L., and Kopito, R. R. (1994). Intracellular turnover of cystic fibrosis transmembrane conductance regulator. Inefficient processing and rapid degradation of wild-type and mutant proteins. J. Biol. Chem. *269*, 25710–25718.

van Weering, J. R. T., and Cullen, P. J. (2014). Membrane-associated cargo recycling by tubule-based endosomal sorting. Semin. Cell Dev. Biol. *31*, 40–47.

Weir, M., and Keeney, J. B. (2014). PCR Mutagenesis and Gap Repair in Yeast. In: Yeast Genetics, ed. J. S. Smith, and ed. D. J. Burke, New York, NY: Humana Press, 29–35.

Welling, P. A., and Ho, K. (2009). A comprehensive guide to the ROMK potassium channel: form and function in health and disease. Am. J. Physiol. Renal Physiol. *297*, F849-63.

Whitesell, L., and Lindquist, S. L. (2005). HSP90 and the chaperoning of cancer. Nat. Rev. Cancer *5*, 761–772.

Wiederkehr, A., Avaro, S., Prescianotto-Baschong, C., Haguenauer-Tsapis, R., and Riezman, H. (2000). The F-box protein Rcy1p is involved in endocytic membrane traffic and recycling out of an early endosome in Saccharomyces cerevisiae. J. Cell Biol. *149*, 397–410.

Wiederkehr, A., Meier, K. D., and Riezman, H. (2001). Identification and characterization of Saccharomyces cerevisiae mutants defective in fluid-phase endocytosis. Yeast *18*, 759–773.

Wolfe, D. M., and Pearce, D. A. (2006). Channeling Studies in Yeast: Yeast as a Model for Channelopathies? NeuroMolecular Med. *8*, 279–306.

Woolford, C. A., Daniels, L. B., Park, F. J., Jones, E. W., Van Arsdell, J. N., and Innis, M. A. (1986). The PEP4 gene encodes an aspartyl protease implicated in the posttranslational regulation of Saccharomyces cerevisiae vacuolar hydrolases. Mol. Cell. Biol. *6*, 2500–2510.

Wright, M. B., Ramos, J., Gomez, M. J., Moulder, K., Scherrer, M., Munson, G., and Gaber, R. F. (1997). Potassium transport by amino acid permeases in Saccharomyces cerevisiae. J. Biol. Chem. *272*, 13647–13652.

Wulff, H., Castle, N. A., and Pardo, L. A. (2009). Voltage-gated potassium channels as therapeutic targets. Nat. Rev. Drug Discov. *8*, 982–1001.

Xia, W.-F., Tang, F.-L., Xiong, L., Xiong, S., Jung, J.-U., Lee, D.-H., Li, X.-S., Feng, X., Mei, L., and Xiong, W.-C. (2013). Vps35 loss promotes hyperresorptive osteoclastogenesis and osteoporosis via sustained RANKL signaling. J. Cell Biol. *200*, 821–837.

Xie, W., Kanehara, K., Sayeed, A., and Ng, D. T. W. (2009). Intrinsic conformational determinants signal protein misfolding to the Hrd1/Htm1 endoplasmic reticulum-associated degradation system. Mol. Biol. Cell *20*, 3317–3329.

Xie, Y., and Varshavsky, A. (1999). The N-end rule pathway is required for import of histidine in yeast lacking the kinesin-like protein Cin8p. Curr. Genet. *36*, 113–123.

Yan, F.-F., Pratt, E. B., Chen, P.-C., Wang, F., Skach, W. R., David, L. L., and Shyng, S.-L. (2010). Role of Hsp90 in Biogenesis of the -Cell ATP-sensitive Potassium Channel Complex. Mol. Biol. Cell *21*, 1945–1954.

Ye, Y., Meyer, H. H., and Rapoport, T. A. (2001). The AAA ATPase Cdc48/p97 and its partners transport proteins from the ER into the cytosol. Nature *414*, 652–656.

Ye, Z., Needham, P. G., Estabrooks, S. K., Whitaker, S. K., Garcia, B. L., Misra, S., Brodsky, J. L., and Camacho, C. J. (2017). Symmetry breaking during homodimeric assembly activates an E3 ubiquitin ligase. Sci. Rep. *7*, 1789.

Yi, B. A., Lin, Y. F., Jan, Y. N., and Jan, L. Y. (2001). Yeast screen for constitutively active mutant G protein-activated potassium channels. Neuron *29*, 657–667.

Yoo, D., Fang, L., Mason, A., Kim, B.-Y., and Welling, P. A. (2005). A phosphorylation-dependent export structure in ROMK (Kir 1.1) channel overrides an endoplasmic reticulum localization signal. J. Biol. Chem. *280*, 35281–35289.

Yoo, D., Flagg, T. P., Olsen, O., Raghuram, V., Foskett, J. K., and Welling, P. A. (2004). Assembly and trafficking of a multiprotein ROMK (Kir 1.1) channel complex by PDZ interactions. J. Biol. Chem. *279*, 6863–6873.

Yoo, D., Kim, B. Y., Campo, C., Nance, L., King, A., Maouyo, D., and Welling, P. A. (2003). Cell surface expression of the ROMK (Kir 1.1) channel is regulated by the aldosterone-induced kinase, SGK-1, and protein kinase A. J. Biol. Chem. *278*, 23066–23075.

Young, J. C. (2014). The role of the cytosolic HSP70 chaperone system in diseases caused by misfolding and aberrant trafficking of ion channels. Dis. Model. Mech. *7*, 319–329.

Yu, L., Jin, X., Cui, N., Wu, Y., Shi, Z., Zhu, D., and Jiang, C. (2012). Rosiglitazone selectively inhibits K(ATP) channels by acting on the K(IR) 6 subunit. Br. J. Pharmacol. *167*, 26–36.

Zaks-Makhina, E., Kim, Y., Aizenman, E., and Levitan, E. S. (2004). Novel neuroprotective K+ channel inhibitor identified by high-throughput screening in yeast. Mol. Pharmacol. *65*, 214–219.

Zaks-Makhina, E., Li, H., Grishin, A., Salvador-Recatala, V., and Levitan, E. S. (2009). Specific and slow inhibition of the Kir2.1 K+ channel by gambogic acid. J. Biol. Chem. *284*, 15432–15438.

Zanetti, G., Pahuja, K. B., Studer, S., Shim, S., and Schekman, R. (2012). COPII and the regulation of protein sorting in mammals. Nat. Cell Biol. *14*, 20–28.

Zeng, W.-Z., Babich, V., Ortega, B., Quigley, R., White, S. J., Welling, P. A., and Huang, C.-L. (2002). Evidence for endocytosis of ROMK potassium channel via clathrin-coated vesicles. Am. J. Physiol. Renal Physiol. *283*, F630-9.

Zerangue, N., Schwappach, B., Jan, Y. N., and Jan, L. Y. (1999). A New ER Trafficking Signal Regulates the Subunit Stoichiometry of Plasma Membrane KATP Channels. Neuron *22*, 537–548.

Zhang, Y., Nijbroek, G., Sullivan, M. L., McCracken, A. A., Watkins, S. C., Michaelis, S., and Brodsky, J. L. (2001). Hsp70 molecular chaperone facilitates endoplasmic reticulum-associated protein degradation of cystic fibrosis transmembrane conductance regulator in yeast. Mol. Biol. Cell *12*, 1303–1314.

Zhong, H., Lai, J., and Yau, K.-W. (2003). Selective heteromeric assembly of cyclic nucleotide-gated channels. Proc. Natl. Acad. Sci. U. S. A. *100*, 5509–5513.

Zhou, C. *et al.* (2014). Organelle-Based Aggregation and Retention of Damaged Proteins in Asymmetrically Dividing Cells. Cell *159*, 530–542.

Zhou, H., Tate, S. S., and Palmer, L. G. (1994). Primary structure and functional properties of an epithelial K channel. Am J Physiol *266*, C809-24.

Zhou, M., Fisher, E. A., and Ginsberg, H. N. (1998). Regulated Co-translational ubiquitination of apolipoprotein B100. A new paradigm for proteasomal degradation of a secretory protein. J. Biol. Chem. *273*, 24649–24653.

Zuzarte, M., Heusser, K., Renigunta, V., Schlichthörl, G., Rinné, S., Wischmeyer, E., Daut, J., Schwappach, B., and Preisig-Müller, R. (2009). Intracellular traffic of the K^+ channels TASK-1 and TASK-3: role of N- and C-terminal sorting signals and interaction with 14-3-3 proteins. J. Physiol. *587*, 929–952.